In Vitro Selection and Characterization of DNA Aptamers against a Multiple Myeloma Monoclonal Protein

Inaugural–Dissertation

to obtain the academic degree
Doctor rerum naturalium (Dr. rer. nat.)
Submitted to the Department of Biology, Chemistry and Pharmacy
of Freie Universität Berlin

by

Yan Wang

from Harbin, China

December, 2008

Diese Arbeit wurde in der Zeit von Januar 2004 bis Mai 2008 unter der Aufsicht von Professor Dr. Volker A. Erdmann am Institut für Biochemie der Freie Universität Berlin angefertigt. Die Verfasserin versichert, die Arbeit eigenständig durchgeführt und alle Hilfsmittel angegeben zu haben.

1st Reviewer: Prof. Dr. Volker A. Erdmann
2nd Reviewer: Prof. Dr. Rudolf Tauber

Date of defence: 11.2.2009

1 Introduction

1.1 Multiple Myeloma (MM)

Multiple myeloma (MM) is a clonal B–cell malignancy, which is characterized by excessive numbers of abnormal plasma cells in the bone marrow (BM) and overproduction of monoclonal immunoglobulin (Ig) (Kyle 1985). MM is associated with a constellation of disease manifestations, including osteolytic lesions due to uncoupled bone metabolism, anemia and immunosuppression due to loss of normal hematopoietic stem cell function, hyper viscosity syndrome and end–organ damage due to monoclonal Ig secretion (Barlogie *et al.* 2001). MM accounts for approximately 1% of all malignant diseases in white population and 2% in black population, and 13% and 33% respectively, of all hematological cancers (Longo 2001). The median age of patients with MM is 65 years but in the past 60 years, a trend towards myeloma patients under 55 years of age was noticed. Men are more frequently affected than women. The cause of MM is unknown and both genetic and environmental factors have been implicated. Despite recent advance in basic biology and treatment, MM remains incurable. Complete remission can be achieved in only 5% of the cases. The median length of survival after diagnosis is 3 to 5 years and a median event–free survival of 24 to 43 months (Hallek *et al.* 1998).

1.1.1 Pathogenesis and Clinical Features of MM

Myeloma cells derive from one clone, so they are identical and produce the same monoclonal Ig, called monoclonal (M) protein or paraprotein, in large quantities. Although the specific M protein varies from patient to patient, there is only one type in each patient (Fig. 1.1). When blood or urine is processed in a laboratory test called electrophoresis, these M proteins show up as a “spike” in the results. In myeloma cells, mutations have occurred in the genes responsible for IgG production. This leads to expression of proteins with

abnormal amino acid sequence and protein structure, which have lost their normal antibody function. So, unlike normal Ig, M protein has no biological functions. Instead, it crowds out normal antibodies. In addition, levels of functional antibodies are depressed in individuals with MM. Although the process is not completely understood, it appears that the functional Igs made by existing normal plasma cells collapse more quickly in MM patients than in healthy individuals. Suppression of normal immune function, increased susceptibility to infection has been reported. Moreover, increased plasma volume and viscosity can cause renal insufficiency as well as the hyperviscosity syndrome in MM patients. Renal insufficiency and recurrent bacterial infections are also major causes of death (Durie 2001).

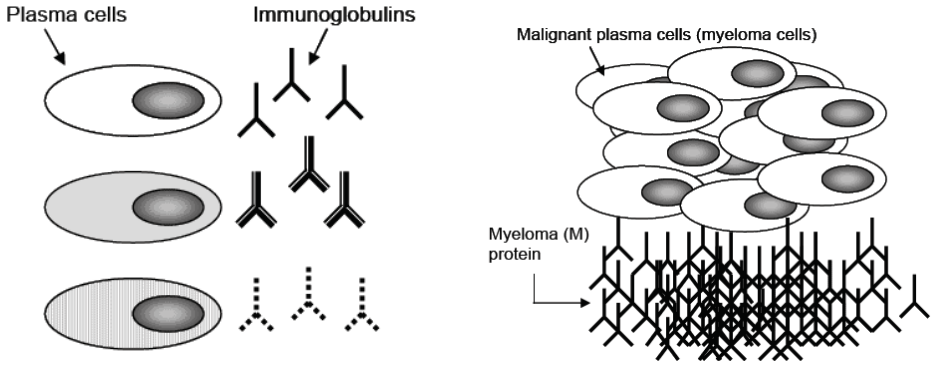

Figure 1.1 Normal plasma cells (left) and myeloma cells (right).

The most common clinical features of MM depend on the progressive accumulation of MM cells within the BM and subsequently the interactions between myeloma cells and the BM microenvironment, by means of cell–cell contact, adhesion molecules, and cytokines. This leads to disruption of the normal bone marrow function (reflected by anaemia), bone marrow failure, bone destruction (diffuse osteoporosis), and damage to the surrounding bone (lytic bone lesions) (Durie 2001). In most patients, multiple discrete lytic lesions can be found at the sites where nests of myeloma cells occur. These so called “punch out lesions” can be visualized by radiography (Fig. 1.2).

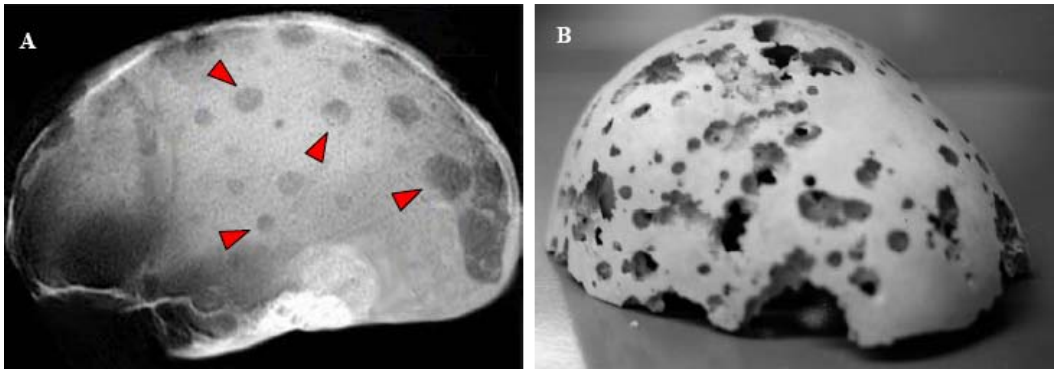

Figure 1.2 Typical bone lesions induced by MM. A) The skull X–ray shows "punched out lesions" (arrowheads) in the skull, which are characteristic of MM. B) Gross examination of the skull reveals severe bone destruction induced by MM.

Patients with myeloma might be diagnosed by chance through screening for other reasons, although they generally displayed common symptoms such as infections, bone lesions, or renal failure, and have one or more M protein or light chain in serum or urine, bone lesions, and BM infiltration with malignant plasma cells. Laboratory investigations that lead to the diagnosis of myeloma are listed in table 1.1 (Sirohi & Powles 2004).

Myeloma cells can proliferate as solitary plasmacytoma or pre–malignant tumor called monoclonal gamopathy of undetermined significance (MGUS). This is the most frequent clonal plasma–cell disorder in the general population which is present in 1% of adults over the age of 25 and progresses to malignant MM in 25–30% of patients (Greipp & Kyle 1982). Both MGUS and MM secrete the same monoclonal Ig, but MM is distinguished from MGUS by having a greater intramedullary tumor–cell content (>10%), the development of osteolytic bone lesions and/or an increasing tumor mass. Smouldering myeloma is a term for disorders half way along the spectrum between MGUS and florid myeloma. It has a stable intramedullary tumor–cell content of >10% but none of the other complications of MM necessarily occur in all of the cases (Riccardi *et al.* 1991).

Table 1.1 Investigations to aid diagnosis of MM.

site and test	what to look for
blood	
• serum immunoelectropheresis and immunofixation	M protein: 53% IgG, 20% IgA and rarely IgM
• immunoglobulin profile	immunoparesis
• β2 microglobulin	high (>2.5 mg/l)
• serum free–light–chain assay	altered ratio
• haematology	low platelet and haemoglobin concentrations, high ESR, plasma cells in peripheral blood
• biochemistry	high creatinine, urea, uric acid, LDH, C–reactive protein, and calcium
urine	
• immunoelectropheresis and immunofixation	Bence–Jones (20% light chain disease)
bone marrow	
• aspirate	plasma cells, morphology, cytogenetics, FISH
• trephine	cellularity, amyloid, MVD (angiogenesis)
bones	
• skeletal survey	lytic lesions, fractures
• DEXA scan	osteoporosis, bone healing
• CT/MRI/PET	if needed for plasmacytomas
whole body	
• serum amyloid protein (SAP)	amyloid load scan

ESR=erythrocyte sedimentation rate. LDH=lactate dehydrogenase.
FISH=fluorescence in–situ hybridisation. MVD=microvascular density.
DEXA: Dual energy X–ray absorptiometry.

1.1.2 Treatment of MM

To date MM remains incurable. However, treatment improves the clinical situation in about 75% of patients and eases the symptoms and significantly improves quality of life. Currently, standard treatments include high–dose chemotherapy and radiotherapy. After treatment, haematopoietic stem cell transplantation (HSCT) may be necessary. Autologous HSCT (Harousseau 2005) uses the patient's own stem cells, whereas allogeneic/syngeneic HSCT

(Crawley *et al.* 2005) employs MHC identical or twin donor bone marrow. If high–dose chemotherapy with HSCT is not an option, conventional chemotherapy, single agent treatment (e.g., dexamethasone) or new treatments (thalidomide, bortezomib) are applied possibly in combination with other drugs.

"Targeted therapies", which include targeted radiotherapy and directed immunotherapy, can greatly reduce toxicity of chemotherapy and radiotherapy and improve the efficacy of treatment (Kuriakose 2005). For example, the original mode of therapeutic delivery – in a beam via an external source – requires knowing the anatomic location of the tumor. Metastases can occur at multiple (and often unknown) sites. And even when the location of a tumor is known, innocent tissues in the line of fire can suffer collateral damage. In contrast to conventional radiotherapy, an outside–in approach–targeted radiotherapy–systemic administration of radioactive agents that home in on a particular tissue, antigen, or receptor type proceeds from the inside out (Goldman 2004). Two radio–labelled monoclonal antibodies (mAbs) to the CD20 antigen are both now approved and in clinical use for non–Hodgkin lymphoma (Garber 2003). Several other radio–labelled antibodies were shown to be successful candidates in early phase clinical trials as well as in preclinical studies. To be effective by themselves, therapeutic agents have to be potent and penetrating, and they need to kill only those cells that express large amounts of the target molecules. As a component of targeted radiotherapy, the antibody is merely a delivery vehicle. The attached radioisotopes do the killing, and their emissions penetrate tumors reaching diseased cells that may or may not express the target antigen. But antibodies are large; whereas, smaller molecules travel faster, penetrate tumor tissue better and are excreted much more swiftly when released into circulation. Research efforts are now shifting to these smaller molecules to improve the effects of radioisotopes. Some of these newer radiopharmaceuticals often conjugated with newly tamed radioisotopes are doing a better job than their older counterparts of targeting cancer cells and providing pain relief, and some are even showing promise as therapeutic agents alone or in combination with other chemotherapeutic agents (Kuriakose 2005).

1.1.3 Idiotype–Specific Immunotherapy in MM Therapy

Immunotherapy is an experimental treatment strategy for MM. Strategies to harness the powerful immune system are mainly at the pre–clinical stage of development for MM, but they are moving towards clinical testing. There is wide variety in the techniques used and the outcomes achieved so far (Chatterjee *et al.* 2006).

Each antibody has a unique antigen–binding site which is formed by hypervariable stretches within the variable part of the immunoglobulin polypeptide chains, the so–called “complementary–determining regions” (CDR) I–III. The CDR III region is created during the antigen receptor gene rearrangement process, in which extensive codon deletions and insertions occur almost at random at the junctions between the rearranging variable (V), joining (J), and diversity (D) segments. During a germinal center reaction, the Ig genes encoding an antigen–binding antibody are further modified by somatic hypermutation. The enormous diversity of Igs resulting from these genetic events implies that an individual antibody molecule should comprise unique epitopes that may be recognized specifically by the immune system and may hence serve as specific targets of a cellular immune response. Collectively, the unique immunological properties of an individual Ig are referred to as “idiotype” (Id).

The Id is a marker unique to a single clone of B cell and hence a fingerprint of an individual clone. It could therefore be exploited to monitor expansion of normal or malignant B cells and to target clonally expanded tumorous B cells specifically. Exploiting myeloma Id as a tumor–associated antigen was proposed over 30 years ago (Lynch *et al.* 2001). The Id also has certain practical advantages as a tumor–specific antigen. Firstly, anti–Id antibodies and protein–based Id vaccines can readily be prepared, because monoclonal Ig can easily be purified from patient serum or transfected cells. Secondly, Id vaccines can be constructed for each patient without too much effort, because the assembled V(D)J gene segment of Ig heavy and light chains may be relatively easily amplified and sequenced from bone marrow samples, tailor–made DNA–based Id vaccines can be constructed for each patient without too much effort (Bogen *et al.* 2006).

1.1.3.1 Anti–Id Antibodies in MM Therapy

Monoclonal antibodies (mAbs) are a new generation of biopharmaceuticals. Currently, approximately 18 mAbs products are already used in disease therapy, and more than 100 mAbs are being tested in clinical trials (Holliger *&* Hudson 2005). MAbs have direct effects on tumor cells, such as blocking of growth and induction of apoptosis, but also indirect effects, which are mediated via the immune system, e.g. complement dependent cytotoxicity (CDC), or antibody dependent cellular cytotoxicity (ADCC). The use of mAbs in cancer therapy has recently been reviewed by Adams and Weiner (Adams *&* Weiner 2001).

In therapy of lymphoma and leukaemia, the use of mAbs directed against specific surface antigens such as CD20 (Rituximab), CD52 (Campath–1H), and CD33 (Myelotarg) has become standard practice. Unfortunately, there is only limited use for these mAbs in MM, since for example CD20 is expressed on less than 20% of MM cells freshly isolated from patients (Treon *et al.* 2001; Lim *et al.* 2004). MM cells lack the presence of suitable surface antigens to develop mAbs with satisfactory specificity and sensitivity for targeting the tumor cells. Antibodies against potential targets such as CD38 (Stevenson *et al.* 1991), CD40 (Tai *et al.* 2005), CD54 (Maloney *et al.* 1999), NY–ESO–1 (Dhodapkar *et al.* 2002), and VEGF (Yang *et al.* 2003) are under current investigation.

Since Id immunoglobulins secreted by myeloma cells may serve as a unique tumor–specific antigen, significant interest has emerged in anti–Id antibodies in MM therapy. Willems and colleagues (1998) used the phage display method and successfully obtained single chain Fv antibodies specifically directed against the Id expressed by myeloma tumor cells. These antibodies showed very promising abilities in myeloma cell detection. Hajifhasemi and colleagues (2006) generated five murine anti–Id mAbs against two human M proteins (IgGs) with hybridoma techniques. Moshitzky *et al*. (2008) confirmed that anti–Id antibodies were effective in retardation of tumor growth *in vivo* .

However, generally the identification and production of mAbs or single chain antibody fragments are laborious and could become very expensive in

search for rare antibodies that require screening of a large number of colonies. Moreover, mouse–derived mAbs are immunogenic and they must be chimerized for clinical applications. These complications surely prevent wide and effective usage of anti–Id treatment in MM patients. Another big obstacle for anti–Id application *in vivo* might be the abundant circulating Id. Experiments in mice have shown that Id–specific antibodies do not play a major role in tumor eradication, the reason being that the large quantities of soluble M protein secreted by myeloma cells block Id–specific antibodies before they can reach the surface of myeloma cells. New strategies need to be developed to eliminate or reduce the level of circulating Id to enhance the therapeutic efficiency.

1.1.3.2 Id–Specific Vaccine in MM Therapy

Cancer vaccines are aimed at inducing tumor–specific immunity by immunizing patients with tumor cells or their antigenic components, known as tumor–associated antigens (TAA). Id can be regarded as a TAA and a potential target in clinical vaccination approaches. It was shown that T–cells and antibodies specific for Id are present in the peripheral blood of MM patients and the presence of expanded T–cell clones is associated with prolonged survival of the patients.

A number of different strategies have been employed for Id–vaccination of MM patients. In some studies, untreated patients with early stage MM were immunized with autologous precipitated myeloma protein, either with (Osterborg *et al.* 1998) or without (Bergenbrant *et al.* 1996) granulocyte–marcrophage colony–stimulating factor (GM–CSF). In other studies, Id vaccination was performed with conjugates of Id–keyhole–limpet hemocyanin (Id–KLH) in association with GM–CSF or interleukin–2 (Bergenbrant *et al.* 1996), or with Id–pulsed dendritic cells (Titzer *et al.* 2000; Yi *et al.* 2002). Some studies were performed after high–dose chemotherapy and stem cell transplantation. Id–specific T–and B–cell responses were detected with variable frequency, but clinical responses were unsatisfactory and not correlated with the induction of tumor–specific immune response. So it is still

too early to conclude that Id–vaccination and elicitation of Id–specific immune responses might improve the prognosis of MM patients (Coscia *et al.* 2004; Rasmussen *et al.* 2003).

1.2 In Vitro Selection of Aptamers

1.2.1 Theory and History

For a long time, nucleic acids were considered mainly as linear carriers of information, whereas most cell functions were carried out by protein molecules which possess complex three–dimensional structures. With the discovery of the catalytic activity of RNAs (Guerrier–Takada *&* Altman 1984; Zaug & Cech 1986), nucleic acids were found to possess both a genotype and a phenotype for the first time. This major discovery was the foundation for the *RNA World* theory (Gilbert *et al.* 1986), which supports the concept that during prebiotic evolution, RNA molecules catalyzed all biological reactions. Because of their ability to catalyze chemical reactions similarly to enzymes, such RNAs are called ribozymes (Pyle 1993).

In 1990, two other ground breaking studies demonstrated that large libraries of RNAs could be screened *in vitro* for RNA ligands that bind T4 DNA polymerase (Tuerk & Gold 1990), and a variety of organic dyes (Ellington & Szostak 1990), respectively. This selection process was termed SELEX (Systematic Evolution of Ligands by EXponential enrichment) by Tuerk and Gold (1990), and RNA ligands were named aptamers by Ellington and Szostak (1990). The term aptamer is derived from the Latin word “aptus”– which means fitting and the Greak word “meros” – which means particle (Ellington & Szostak 1990). Aptamers are short single–stranded DNA (ssDNA) or RNA with a specific and complex three–dimensional shape characterized by stems, loops, bulges, hairpins, pseudoknots, triplexes, and/or quadruplexes. Based on their three–dimensional structures, aptamers can bind to a wide variety of targets. Binding of the aptamer to the target molecule results from structure compatibility: stacking of aromatic rings, electrostatic

and van der Waals interactions, hydrogen bindings, or from a combination of these effects (Hermann & Patel 2000).

The SELEX process starts by generating a large library of randomized nucleotide sequences folding into different structures depending on their particular sequence. The library is then incubated with the target of interest, and those sequences present in the library that bind to the target are separated from those that do not. The retained ligands are then amplified to generate a pool of sequences that have been enriched for those that bind the target of interest. This selection and amplification process is repeated (usually 8–12 rounds) until the ligands with the highest affinity for the target protein are isolated. The winning aptamers are then cloned and sequenced (Fig. 1.3).

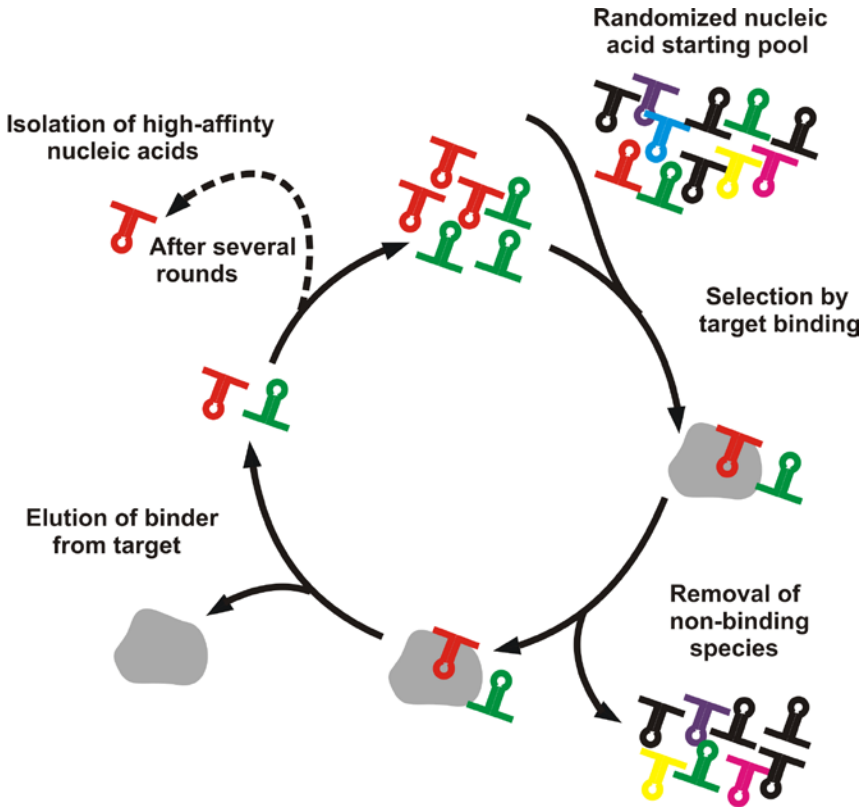

Figure 1.3 General scheme of the SELEX procedure. (I) A pool of 3–D folded, random nucleic acids is incubated with the target. (II) Nonbinding sequences are partitioned away. (III) Binding sequences are eluted from the target and (IV) reamplified to yield an enriched pool with respect to binding to the corresponding target. After several rounds, aptamers can be selected with high affinity and specificity.

1.2.2 Technology

1.2.2.1 Random DNA Oligonucleotide Library

The starting point of a SELEX process is a chemically synthesized random DNA oligonucleotide library. This library consists of a multitude of ssDNA fragments (~10^{15} molecules) comprising a central random region of 20–80 nt flanked by different specific sequences of 18 to 21 nt, which function as primer binding sites in the PCR. Important aspects for designing the oligonucleotide library include the size of the randomized region, the type of randomization and chemical modifications of the nucleotides.

The size (n) of random domain determines the complexity of the library, which can be calculated easily as 4^n. For example, the complexity of a library with thirty–five fully randomized nucleotides is 4^{35} or 10^{21}. Use of enough randomized nucleotides is critical to get a high affinity ligand and probably a stable structure. In the SELEX experiments published so far the successful aptamers selected represented 1 in 10^9 to 10^{13} of the molecules in the starting library (Gold 1995). In practice, the libraries containing 10^{14} to 10^{15} different species with the random domain from 20 to 80 nt are commonly used for *in vitro* selection. The arrangement and type of randomization are also variable. Total randomization of a block of contiguous nucleotides, partial randomization of a block (Davis & Szostak 2002; Nutiu & Li. 2005), short blocks interspersed with fixed sequences, or linkage of blocks of random sequences to create a very large random region (>200 positions) are all viable strategies for SELEX. Chemically modified oligonucleotide libraries were used in some SELEX experiments with the goal to increase the complexity of a library, to introduce new features like functional groups providing new possibilities for the interaction with target molecules, to enhance the stability of oligonucleotide conformations, or to increase the resistance to nucleases, which is important for many applications (Kopylov & Spiridonova 2000; Kusser 2000). Typical modifications concern the 2'–position of the sugar in RNA libraries. The ribose 2'–OH group of pyrimidine nucleotides is replaced with a 2'–NH_2 or F group, which protects the RNA from degradation by nucleases (Kopylov & Spiridonova 2000; Kusser 2000). A series of C–5–modified dUTPs bearing amino acids were used to prepare a variety of modified DNAs. The

authors mentioned that such modified oligonucleotides with new functionalities are applicable to *in vitro* selection experiments particularly to select DNA aptamers for anionic target molecules (Kuwahara *et al.* 2006). Modifications of the phosphate backbone of nucleic acids were also applied. For example, replacement of the non–binding oxygen in the phosphodiester linkage by sulfur can increase the resistance of phosphoRothe, Germanyioate oligonucleotides against nuclease digestion (Andreola *et al.* 2000).

Another technique investigated to overcome aptamer instability is the creation of spiegelmers – a very elegant solution to the problem. The idea is that aptamers composed of natural D–oligonucleotides can be selected against mirror image targets, such as D–amino acid peptides, rather than natural L–amino acid peptides. Once the aptamers are isolated, they can be chemically synthesized as L–oligonucleotide, called Spiegelmer, and will bind to the natural L–amino acid peptide targets (Klussmann *et al.* 1996; Nolte *et al.* 1996). Because Spiegelmers are composed of unnatural monomers, they are insensitive to nuclease degradation and have shown to stable over 60 h in biological fluid (Klussmann *et al.* 1996; Eulberg *&* Klussmann 2003).

Principally, aptamers can be developed for any target molecule. Several reviews summarized the various target molecules according to certain aspects (Famulok 1999; Stoltenburg *et al.* 2007). Aptamers can be developed for molecules connected with nucleic acids and for nucleic acid binding proteins like enzymes or regulatory proteins, but also for molecules by nature not associated with nucleic acids like growth factors (Green *et al.* 1996) or organic dyes (Ellington & Szostak 1990). Besides organic molecules, divalent metal ions also served as targets in SELEX experiments. The selection of RNA aptamers with affinities for Zn^{2+} (Ciesiolka *et al.* 1995) and Ni^{2+} (Hofmann *et al.* 1997) were described, respectively. Even nucleic acid structures could be used to select aptamers for different purposes (Duconge & Toulme 1997; Toulme *et al.* 2003). In addition to single molecule targets, SELEX technology can also be applied to complex target mixtures, whole cells, tissues, and organisms.

1.2.2.2 Selection Process

A typical SELEX round involves three processes, namely, selection of ligand sequences that bind to a target; partitioning of aptamers from non–aptamers via affinity methods; and amplification of bound aptamers. During the selection process, the nucleotide pool is incubated with the target molecule of interest under appropriate buffer and at a temperature that depends on the requirements. After binding, partitioning of the aptamer–target complex from nonspecific molecules can be achieved by various techniques. The most commonly used method for protein targets is nitrocellulose filters (Bianchini *et al.* 2001). Alternatively, the immobilization of a target molecule on a particular matrix, such as sepharose (Ciesiolka *et al.* 1995) or agarose (Tombelli *et al.* 2005) or magnetic beads (Stoltenburg *et al.* 2005) is also a conventional method for the separation step. During recent years, more effective separation methods are reported, e.g. Capillary Electrophoresis (CE), Flow Cytometry (FC) (Davis *et al.* 1997) and Electrophoretic Mobility Shift Assay (EMSA) (Tsai & Reed 1998), Surface Plasmon Resonance (SPR) (Misono & Kumar 2005) or centrifugation (Rhie *et al.* 2003). For review see Gopinath (2007).

High background during the partitioning step increases the number of rounds and, in the worst situation, leads to the isolation of sequences that partition without facilitation by the target molecule. For example, nitrocellulose filter–specific ligands or agarose–specific ligands are often found, especially if they are more abundant in the library than the oligonucleotides that bind tightly to the intended target. Therefore, counter–selection against the partitioning matrix or alternate partitioning protocols can be very important (Gold *et al.* 1995).

The bound sequences are then eluted and amplified to generate a new pool for the next round of selection. This selection and amplification process is repeated (usually 8 to 12 rounds) until the ligands with the highest affinity for the targets are isolated. The winning aptamers are then cloned and sequenced.

1.2.2.3 RNA SELEX and DNA SELEX

The basic process of *in vitro* selection can be applied for both RNA SELEX and DNA SELEX. For the selection of RNA aptamers, the random DNA oligonucleotide library has to be transformed into a RNA library before starting the first round of a RNA SELEX process. A special sense primer with an extension at the 5'–end containing the T7 promoter sequence and an antisense primer are necessary to convert the ssDNA library into a double–stranded (dsDNA) library by PCR. The dsDNA is then *in vitro* transcribed by the T7 RNA polymerase resulting in a randomized RNA library, which is used to start an RNA SELEX. During this SELEX process the selected RNA of each round has to be reverse transcribed and subsequently amplified by RT–PCR using the same primer as described above. The new RNA pool for the next SELEX round is then generated again by *in vitro* transcription (Fig. 1.4).

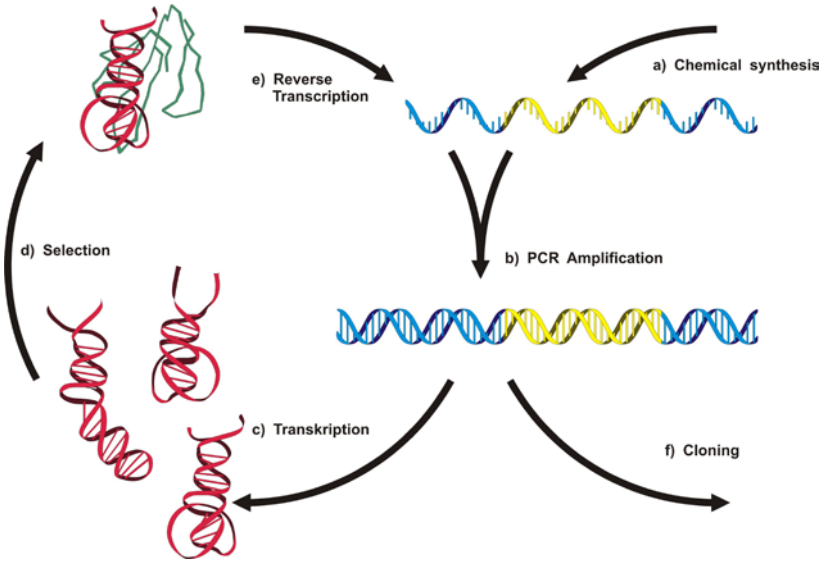

Figure 1.4 Scheme of RNA SELEX. The selected RNA is reamplified by RT–PCR and then transcribed into RNA to yield an enriched RNA pool.

Yet, the procedure for DNA SELEX (Fig. 1.5) is simpler since it involves only the PCR amplification as enzymatic step. For the selection of DNA aptamers, the library can be used directly in the first round of the SELEX process. Sense and antisense primer derived from the specific sequences at

the 5'– and 3'–end enable the amplification of the selected oligonucleotides in each SELEX round.

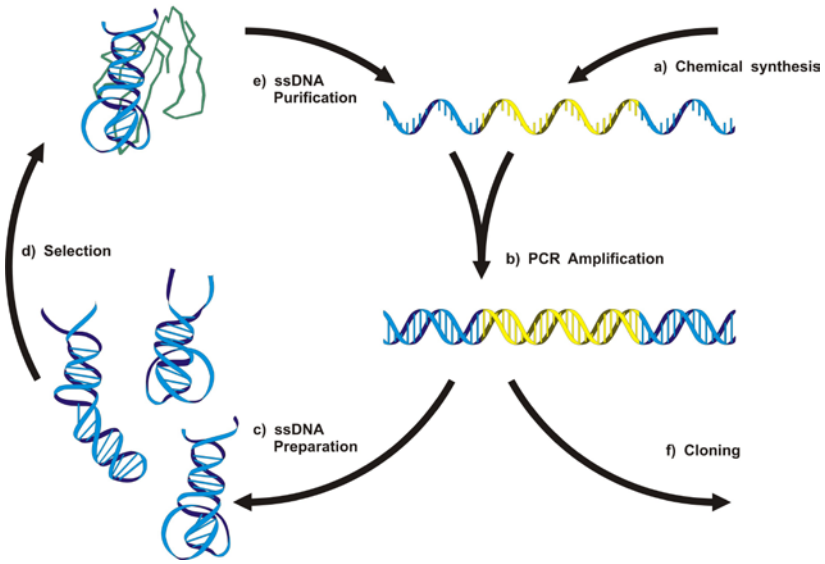

Figure 1.5 Scheme of the DNA SELEX. The selected DNA is amplified with PCR and ssDNA is prepared for the next round of selection.

After PCR amplification, ssDNA preparation must be performed to generate a ssDNA pool for the next round. There are several commonly used methods for ssDNA preparation:

(1) A biotin residue is introduced into one of the primers used for amplification, and DNA strands are separated under denaturing conditions on a column with streptavidin (Murphy *et al.* 2003);

(2) Asymmetric PCR amplification is used in which replication initiated by one PCR primer is relatively inefficient, leading to the accumulation of ssDNA synthesized from the other primer (Ellington & Szostak 1992);

(3) A hexaethyleneglycol (HEGL) spacer and an extension of several adenine nucleotides (polyA) are added at the 5'–end of the reverse primer. The HEGL–spacer acts as a terminator for Taq polymerase. The elongation of the (+) strand stops, while the (–) strand grows further. The two strands can be separated by size using electrophoresis under denaturing conditions ((Williams & Bartel 1995);

(4) A phosphate group is introduced into the 5'–end of one primer and the dsDNA obtained by amplification is treated with the phage lambda exonuclease that cleaves the phosphorylated strand of DNA (Fitter *&* James 2005).

Until now, a number of both DNA aptamers and RNA aptamers have been selected against various targets. Analysis shows that there is no difference between RNA and DNA aptamers in terms of affinity and specificity (Gold 1995a). Compared with RNA aptamers, DNA aptamers have certain advantages. The selection process for DNA aptamer is simpler and faster. Moreover, DNA aptamers have greater stability than RNA aptamers, which make them more suitable for potential clinical use. Therefore, DNA aptamers have become more and more widespread during recent years (Breaker 1997).

1.2.3 Improvements in Selection Technologies

Whereas the basic SELEX technology has been proven robust for the identification of high affinity aptamers against a variety of important targets, continued improvements are needed to generate aptamers more efficiently and with even higher affinities. In particular, automated SELEX offered a fast and parallel development of multiple aptamers, using CE it is possible to select aptamers with extremely well–defined affinity profiles, whereas cell surface selection of aptamers enable the identification of aptamers even in the absence of known biomarkers.

Automation of the selection procedure means the integration and automation of different molecular biology methods (for binding, partitioning, elution, amplification, conditioning) and is thus a very complex automation challenge. Cox and colleagues used a system based on an augmented Beckmann Biomek 2000 Pipetting robot which was adapted to the selection of aptamers for a protein by some modification and generated aptamers to hen egg white lysozyme (Cox *&* Ellington 2001) and some other proteins (Cox *et al.* 2002a). The authors declared that this robotic work station can carry out eight selections in parallel and will complete 12 rounds of selection in two days. Aptamers against 120 targets should be produced in one month, which is

about 10 to 100 times faster than manual selection (Breaker 1997). A further extension of the automatic work station consists in the generation of protein targets directly transcribed and translated from the respective gene *in vitro* on the robotic work station (Cox *et al.* 2002b). This would further accelerate aptamer selection for proteins and increase the utility of aptamers as reagents in proteome analysis. Eulberg and colleagues (2005) have developed an automated SELEX procedure with high flexibility and versatility in terms of choice of buffers and reagents as well as stringency of selection conditions. This selection robot is based on a RoboAmp 4200 E instrument (MWG Biotech, Ebersberg, Germany) with further modifications for ultrafiltration, fluorescence detection, and semi–quantitative PCR. It can perform two selection rounds per day with increased chance of success.

Another form of automated SELEX is an automated microfluidic, microline–based assembly that uses LabView–controlled actuatable valves and a PCR machine (Hybarger *et al.* 2006). The system is organized in a modular fashion, which enables the modification and evaluation of individual processes. The microfluidic platform for automated SELEX experiments should lead to the development of standardized protocols, making automated aptamer selection easier accessible to many investigators. The possibility of high–throughput SELEX would enable producing a multitude of aptamers in a short time, which can be used as ligands for proteomics and metabolomics.

CE has been used for the precise and sensitive separation of different species and complexes for years. Recently, it is applied in SELEX (CE–SELEX) (Mendonsa & Bowser 2004a and 2004b; Drabovich *et al.* 2005; Berezovski *et al.* 2005). A big advantage of CE over traditional selection methods is that the partition efficiency is much higher than filtration or affinity chromatography and, thus, only a few rounds of selection are required to obtain high–affinity aptamers. Krylov's laboratory (Berezovski *et al.* 2005) selected a DNA aptamer against the protein farnesyltransferase with a dissociation constant (K_d) of 0.5 nM in just one round of selection on the CE. Moreover, aptamers with even higher affinity can be obtained by CE–SELEX. DNA aptamer against HIV–1 RT isolated by CE–SELEX (Mosing *et al.* 2005) had a K_d of 340 pM, better than previously selected ssDNA aptamers (Schneider *et al.* 1995).

Aptamers can be selected not only against purified targets or antigens, but also against heterogeneous mixtures of targets, such as whole cells. Such SELEX is so called “complex target SELEX” (Morris *et al.* 1998). It enables isolation of potent and selective aptamers directed against a variety of cell–surface proteins, including receptors and markers of cellular differentiation, as well as determinants of disease in pathogenic organisms. It also enables aptamers to be generated even when biomarkers are not known in advance. So “complex target SELEX” can facilitate the identification of new biomarkers, which have wide therapeutic and diagnostic utility (Shamah *et al.* 2008). In one of the most intriguing examples to date, Homann and Göringer (1999) were able to select aptamers against whole trypanosomes, and the target was dertermined to localize to the flagellar pocket by photocrosslinking experiments.

1.2.4 Aptamers in Clinical Applications

1.2.4.1 Overview

Antibodies are the most popular and widely used class of molecules providing molecular recognition, which plays an essential role in basic research as well as in clinical practice. They have made substantial contributions to the advancement of diagnostic assays, and novel mAb has become indispensable in most diagnostic tests that are used routinely in clinics today. However, there are certain limitations associated with antibodies. Several properties of aptamers make them more attractive diagnostic and therapeutic agents that rival, and in some cases even surpass antibodies (Table 1.2).

Aptamers act in the same way as antibodies by folding into three–dimensional structures based on their nucleotide sequences to bind to their targets. Aptamers bind to their targets with the same high affinity as antibodies with K_ds in the low picomolar to low nanomolar range. The binding specificity of aptamers is also very high, with the ability to discriminate between related proteins that share common sets of structural domains. Moreover, aptamers display low to no immunogenicity when administered in

preclinical doses 1000–fold greater than doses used in animal and human therapeutic applications (Eyetech Study Group. 2002 and 2003). Reporter molecules such as fluorescein and biotin can be attached to aptames at precise locations identified by the user. Functional groups that allow subsequent derivation of aptamers with other molecules can also be attached during the chemical synthesis of aptamers. Truncated aptamers are 25 to 40 nt long and weigh 8 to 14 kDa (Fig. 1.4). This small size enables them to travel in circulation faster, penetrate tissues better and distribute in organs more efficiently.

Table 1.2 Properties of aptamers versus antibodies

	aptamers	**antibodies**
binding affinity	in low nanomolar to picomolar range	in low nanomolar to picomolar range
selection procedure	chemical process carried out *in vitro* and therefore can target any protein	requires a biological system and therefore difficult to raise antibodies to toxins or non–immunogenic targets
working conditions	can select for ligands under a variety of conditions for *in vitro* diagnostics	limited to physiologic conditions for optimizing antibodies for diagnostics
time and expense	fast and cheap	laborious and very expensive
activity	uniform, regardless of batch synthesis	vary from batch to batch
size	small, MW: 8–12 kDa	large, MW: 150 kDa
kinetic parameters	can be changed on demand	difficult to modify
target site	can be determined by investigator	immune system determines target site
modification	wide variety of chemical modify–cations to molecule for diverse functions	limited
temperature stability	return to original conformation after temperature insult	sensitive to temperature and undergo irreversible denaturation
shelf–life	unlimited	limited
immunogenicity	none	significant

The small size of aptamer also results in renal clearance in minutes. In order to reduce drug clearance, aptamers can be modified by site specific addition of polyethylene glycol (PEG) and other moieties or attachment to a liposome surface (Willis *et al.* 1998; Tucker *et al.* 1999). Insufficient stability is often cited as the major potential drawback of nucleic acids as therapeutic agents. This can easily be overcome by using libraries with amino– or fluoro–modification at the 2' position of pyrimidines (Jellinek *et al.* 1995) as well as postselection substitutions of O'–methyl for OH residues at the 2' position of purines in a given aptamer (Beigelman *et al.* 2006).

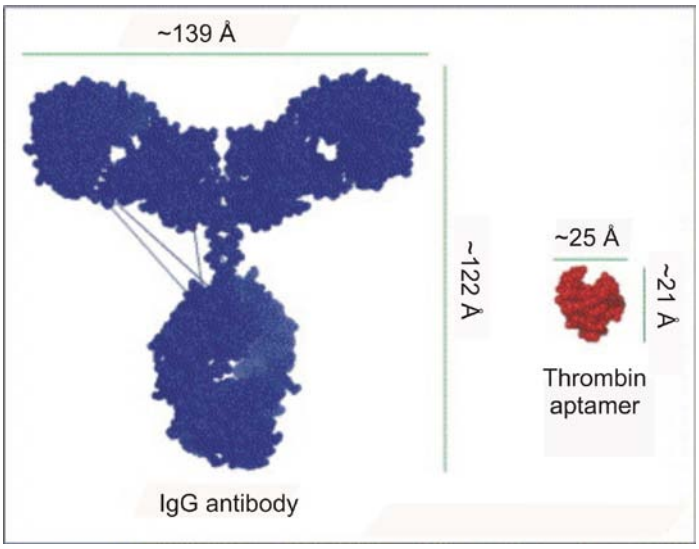

Figure 1.4 Antibody–aptamer size comparison. An estimated comparison of the size difference between an antibody (human IgG) and a selected aptamer (anti–thrombin DNA aptamer) is shown with space–filling models of both. The anti–thrombin aptamer is only 17 residues in length (Lee *et al.* 1992).

Conclusively, aptamers can be thought of as "chemical antibodies" in that they offer the advantages of antibodies – high specificity and affinity – in a relatively small, chemically synthesized molecule without immunogenicity. Because of their unique properties and proven clinical efficacy, aptamers hold extraordinary potential in the diagnosis and therapy of diseases. One aptamer–based drug was approved by the U.S. Food and Drug Administration (FDA) in treatment for age–related macular degeneration (AMD). Numerous

aptamers are in pre–clinical development, and a few of them will begin clinical evaluation soon.

1.2.4.2 Aptamers in Diagnostics

Aptamers have proven to be appropriate tools in many assay forms such as two–site binding assay, flow cytometry or *in vivo* imaging. Two–site binding assay, also referred to as sandwich assay, is one of the most commonly used diagnostic formats today. In this assay, a capture antibody is used, usually immobilized on a solid surface, to bind the analyte. A second antibody, whether monoclonal or polyclonal aimed at a different epitope, is then used to detect the bound protein, the second antibody is usually detected by fluorescence or a colorimetric assay. Aptamers can be used in two–site binding assays to take the place of antibodies. In one example, a RNA aptamer selected against vesicular endothelial growth factor (VEGF) with high affinity and specificity was used as the detector ligand in the sandwich assay format (Drolet *et al.* 1996). The aptamer was labelled with fluorescein at the 5'–end and detected by anti–fluorescein Fab fragment conjugated to alkaline phosphatase. Aptamers can function as the capturing reagent as well as the detector reagent in a two–site binding assay. Ikebukuro and colleagues (2005) developed a novel electrochemical sensor system based on two different aptamers recognizing different epitopes of thrombin for the detection of thrombin. One of the aptamers was thiol–modified and immobilized on a gold electrode for capturing thrombin, while the other aptamer, which was labelled with a pyrroloquinoline quinone glucose dehydrogenase, indicated complex formation. The big market of immunological diagnostics in the medical area will create an increasing competition between antibody– and aptamer–based kits. Some working groups are already starting to transfer antibody based diagnostic platforms to aptamers. In all probability, aptamers will be applied in standardized diagnostic test kits in the near future.

Biosensor is a very powerful tool in research as well as in clinical area. Kleinjung and colleagues (1998) were the first to develop an aptamer–based biosensor. Liss and colleagues (2002) used an IgE–binding aptamers in

quartz crystal biosensor to detect native IgE in solution. The aptamers were immobilized on a gold surface in a dense and oriented manner. They showed that sensor layers based on aptamer receptors could be regenerated more effectively and more often, and these layers were more stable compared to the antibody system. In microscopy studies, aptamers have also been shown to function as histological markers. For example, Blank and colleagues (2001) used a fluorescein isothiocyanate (FITC)–conjugated aptamer as a novel tumor marker to selectively visualize the paths and the branching of neoangoigenetic, pathologic microvasculature in tissue sections of rat brain glioblastoma. In the field of cytomics, where the target is often complexed in its natural surrounding, the small aptamers have shown their superiority compared to antibodies, which often fail in target binding due to sterical hindrance. Lorger and colleagues (2003) selected aptamers against a variant surface glycoprotein (VSG) of the *Trypanosoma brucei* parasite, which causes sleeping sickness in humans. As demonstrated by fluorescence microscopy, the VSG structures could be visualized by incubating trypanosomes with biotinylated aptamers followed by staining with fluorophore–conjugated streptavidin. In another example, a competitive fluorescent dye–linked aptamer assay (FLAA) was designed to detect daunomycin (Wochner *et al.* 2008), in which the preincubated nucleic acid–antibiotic mixtures were added to the daunomycin–coated microtiter plates, and the binding was monitored by fluorescence of OliGreen.

Another very promising field for aptamer in diagnostic application is *in vivo* imaging. For successful *in vivo* imaging, the targeting agents should not reside long in the blood or in the organs of metabolism. The small size and polyanionic nature of aptamers may lead to rapid blood clearance and tissue uptake. At the same time it may minimize the residue in liver and kidney, providing some potentially useful features for imaging and radiotherapy (Cerchia *et al.* 2002; Guhlke *et al.* 2003). An initial experiment to address aptamer suitability for *in vivo* imaging was reported by Charlton *et al.* (1997a and 1997b), and the selected aptamers against neutrophil elastase were successfully used for diagnostic imaging of inflammation in rats. Compared with IgG, which is used clinically in diagnostic imaging of inflammatory diseases, the aptamer achieved a significantly higher target–to–background

ratio in less time. This ratio was achieved primarily by the rapid clearance of the aptamer from the peripheral circulation. Studies designed to elucidate oligonucleotide biodistribution properties have also been reported (Tavitian *et al.* 1998; Zhang *et al.* 2000). Hicke and colleagues (2006) utilized an aptamer with high affinity for a protein, tenascin–C, that is overexpressed in tumor tissues to target tumor and perform *in vivo* imaging. The radio–labelled aptamer was taken up by a variety of solid tumors including breast, glioblastoma, lung, and colon. Rapid uptake by tumors and rapid clearance from the blood and other nontarget tissues enabled clear tumor imaging.

Some interesting approaches such as the possibility of developing a diagnostic system incorporating Photo–SELEX evolved aptamers (Petach & Gold 2002) capable of simultaneous quantification of a large number of analyte molecules, have been presented (Bock *et al.* 2004). The aptamers selected are so called photoaptamer – which are RNA or DNA aptamers bearing a 5'–iodo or 5'–bromo–substituted uridine 5'–triphosphate (UTP) or 2'–deoxy uridine 5'–triphosphate (dUTP) – allows cross–linking of the immobilized aptamer to a targeted protein using UV photoexcitation. Photoaptamers have for this reason, greater sensitivity and specificity than those aptamers selected through conventional selection methodologies. The aptamers were fixed to a chip and incubated with the sample (e.g., patient serum). After washing, the chip is irradiated with UV light, which causes covalent bond formation between aptamer and target and a universal fluorescent dye is added to conjugate specific amino acids of the covalently bonded proteins, so quantitatively detect the target molecules. The diagnostic array benefits from: (1) the small aptamer size allowing high–density aptamer coupling to the chip surface; (2) convenient and site–specific labeling with chemical cross–linkers (After UV induction of covalent bonds, the aptamer "chip" can be washed under harsh conditions to remove nonspecifically bound proteins from the array surface); and (3) the fact that the analytes (proteins/peptides) are different from the capturing reagent (nucleic acids), generic protein stains can be used to visualize positive molecular recognition of the aptamers. All these factors add up to a microarray system characterized by low detection levels, a high dynamic detection range, and an

unprecedented reduction in the number of false–positive signals (Proske *et al.* 2005).

1.2.4.3 Aptamers in Therapeutics

The concept of using aptamer as therapeutic agents is now more then 15 years old. With the FDA approval of the first aptamer drug “Macugen” (pegaptamib, by Pfizer and Eyetech) (Rakic *et al.* 2005; Ng *et al.* 2006) for the treatment of AMD at the end of 2004, aptamer technologies achieved a breakthrough in therapeutic application. So far, aptamers have been validated as therapeutics in the areas of anti–infectives, anticoagulation, anti–inflammation, antiangiogenesis, antiproliferation, and immune therapy (Nimjee *et al.* 2005). Some examples of aptamers selected for therapeutic applications are listed in table 1.3.

Macugen is a specific anti–VEGF–165 aptamer. VEGF is the main target for anti–angionenesis work and has also been implicated in the leakage of blood vessels. Anti–VEGF therapy, therefore, could have a dual effect, both inhibiting angiogenesis and blocking blood vessel leakage. Macugen has a K_d of approximately 50 pM and inbibits the binding of VEGF–165 to its receptors. Using experimental models, Macugen inhibited VEGF–mediated vascular leakage as measured by a corneal micropocket assay (Miles assay) in guinea pigs (Eyetech Study Group, 2002). Macugen has also shown anti–angiogenesis effect in a rat corneal angiogeneses model and a mouse retinopathy of prematurity model (Proske *et al.* 2005). Macugen was also effective in the inhibition of blood–retinal barrier breakdown in a diabetic rat model (Ishida *et al.* 2003). The half–time of Macugen is about 94 h when administered by intravitreal injection at a dose of 1 mg/eye in monkeys (Drolet *et al.* 2000). Preclinical toxicity studies in rhesus monkeys demonstrated no toxic effects and no immune response to Macugen (Vinores, 2003). In Phase II/III trial (Eyetech Study Group, 2003), all patients in the Macugen group had significantly less disease progression than patients in the untreated group. As the first aptamer drug, the early results are very promising.

Table 1.3 Examples of medically relevant aptamers.

target	K_d (nM)	therapeutic applications	reference
anti–viral			
Rous Sarcoma Virus (RSV)	40	Avian sarcoma	(Pan *et al.* 1995)
hepatitis C NS3	10	Viral replication	(Fukuda *et al.* 2000; Kumar *et al.* 1997)
human cytomegalo virus	351	Viral replication	(*Wang et* al. 2000)
influenza	NA	Viral replication	(Jeon *et al.* 2002)
HIV–1 reverse transcriptase	1	HIV replication	(Tuerk *et al.* 1992 Schneider *et al.* 1995)
HIV–1 integrase	10	HIV replication	(Allen *et al.* 1995)
HIV–1 Rev	<1	HIV replication	(Giver *et al.* 1993)
HIV–1 nucleocapsid	2.3	HIV replication	(Berglund *et al.* 1997))
HIV–1 Tat	0.1	HIV replication	(Tuerk *et al.* 1993; Yamamoto *et al.* 2000)
cell growth & tumor genesis			
alpha–thrombin	25	thrombosis	(Bock *et al.*1992; Kubik *et al.*1994)
activated protein C	110	thrombosis	(Gal *et al.* 1998)
protein tyrosine phosphatase	18	oncogenesis, viral regulation	(Bell *et al.* 1998)
beta–2–integrin cell adhesion	81	apoptosis	(Lebruska *et al.* 1999)
human TNF–α	n/a	regulation of immune defense	(Yan *et al.* 2004)
basic fibroblast growth factor	0.35	angiogenesis	(Jellinek *et al*. 1993)
keratinocyte growth factor	0.0003	epithelial hyperproliferative disease	(Pagratis *et al.* 1997)
platelet derived growth factor	0.1	tumor development	(Green *et al.* 1996)
VEGF	0.14	neovascularization	(Green *et al.* 1995)
tumor microvessels		glioblastoma detection	(Blank *et al.* 2001)
tenasin–C	5	tumor cell detection	(Hicke *et al*. 2001)
nuclear factor of activated T–cells	10–100	T–cell differentiation and immune response	(Cho *et al*. 2004)
wilm's tumor suppressor	700	renal cancer	(Bardeesy *et al*. 1998)
HER3	45	carcinomas	(Chen *et al*. 2003)
immune response and inflammation			
human neutrophil elastase	n/a	inflammation	(Charlton *et al*. 1997a)
neutrophil elastase	n/a	inflammatory response	(Bless *et al*. 1997)
L–selectin	3	inflammation	(O'Connell *et al*. 1996)
immunoglobin E (IgE)	10	allergies	(Wiegand *et al*. 1996)
anti–acetylcholine autoantibodies	60	myasthenia gravis	(Hwang *et al*. 2002 and 2003)
Ku protein	<2	DNA repair, autoimmune disorders, cancer	(Yoo *et al.* 1998;)

Another aptamer that blocks coagulation also appears to be a promising drug candidate. One anti–thrombin aptamer, termed ARC183, was originally selected at the company Gilead (Ginsberg *et al.* 2001). ARC183 has key advantages in that it avoids heparin use and the risk of associated thrombocytopenia, is a specific inhibitor with rapid onset, is effective at inhibiting clot–bound thrombin, and has a short *in vivo* half–life of approximately two minutes, which allows for rapid reversal of its effects and the avoidance of dose–adjusting complications of heparin and protamine. ARC183 promotes transient anticoagulation activity during coronary artery bypass graft surgery and has passed Phase I clinical trials.

Spiegelmers are also beginning to make their way to the clinic. The company NOXXON has developed Spiegelmers against ghrelin, a peptide hormone associated with increase of appetite and weight gain. So this Spiegelmer can serve as an anti–obesity drug, and the animal test has already proved the weight loss effect in mice (Shearman *et al.* 2006).

Given their small size, ease of synthesis, and low cost, aptamers have been proven to be a promising novel drug agent in therapeutic applications. Medically relevant targets have yielded aptamers with high affinities and specificities. Additionally, a number of approaches have been validated for stabilizing and delivering aptamers, and animal and preclinical experiments with aptamers are bringing alone the next drugs in the pipeline. In the future, one of challenges will be to continue to explore the use of aptamers against intracellular targets in gene therapies.

1.2.5 Aptamers against Antibodies

Antibodies are involved in the pathology of various diseases, including cancers, inflammation, and autoimmune disorders. Ligands that can recognize and target these antibodies with high affinity and specificity can be used in disease diagnosis and therapy. For example, specific anti tumor antibodies have been exploited in immunotherapeutic approaches for haematological malignancie (Terness *et al.* 1997; Würflein *et al.* 1998). Another application of targeting antibody could be the generation of immunoaffinity matrices for the

purification of antibodies (Miyakawa *et al.* 2008). Due to their special characters, aptamers have been used to target antibodies for different purposes.

An early antibody target for SELEX was serum prepared against a 13–amino acid sequence (NH2–MASMTGGQQMGRC–COOH) from the amino terminus of the bacteriophage T7 gl0 protein (Tsai *et al.* 1992). The RNA library contained only 10 randomized positions within the loop of a fixed hairpin. After three SELEX rounds, one winning sequence was found. The resultant ligand binds to the anti–g10 antibodies at the antigen recognition site, demonstrated through binding competition. Oligonucleotides can mimic a protein antigen even though that antigen is not a polyanion.

The abnormal targeting of self–antigens by autoantibodies, leading to tissue destruction and other pathologies, is the main cause of autoimmune disorders. These autoantibodies could become possible targets in the management of these conditions (Deitiker *et al.* 2000). Until now, the treatment of such diseases has relied on the non–specific suppression of the immune system, with its fate of side effects. New treatments that would target specifically the autoantibodies involved in the inappropriate autoimmune response are likely to bring significant progress in the management of this frequent pathology. Inhibitory peptides have been proposed but they can themselves induce an immune response. Because aptamers seem devoid of immunogenicity, they could represent a good alternative. RNA aptamers have been selected against anti–DNA autoantibodies involved in systemic lupus erythematosus (SLE). Aptamers display *in vitro* higher affinity to their target autoantibody than its cognate antigen dsDNA (Kim *et al.* 2003). However, aptamers are so specific that they do not recognize similar autoantibodies against other dsDNA. Using different autoantibodies as targets during SELEX has been proposed to circumvent this problem. In myasthenia gravis (MG), autoantibodies against nicotinic acetylcholine esterase receptors (AChRs) inhibit the neuromuscular activation leading to muscular weakness and fatigability. A 2'–amino–pyrimidine modified RNA aptamer against these autoantibodies can inhibit the autoimmune response in animal models of MG (Hwang *et al.* 2002 and 2003). Interestingly, two SELEX experiments were performed to obtain this aptamer. A first SELEX identified an aptamer, with

which a second SELEX was performed after addition of a random stretch of 20 nt at the 3' extremity. This second SELEX allowed the identification of an additional motif which increased by five–fold the inhibition efficiency of the first aptamer in an *in vitro* assay (Hwang *et al.* 2002). Furthermore, this aptamer conjugated with PEG at its 5' extremity, showed *in vivo* a protective effect on experimental autoimmune MG induced in rats (Hwang *et al.* 2003).

Autoantibodies secreted against insulin receptor are involved in insulin resistance (Zhang & Rothe, Germany 1991). Doudna and colleagues (1995) reported the identification of an RNA sequence that bound MA20, a murine insulin receptor antibody, which shares an α subunit epitope with the human one, with a K_d of 2 nM. The RNA can act as a decoy, blocking the antibody from binding the insulin receptor. Strikingly, the RNA cross–reacts with autoantibodies from patients with extreme insulin resistance. These results suggested that the selected RNA may structurally mimic the antigenic epitope on the insulin receptor protein. A 2'–aminopyrimidine–modified RNA selection was conducted on MA20 to isolate nuclease–resistant aptamers (Lee & Sullenger. 1996). The isolated RNA aptamer bound to MA20 with a K_d of 30 nM and exhibited superior nuclease resistance. A large fraction remained after 24 h of incubation in 10% human serum, whereas the unmodified aptamer degraded completely in 15 sec. The aptamer also inhibited MA20 binding to the insulin receptor by 95% on human lymphocytes, and it protected cells from MA20–dependent and autoantibody–dependent down regulation of the insulin receptor expression by up to 90% and 80%, respectively. Interestingly, the sequences of these 2'–amino RNAs were very different from the sequences of unmodified RNAs that we previously generated to bind to MA20 (Doudna *et al.* 1995).

Besides autoimmune antibodies, aptamers against immunoglobulin E (IgE) have been selected with implications in allergic diseases. IgE has been implicated in response to protect mammals from parasites (Gounni *et al.* 1994). Overproduction of IgE due to exposure to environmental antigens, however, can result in diseases such as allergies, atopic dermatitis, and allergic asthma (Sutton & Gould 1993). A 2'–NH_2 pyrimidine–modified RNA aptamer selection and a DNA aptamer selection were performed against human IgE and yielded aptamers that bind to human IgE with high affinities

(RNA, K_d =30 nM; DNA, K_d =9 nM) (Wiegand *et al.* 1996). The aptamers inhibited IgE binding to its receptor FcεRI, resulting in a inhibition constant (K_i) of 21 nM for the RNA aptamer and a K_i of 6 nM for the DNA aptamer. The aptamers also prevented IgE–mediated cellular degranulation in serum of patients with a grass allergy. In patients exposed to grass extract, the 50% inhibitory concentrations (IC_{50s})for the RNA and DNA aptamers were 2 to 6 μM, and when triggered by anti–IgE antibodies, the IC_{50s} were 200 to 300 nM.

New methodologies were developed for antibody selection. Mendonsa & Bowser (2004) utilized CE–SELEX to select aptamers with high affinity for IgE in only four rounds. The selected aptamers had an average K_d of 29 nM. Like other SELEX experiments against the same target, the sequences they obtained were totally different from those in the IgE SELEX before (Wiegand *et al.* 1996). Missailidis and colleagues (2005) developed a new method based on the adsorption of the antibodies to the surface of a PCR tube and the performance of SELEX selection in the PCR tube. In this experiment, the anti–MUC1 mAb C595 was immobilized on wall the PCR tube and the selection was carried out inside the tube. After binding and washing, the PCR reaction was performed in the same tube without extra elution step due to the reason that denaturation of the antibody can take place in the first PCR cycle. This method is very easy to perform and does not require special instrumentation. It offers the possibility of rapidly selecting aptamers for antibody targeting and can also be potentially useful in raising aptamers against other protein targets. Aptamers selected against C595 with this method were found to bind to their target with a higher affinity than the natural antigenic peptide, and they were able to displace the antigens from the antibody binding pockets.

Aptamers binding to mAbs were found to inhibit or block the biological function of the antibodies or could displace the natural antigens, which indicate that the binding sites of the aptamers are the binding pockets of the antibody or close to them. However, aptamers can be selected to bind to the constant region of antibodies as well and also have certain applications. Such aptamers can serve as probing agent instead of the usual secondary antibody in antibody–based detection systems or as immobilized resins for antibody

purification. In one example, an aptamer bound specifically to the constant region of rabbit IgG with a K_d of as low as 15 pM (Yoshida *et al.* 2008). Moreover, this aptamer recognized only the native form of rabbit IgG but not the SDS–denatured from. In another example, high affinity and specificity RNA aptamers against human IgG was isolated (Miyakawa *et al.* 2008). The 23–nt aptamer was observed to bind to the constant region of human IgG and compete with protein A in binding. Therefore, it could be used as a protein alternative for affinity purification.

2 Objective

The goal of this research project is to obtain and characterize DNA aptamers against a multiple myeloma (MM) monoclonal protein (M protein), and to evaluate potential clinical applications of these aptamers. MM is a clonal B–cell tumor, which remains incurable despite recent advances in basic biology and treatment. The idiotype (Id) of the M protein is a well–defined, tumor–specific marker. Therefore, aptamers binding to the Id tightly and selectively could be exploited to monitor expansion of malignant B cells and to target tumor cells specifically, which would be useful in MM diagnostic and therapeutic applications. Even though this is an appealing task, aptamers against the Id of M proteins have not been reported yet.

First, DNA aptamers against a M protein will be isolated using *in vitro* selection (SELEX). This antibody was purified from a MM patient. The DNA sequences will be cloned and characterized after complete enrichment is achieved. Once the aptamers are isolated, the possible binding sites of apatmers on the MM antibody will be studied to obtain aptamers against the Id of the antibody, since antibodies are big molecules possessing multiple structural solutions to high–affinity aptamers. According to the publications of aptamers against mAbs, almost all selected aptamers bind to the binding pockets of the antibody. Thus, it may be possible to obtain Id–specific aptamers. To confirm this, binding tests with the MM antibody fragments and M proteins from other patients will be performed. The binding dissociation constants will be determined and the structural and functional features of selected aptamers will be studied.

Second, potential of the M protein specific aptamers in clinical applications will be evaluated. Serum stability assay will be performed and the effect of immobilization and different buffers on aptamer binding will be tested. Moreover, aptamer–based ELISA and affinity capture assays will be designed and established for the detection and elimination of M proteins from patient serum. This could be the first step in the development of DNA aptamers in MM diagnosis and therapy.

3 Methods

3.1 DNA Technology

3.1.1 Conventional Polymerase Chain Reaction (PCR)

Developed in 1983 by Kary Mullis (Bartlett & Stirling 2003), the polymerase chain reaction (PCR) is now a common and often indispensable technique used in medical and biological. *Taq* polymerase was used in this work. One of *Taq*'s drawbacks is the relatively low replication fidelity. It lacks a 3' to 5' exonuclease proofreading activity, and has an error rate measured at about 1 in 9,000 nucleotides. But since more diversity of the selection pool is desired, this character is an advantage rather than a disadvantage for SELEX experiments. Furthermore, *Taq* polymerase makes DNA products to have overhanging adenosines (As) at their 3' ends, which is useful for TA cloning.

Usually 10 to 100 ng template DNA was used per PCR reaction. To label DNA for quantification, 1 μl α–^{32}P–dCTP was mixed into 100 μl PCR reaction system. All PCR reactions were carried out in volume of 100 μl as follows. An initial denaturing step of 95°C for 2 min was used to ensure the complete denaturation of the DNAs. This was followed by twenty rounds standard PCR protocol, with a denaturing step at 95°C for 30 s, an elongation step at 56°C for 30 s and an extension step at 72°C for 30 s. A final extension step was performed at 72°C for 2 min.

stock	final concentration	volume
template DNA	10–100 ng	0.5–1 μl
10×Taq Buffer	1×	10
10 mM dNTPs	0.2 mM	2 μl
100 mM forward primer	2 μM	2 μl
100 mM reverse primer	2 μM	2 μl
Taq Polymerase (5U/μl)	25 U/ml	0.5 μl
H_2O		ad 100μl

3.1.2 PCR Screen of Bacteria

The PCR screen is an adapted protocol of the conventional PCR. This method allows for quick control of a plasmid or insert present in large numbers of bacteria without the need of plasmid isolation. However, this method is only a rough screen for putative positive clones. There is a risk of obtaining false positives or of missing truly positive clones. The need of plasmid isolation (section 3.1.11) and proper analysis of the plasmid DNA by PCR and/or restriction digestion persists for accurate results.

The PCR screen was usually carried out in 0.2 ml PCR tubes or 96–well PCR–plates depending on the number of screened clones. With a sterile toothpick a tiny amount of cells is transferred from a single clone into the tube or plate, by lightly streaking the cells off on the bottom wall of the tube. With the same toothpick a LB–agar masterplate is dotted, which is necessary for subsequent identification and amplification of the positive clones. Depending on the number of reactions, a PCR mastermix was set up, including the no template control. Mastermix of 20 µl was added to each tube or well. To ensure that a cross contamination with bacteria can be detected, the no template control reaction should be the last well to be pipetted in order. The same conditions were used as for a conventional PCR (section 3.1.1).

Mastermix (for one reaction)

stock	**final concentration**	**volume**
10×Taq Buffer	1×	10
10 mM dNTPs	0.2 mM	2 µl
100 mM forward primer	2 µM	2 µl
100 mM reverse primer	2 µM	2 µl
Taq Polymerase (5U/µl)	25 U/ml	0.5 µl
H_2O		ad 20µl

3.1.3 Gel Electrophoresis

3.1.3.1 Agarose Gel Electrophoresis

Agarose gel electrophoresis is an easy way of separating and analyzing DNAs. In this work, 2% agarose gels were prepared for dsDNA with less than 100 bp, and 1% gels for large DNA fragments. The gels were prepared with 1×TAE buffer and 0.5 µg/ml Ethidium Bromide (EtBr). The gels were run in 1×TAE buffer with a current of 8 V/cm. The gels were visualized under ultraviolet (UV) light.

3.1.3.2 Denaturing Urea–Polyacrylamide Gel Electrophoresis (PAGE)

Polyacrylamide gels are chemically cross–linked gels formed by the polymerization of acrylamide with a cross–linking agent, usually N, N'–methylene bisacrylamide (Bis). Urea denaturing gels polymerized in the presence of urea to suppress base pairing in nucleic acids. Denatured DNA migrates through these gels at a rate that is almost completely independent of its base composition and sequence.

In this work, polyacrylamide gel electrophoresis (PAGE) was used to separate and purify ssDNA. Gels containing 8 M Urea and 10% acrylamide were prepared for ssDNA with less than 100 nt. The gels were run at 15 V/cm in 1×TBE buffer.

content for one gel:

acrylamid concentration	**10 %**
40% Acrylamid/bisacrylamide (29:1)	25 ml
10×TBE buffer	10 ml
Urea	48 g
H_2O	Ad 100 ml
APS (10%)	1 ml
TEMED	100 µl

3.1.4 Determination of Nucleic Acids on Gels

3.1.4.1 Ethidium Bromide (EtBr) Staining

EtBr is a heterocyclic and cationic fluorescence dye, which interacts with the bases of nucleic acids. It is an intercalating agent commonly used as a nucleic acid stain for agarose gels and polyacrylamide gels. The gels were stained by soaking in EtBr solution (1 μg/ml) solution for 30 min and visualized on an ultraviolet transilluminator at 302 nm.

3.1.4.2 Autoradiography

An autoradiograph is an image on an X–ray film or nuclear emulsion produced by the pattern of decay emissions from a distribution of a radioactive substance. The gels with radioactively labelled nucleic acids were placed in a cassette with X–ray films on the top of them. After certain time (depending on the intensity of the lablled radioactivity) of exposure, the films were developed and fixed.

3.1.5 Extraction of Nucleic Acids from Gels

3.1.5.1 Extraction from Agarose Gels

NucleoSpin Extract II kit was used for the extraction of DNA from an agarose gel. The gel was visualized on an ultraviolet transilluminator at 302 nm, and the desired band was cut out precisely from the gel. The gel was then chopped into small pieces and put into a 1.5 ml tube. Per 100 mg gel, 200 μl NT buffer was added and incubated at 50°C for 5 min to dissolve the gel. The solution was then transferred into a spin column and centrifuged at 11,000 g for 1 min. The membrane was washed with 600 μl NT_3 buffer and centrifuged at 11,000 g for 1 min. The membrane was dried by centrifugation at 11,000 g for 2 min. Finally, the purified DNA was eluted from the membrane with 15 μl NE buffer by incubation at RT for 1 min and centrifugation at 11,000 g for 1 min.

3.1.5.2 Extraction from Polyacrylamide Gel

To extract DNA from a polyacrylamide gel, the gel was visualized on an UV transilluminator at 302 nm, and the desired band was cut out precisely from the gel. The gel was then chopped into small pieces and put into a 1.5 ml tube. About two volumes of water was added to the tube and incubated at RT with shaking for 4 h or overnight. The sample was then centrifuged and the supernatant was recovered carefully. The purified nucleic acids could be obtained by ethenol precipitation.

3.1.6 Ethanol Precipitation

Ethanol precipitation is a widely used method to concentrate nucleic acids. The mechanism is that nucleic acids are polar and soluble in water, which is polar too, while insoluble in the relatively nonpolar ethanol. Before precipitation, the salt concentration of the sample was adjusted to 0.3 M by adding 1/10 volume of 3 M sodium acetate. Two volumes of cold 100% ethanol was added to the sample, and then placed at –20°C for 2 h or overnight. The sample was spun at 11,000 g in a microfuge for 30 min to harvest the precipitated DNA. The supernatant was decanted carefully. The pellet was washed by adding 1 ml of 70% ethanol and spinning for 5 s. The supernatant was then decanted carefully. The pellet was air dried and suspended in 50 µl TE buffer or distilled H_2O.

3.1.7 Lambda Exonuclease (λ) Digestion for ssDNA Preparations

The lambda (λ) exonuclease is a highly processive 5’ to 3’ exodeoxyribonuclease. It selectively digests the phosphorylated strand of dsDNA (Fig. 3.5). The enzyme exhibits greatly reduced activity on ssDNA and non–phosphorylated DNA. Higuchi and Ochman (1989) firstly described the use of λ exonuclease to produce ssDNA for PCR products. In this work, λ exonuclease was utilized to generate ssDNA after amplification of binders obtained in each round of selection.

Different enzyme concentrations, incubation time and different buffer conditions were tested to optimize the digestion condition of λ exonuclease. PCR products with unequal length (Williams & Bartel 1995) were utilized to monitor the digestion. The reverse primer was 5'–phosphorylated, while the forward primer was synthesized with a terminator and a lengthener of 20 As at the 5'–end. Therefore, the positive strand of the PCR product was 20 nt longer than the negative one, and they could be separated clearly by denaturing PAGE.

The PCR product was purified with Nucleospin® Extract II kit before digestion. The concentration of the dsDNA was calculated from absorbance readings at 260 nM. For about 4.0 µg purified dsDNA, 10 U and 20 U was tested in a total volume of 100 µl in 1× λ exonuclease buffer. The mixture was incubated at 37°C. Aliquots of 10 µl were taken out at different time points of 0, 10, 20, 30, 40, 50 min, and the reaction was terminated by incubation at 80°C for 10 min. Samples were loaded on denaturing (8.3 M Urea) 10% polyacrylamide gels (Fig 3.5).

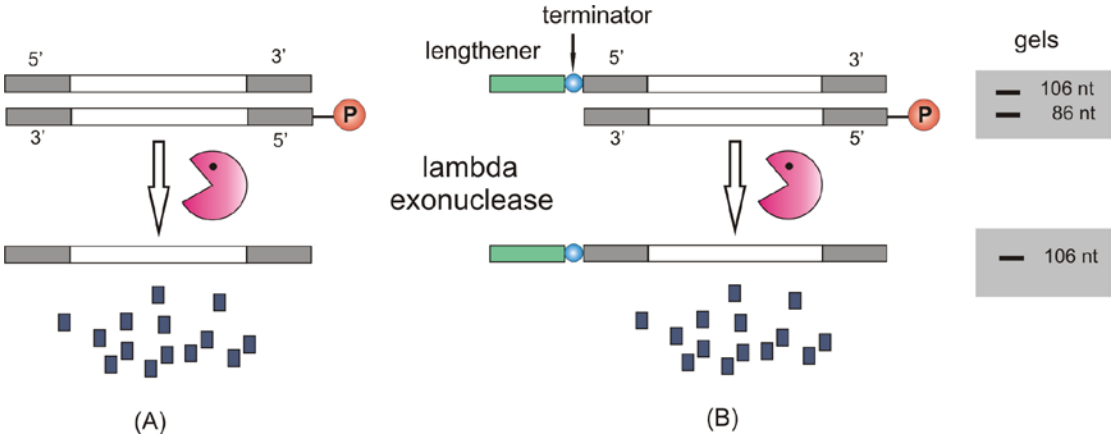

Figure 3.5 Lambda exonuclease digestion for ssDNA preparation. (A) Mechanism of λ exonuclease digestion. (B) Lambda exonuclease digestion of dsDNA of PCR product with unequal strands.

3.1.8 Determination of Nucleic Acid Concentration

The absorbance at wavelength 260 nm (A_{260}) can be used for determination of nucleic acid concentration in solution. The function describing the concentration to absorbance relation is the Lambert–Beer Law:

$$OD = e * c * d$$

The optical density (OD) is the product of the substance specific extinction coefficient (*e*), the concentration of the absorbing sample (*c*), and the optical pathlength in cm (d). The commonly accepted absorbance to concentration conversion for nucleic acids is listed below (Sambrook *et al.* 1989):

dsDNA:	1 OD_{260}= 50 µg /ml
ssDNA:	1 OD_{260}= 33 µg /ml
RNA:	1 OD_{260}= 40 µg /ml

The absorbance at wavelength 280 nm (A_{280}) was used to measure protein concentration. A ratio of A_{260}/A_{280}>1.8 suggested that there was little protein contamination in a DNA/RNA sample.

3.1.9 DNA Cloning

All cloning was performed with pGEM®–T Easy vector systems. The vectors supplied were pre–treated by cutting the vector with *Eco*R V and adding a 3' terminal thymidine (Promega, USA). This singe 3'–T overhangs at the insertion site greatly improved the efficiency of ligation of a PCR product into the plasmids by preventing recircularization of the vector and providing a compatible overhang for PCR products generated by *Taq* polymerases. PCR products of the 9th round were purified for the cloning using the Nucleospin® Extract II kit, which removed unincorporated nucleotides, primers and polymerase. The ligation reactions were set up as described below. The reactions were mixed by pipetting and incubated at 4°C overnight.

ligation mixture

	reaction	control
2× Rapid Ligation Buffer, T4 DNA lagase	5 µl	5 µl
pGEM®–T Easy vector (50 ng)	1 µl	1 µl
PCR product (200 ng)	1 µl	–
T4 DNA ligase (3 Weiss units/µl)	1 µl	1 µl
deionized water to a final volume of	10 µl	10 µl

3.1.10 Transformation

E. coli JM109 High Efficiency Competent Cells were used for transformation. The tube of frozen cells were removed from –70°C and placed in an ice bath until it was just thawed. The cells were mixed by gently flicking the tube. For each transformation reaction, 50 µl cells were mixed with 2 µl ligation solution. The tubes were gently mixed and then placed on ice for 20 min. The cells were heat–shocked for 45 to 50 s in a water bath at exactly 42°C, then immediately returned to ice for 2 min. SOC medium of 950 µl at RT was added to the tubes. The tubes were then incubated for 1.5 h at 37°C with shaking (~ 150 rpm). For each transformation, 100 µl cell culture was plated onto duplicate LB/ampicillin/IPTG/X–Gal plates. The plates were incubated overnight at 37°C.

3.1.11 Isolation of Plasmid DNA

For small scale preparation of plasmid DNA, 3 ml culture of LB medium containing the appropriate antibiotic (ampicillin, 100 mg/ml) was inoculated with a single bacterial colony. The culture was placed at 37°C for 16 h in a rotating incubator. The preparation of the plasmid was conducted using the NucleoSpin® Plasmid. Briefly, 2 ml cell culture was centrifuged for 30 s at 11,000 g to pellet the bacteria. Buffer A1, A2 and A3 were added to the pellet in turn to lyse the cell. The tube was centrifuged for 5 to 10 min at 11,000 g to clear the lysate. The supernatant was loaded onto a NucleoSpin® Plasmid column and centrifuged for 1 min at 11,000 g to bind the plasmid DNA to the

silica membrane. The membrane was then washed with 600 µl buffer A4 and centrifuged for 5 s. To elute the DNA, 50 µl AE buffer was added to the membrane and incubated for 1 min at RT, then the tube was centrifuged for 1 min at 11,000 g to collect the eluted DNA.

3.1.12 DNA Sequencing

Before sequencing, the quality of the purified plasmids was checked by 0.7% agarose gel electrophoresis. For sequencing of clones, 0.6 µg purified plasmid DNA was mixed with 20 pmol pUC forward primer in a 100 µl PCR tube. The sequencing was performed by the Sequence Laboratories Göttingen GmbH.

3.2 Protein Technology

3.2.1 Sodium Dodecyl Sulfate Polyacrylamide Gel Electrophoresis (SDS–PAGE)

Sodium dodecyl sulfate polyacrylamide gel electrophoresis (SDS–PAGE), is a technique to separate proteins according to their electrophoretic mobility. SDS, an anionic detergent, which denatures secondary and non–disulfide–linked tertiary structures, applies a negative charge to each protein in proportion to its mass. So SDS–protein complexes can migrate through the gel in accordance to the size of protein.

A discontinuous buffer system with stacking gel and separating gel is used to increase the resolution of protein separation during SDS–PAGE. The stacking gel contains chloride ions, the leading ions, which migrate more quickly through the gel than the protein sample, while the electrophoresis buffer contains glycine ions, the trailing ions, which migrate more slowly. The protein molecules are trapped in a sharp band between these ions. As the protein enters the separating gel, which has a smaller pore size, a higher pH and a higher salt concentration, the glycine is ionized, the voltage gradient is dissipated and the protein is separated based on size. Ges were prepared in

a BioRad mini–gel set (Bio–Rad, USA) wih 10% separating gel and 4% stacking gel.

content of SDS–PAGE for one gel

separating gel solution (10% acrylamide)

H_2O	3.19 ml
1.5 M Tris–HCl, pH 8.8	1.9 ml
10% (w/v) SDS	75 µl
Acrylamide/Bis–acrylamide (30%/0.8% w/v)	2.25 ml
10% (w/v) ammonium persulfate (APS)	75 µl
TEMED	7.5 µl

stacking gel solution (4% acrylamide)

H_2O	1.7 ml
0.5 M Tris–HCl, pH 6.8	315 µl
10% (w/v) SDS	25 µl
Acrylamide/Bis–acrylamide (30%/0.8% w/v)	415 µl
10% (w/v) ammonium persulfate (APS)	50 µl
TEMED	2.5 µl

The samples were mixed with 2×SDS–PAGE loading buffer and boiled at 95°C for 5 min. The gels were run in 1×Laemmli buffer at 8 V/cm. Proteins were visualized using Colloidal Coomassie Blue stain.

3.2.1.1 Reducing SDS–PAGE

Besides the addition of SDS, proteins may optionally be briefly heated to near boiling in the presence of a reducing agent, such as dithiothreitol (DTT), which further denatures the proteins by reducing disulfide linkages, thus overcoming some forms of tertiary protein folding, and breaking up quaternary protein structure. This is known as reducing SDS–PAGE. On reducing SDS–PAGE, IgG shows two bands, one with a size of 25 kDa of Fab fragments and one with a size of 50 kDa of the Fc fragments.

3.2.1.2 Non– Reducing SDS–PAGE

Non–reducing SDS–PAGE (no reducing agent) was used to analyze protein samples when native structures were investigated. Without reducing the disulfide linkages, IgG remains one band with a size of 150 kDa on the gel.

3.2.2 Bradford Protein Assay

The Bradford protein assay is based on the observation that the absorbance maximum for an acidic solution of Coomassie Brilliant Blue G–250 shifts from 465 nm to 595 nm when it binds to proteins. Bradford (1976) first demonstrated the usefulness of this principle in a protein assay. Spector (1978) found that the extinction coefficient of a dye–albumin complex solution was constant over a 10–fold concentration of protein by selecting an appropriate ratio of dye volume to sample concentration. Over a broader range of protein concentrations, the dye–binding method gives an accurate, but not entirely linear response.

In this work, the Bradford protein assay (Bio–Rad, USA) was used to check the retention ability of the nitrocellulose filters to the antibody. The sensitivity of this method was 1 µg/ml. First, a standard curve for the Bio–Rad protein micro assay was performed with normal human IgGs. The standard curve was made according to OD_{595} versus concentration of standards. To test the retention ability of the nitrocellulose filters, 1 ml human IgG (25 µg/ml) was filtrated through filter, the filter was then washed twice with 1 ml PBS. The flow through and the washing fractions were collected to measure the protein concentration. Concentrated dye reagent (0.2 ml) was added to the each tube containing 0.8 ml standards or samples. The tubes were mixed by vortex carefully. After incubation at RT for about 10 min, A_{595} was measured versus reagent blank. Unknowns were read from the standard curve.

3.2.3 StrataClean Resin Purification

StrataClean resin is a phenol–free technique for DNA purification. The solid phase silica–based resin contains hydroxyl groups that react with

proteins in a similar manner as the hydroxyl group of phenol. DNA can be rapidly and efficiently separated from all proteins by treatment with the resin.

In this work, this resin was used to separate λ exonuclease from ssDNA after digestion. For a 100 µl reaction, 10 µl resin was added according to the instruction of the supplier (Stratagene, USA). Before use, the slurry was completely resuspended by vortexing. After adding the resin, the sample was mixed by vortexing for 15 s and then incubated at RT for 1 min. The mix was spun in a microfuge at 2,000 g for 1 min. The supernatant containing the DNA was carefully removed to a fresh tube. After extraction, the absorbance of A_{260} and the ratio of A_{260}/A_{280} were measured to decide whether a second extraction was needed.

3.2.4 Preparation of Antibody–Free Serum

The serum of the myeloma patient is needed to evaluate the efficacy of the aptamer in clinical applications. A mimic serum was prepared because the serum of the patient was unavailable according to the information from the company supplying this antibody. Antibody–free serum fraction was generated as described by Goore and colleagues (1973). Solid ammonium sulphate was added to 50% saturation and incubated at 4°C for 2 h. The sample was centrifuged at 10,000 g for 10 min. The antibody–free supernatant fluid was carefully removed to a new tube. The sample was then desalted with the YM–3 spin column (Millipore) and eluted in PBS buffer. The MM antibody was added to the antibody–free serum at a final concentration of 20 mg/ml to mimic the serum of myeloma patient.

3.3 In Vitro Selection

3.3.1 Nitrocellulose Membrane Filter Partition Method

Nitrocellulose membrane filters (nitrocellulose/cellulose acetate–mixed matrix, 0.45 µm pore size; Millipore Corp.) were used to separate the DNA–antibody complexes from the unbound ssDNAs. The basis of the methodology

is the observation that most proteins bind to nitrocellulose nonspecifically. If a protein is associated with a nucleic acid, then the complex can also be retained on the nitrocellulose filter.

To reduce the non–specific adsorption of nucleic acids to the filters, the filters were pre–treated with alkali as described (McENtee *et al.* 1980). The disks were soaked in 0.5 M KOH at RT for 20 min, then washed extensively with distilled H_2O. The disks were washed for 45 min in binding buffer by shaking and stored in new buffer at 4°C. A mini vacuum device was designed and used for the *in vitro* selection (Fig. 3.1).

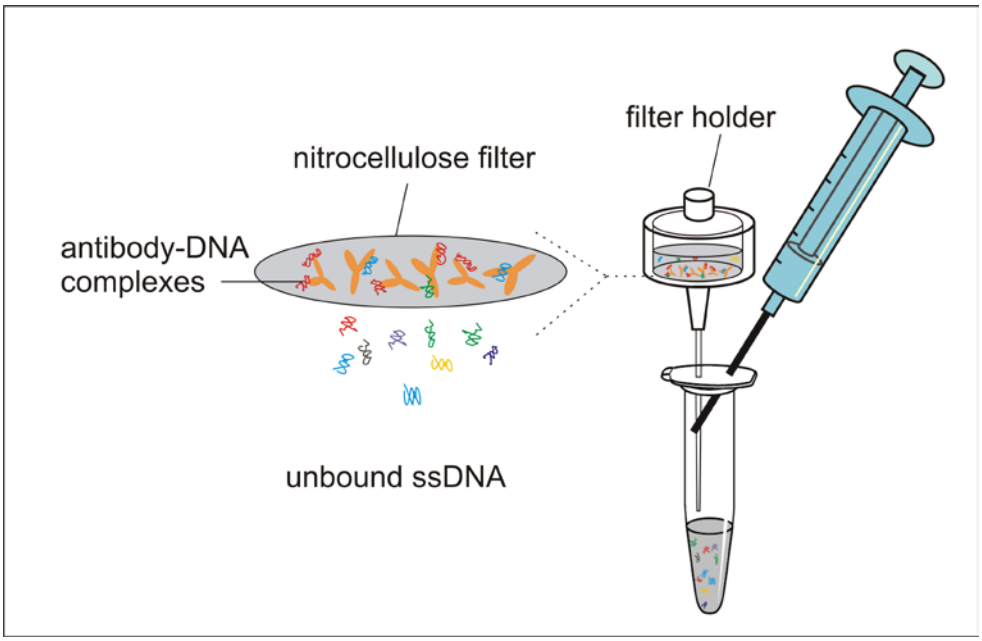

Figure 3.1 Mini vacuum device for the nitrocellulose filter partition method

The filter holder and a syringe were inserted into a 1.5 ml tube through the cap. After incubation of ssDNA with antibody, the mixture was loaded carefully on top of the filter without touching it. By pulling the syringe, a vacuum condition was generated. The unbound ssDNAs were sucked through the filter and collected in the tube. The DNA–antibody complexes were retained on the filter. The advantage of this mini vaccum device is that the unbound DNA in the follow–through fraction could be easily collected for further analysis.

3.3.2 Selection Procedure

The target molecule of the *in vitro* selection was a myeloma protein (MM IgG1), which was purified from a myeloma patient. The binding buffer was phosphate buffered saline (PBS), pH 6.0. A ssDNA library (5 nmol, about 3.0×10^{15} different molecules) was used for the first round of selection. To monitor the formation of antibody–DNA complexes, a small fraction of the library (1%, 50 pmol) was 5'–end labelled with γ–^{32}P–ATP by T4 polynucleotide kinase, purified from a 10% polyacrylamide 8.3 M urea gel and added back. The library then was dissolved in 1 ml binding buffer, heated to 95°C for 3 min and immediately placed at 4°C for 30 min. The renatured DNA was filtrated through a nitrocellulose filter in the absence of target molecules to get rid of the matrix binders. This procedure was called pre–selection. The flow–through fraction containing the unbound ssDNA was then incubated with 0.5 nmol target antibody at RT for 30 min. The reaction mixture was aspirated through the filter disk. Nonbinding oligonucleotides were removed by extensive wash steps (3×1 ml) with the same buffer. Bound ligands were recovered from the membrane by denaturing with 7 M urea incubated at 95°C for 30 min and assessed by Cerenkov counting. The selected ssDNA was then ethanol precipitated, PCR amplified, λ exonuclease digested and purified to generate a new ssDNA pool for the next round of selection.

Subsequent rounds of selection were performed similarly. The DNA was labelled with α–^{32}P–dCTP through PCR amplification. The pre–selection procedure was carried out before selection in each round. After pre–selection about 70 pmol ssDNA was used for the next selection. A molar ratio of DNA to antibody of 10 to 1 was kept for all rounds. The total reaction volume was 200 µl. PCR products from round 9 were cloned into the pGEM®–T vectors, sequenced and characterized.

3.3.3 Secondary Structure Prediction

Secondary structures of the selected aptamers were predicted by the Zuker algorithm (Zuker, 2003), using Mfold (version 3.2, http://mfold.bioinfo.rpi.edu/cgi-bin/dna-form1.cgi) with conditions set up at 0.15 M NaCl and 25°C.

3.4 Biochemical and Biophysical Assays

3.4.1 Nitrocellulose Filter Binding Assay

Nitrocellulose filter binding assays (NCFBAs) have been used for many years to qualitatively and quantitatively determine protein–nucleic acid affinities. They were used to test the binding ability of single clones, to determine the equilibrium dissociation constants (K_d) of the best binder and the truncated ligands, as well as to determine the binding specificity.

The filter used in NCFBAs and the pre–treatment procedure were the same as described in the *in vitro* selection part. Briefly, after incubation of radioactivity labelled ssDNA and target antibody, the mixture was filtrated through the nitrocellulose filter sitting on a filter holder connected with a vacuum device. The filter was then washed three times with 1 ml PBS buffer. Bound ligands were recovered from the membrane by denaturing with 7 M urea incubated at 95°C for 30 min and assessed by Cerenkov counting.

The binding tests of single clones and the binding specificity tests were carried out in a 20 µl reaction containing ^{32}P–labelled ssDNA and target at a concentration of 100 nM each. To determine the K_d, an aliquot of 20 µl reactions containing 1.5 pmol ^{32}P labelled aptamer and MM IgG1 ranging from micromolar to nanomolar concentrations were mixed in binding buffer and incubated at RT for 30 min. Then the mixture was filtrated and washed as described above. K_ds were determined graphically by plotting the fraction of bound RNA versus the log of the antibody concentration.

3.4.2 K_d Determination

The dissociation constant (K_d) of a complex is defined by the following equation:

$$K_d = \frac{[D]_f * [L]_f}{[DL]} \qquad (1)$$

Where:

$[D]_f$: concentration of free DNA

$[L]_f$: concentration of free ligand (IgG1 in this case)

[DL]: complex of DNA bound to its ligand

The total DNA concentration consists of the concentration of free DNA and the concentration of ligand–bound DNA, and the same is true for the ligand as well:

$$[D]_f = [D]_t - [DL] \quad (2)$$

$$[L]_f = [L]_t - [DL] \quad (3)$$

With:

$[D]_t$: total DNA concentration

$[L]_t$: total ligand concentration

Therefore, when substituting the variable for the free ligand concentration in equation (1) with equation (2):

$$K_d = \frac{[L]_f * ([D]_t - [DL])}{[DL]} \quad (4)$$

Re–arranging of equation (4) results in the Langmuir–Hill equation (9):

$$K_d * [DL] = [L]_t * [D]_f - [DL] * [D]_f \quad (5)$$

$$K_d * [DL] + [DL] * [D]_f = [L]_t * [D]_f \quad (6)$$

$$[DL] * (K_d + [D]_f) = [L]_t * [D]_f \quad (7)$$

$$[DL] = [D]_t * \frac{[L]_f}{K_d + [L]_f} \quad (8)$$

$$\frac{[DL]}{[D]_t} = \frac{[L]_f}{K_d + [L]_f} \quad (9)$$

Based on equations (2) and (3):

$$[DL] = [D]_t - [D]_f = [L]_t - [L]_f \quad (10)$$

$$[L]_f = [L]_t - [D]_t + [D]_f \quad (11)$$

When replacing the variable for $[D]_f$ in equation (9) with equation (11), the resulting equation representing the fraction of bound ligand results in:

$$\frac{[D]_{bound}}{[D]_{total}} = \frac{[DL]}{[L]_t} = \frac{[L]_t - [D]_t + [D]_f}{K_d + [L]_t - [D]_t + [D]_f} \quad (12)$$

Due to the experimental difficulty in measuring the amount of free RNA, it is crucial for the following assumption to be valid for accurately determining the K_d using the amount of total DNA in the calculation. At large ratios of aptamer to ligand concentration, the total concentration of the ligand can be regarded as sufficiently small to be ignored (e.g. at a 25–fold excess of aptamer, the error would be 2% and even decreasing at larger ratios). Therefore:

$$\text{if } [D]_t << [L]_t \text{ , then } [L]_t - [D]_t + [D]_f \sim [L]_t \qquad (13)$$

$$\frac{[D]_{bound}}{[D]_{total}} = \frac{[L]_t}{K_d + [L]_t} \qquad (14)$$

Therefore, at $[L]_t = K_d$:

$$\frac{[D]_{bound}}{[D]_{total}} = \frac{1}{2}$$

3.4.3 Serum Stability Assay

The susceptibility of natural nucleic acids to nucleolytic degradation is a serious hurdle for their applications in biological fluids. Serum stability assays were performed to evaluate the stability of the aptamer in human serum. Assessment of stability was essentially performed as described (Klussmann *et al.* 1996). The annealed MA–01 was incubated at a concentration of 8 µM in 90% human serum buffered with PBS, pH 7.2 at 37°C. To maintain conditions of constant pH and sample concentration, lengthy incubations were performed in an incubator at 37°C, 94.5% humidity and 5% carbon dioxide. Aliquots were mixed with equal volumes of stop solution (8 M urea, 50 mM EDTA) and frozen at –20°C. The samples (10 pmol DNA each) were separated on 10% denaturing (8.3 M urea) polyacrylamide gels. The gels were stained in EtBr (1 µg/ml), and visualized at 254 nm.

3.4.4 Circular Dichroism (CD) Spectroscopy

Circular dichroism (CD) is a form of spectroscopy based on the differential absorption of left– and right–handed circularly polarized light. This polarized light passes through the sample to a photomultiplier detector. If the sample is not optically active, the light beam does not vary through this cycle. With the introduction of an optically active sample, a preferential absorption is seen during one of the polarization periods and the intensity of the transmitted light now varies during the modulation cycle. The variation is directly related to the CD of the sample at that wavelength. Successive detection is performed at various wavelengths leads to the generation of the full CD spectrum. CD spectra for distinct types of secondary structure present in peptides, proteins and nucleic acids are different. The analysis of CD spectra can therefore yield valuable information about the secondary structure of biological macromolecules.

In this experiment, CD measurements were carried out on a JASCO J–610 spectropolarimeter in a quartz cell with an optical path length of 10 mm. The CD spectra were obtained by taking the average of 10 scans made from 350 nm to 200 nm. The measuring condition was 2 µM oligonucleotide in 10 mM Tris/HCL buffer (pH 7.5) with or without 100 mM NaCL or 100 mM KCL or in PBS buffer. The samples were heated to 95°C for 5 min and annealed either by slowly cooling to 25°C in water bath over a period of 12 h or by fast cooling to 4°C by putting them on ice immediately. Buffer baselines were collected in the same cuvette and subtracted from the sample spectra. Final spectra were normalized to get rid of the sample concentration and the cuvette path length and have zero ellipticity at 320 nm.

3.4.5 Thermal Denaturation–Renaturation using UV–Visible Spectroscopy

The stability of various conformational forms of nucleic acids can be measured by a thermal denaturation–renaturation experiment. Heating a structured nucleic acid leads to changes in its ultraviolet absorbance, which reflect the conformational change of the molecule in solution, specifically a

disruption of base–stacking interactions. Such melting experiments can be analyzed to determine the thermodynamic basis of DNA or RNA structure stability. In most cases, one may perform thermal denaturation experiments by recording absorbance at 260 nm as a function of temperature. However, it may also be preferable to record absorbance at other wavelengths. For example, quadruplex denaturation does not lead to large variation in absorbance at 260 nm. It is, however, possible to follow this denaturation at other wavelengths such as 295 nm (Mergny *et al.* 1998).

Oligonucleotides were resuspended at a final concentration ranging from 1 µM to 2 µM, depending on the length. Oligonucleotides were annealed in buffers by boiling for 5 min, and slow cooling to room temperature. Thermal denaturation–renaturation was carried out using a Hewlett Packard Agilent 8452 Diode Array Spectrophotometer equipped with a Peltier effect heated cuvette holder and temperature controller. Samples (1.2 ml, which filled the cuvette) were placed in a quartz cuvette of 1 cm path length and were allowed to reach ambient temperature before beginning each experiment. A temperature range of 20°C to 95°C was used to monitor absorbance at 260 nm and 295 nm at a heating/cooling rate of 0.5°C/min. The melting and annealing temperatures (T_ms) were calculated as the temperature, where the absorbance was halfway between the absorbance of the annealed species and the absorbance of the denatured species.

3.5 Aptamer–Based Immuno–Assays

3.5.1 Aptamer–Based ELISA

The enzyme–linked Immunosorbent Assay (ELISA) combines the specificity of antibodies with the sensitivity of simple enzyme assays, by using antibodies or antigens coupled to an enzyme. The ELISA can be used to detect the presence of antigens that are recognized by an antibody or it can be used to test for antibodies that recognize an antigen.

An indirect aptamer–based ELISA was established for the detection of myeloma antibody in human serum (Fig. 3.2). The SELEX derived aptamer

served as a capture agent in the assay. Reacti–Bind™ streptavidin coated 96–well plates were used (Pierce) to develop this assay. The plates were already blocked with Blocker™ BSA by the supplier. The binding capacity of the plate was about 10 pmol biotin per well. Aptamer MA–01a was synthesized with a biotin and a TEG at the 3' end and named 3'–Bio–TEG–01a. To get a maximum coating effect, 30 pmol renatured aptamer in a total volume of 30 µl PBS buffer pH 6.0 and control (PBS buffer) was immobilized onto each well in a 30 min incubation step. The plate was then washed three times with 200 µl PBS buffer to remove any unbound molecules.

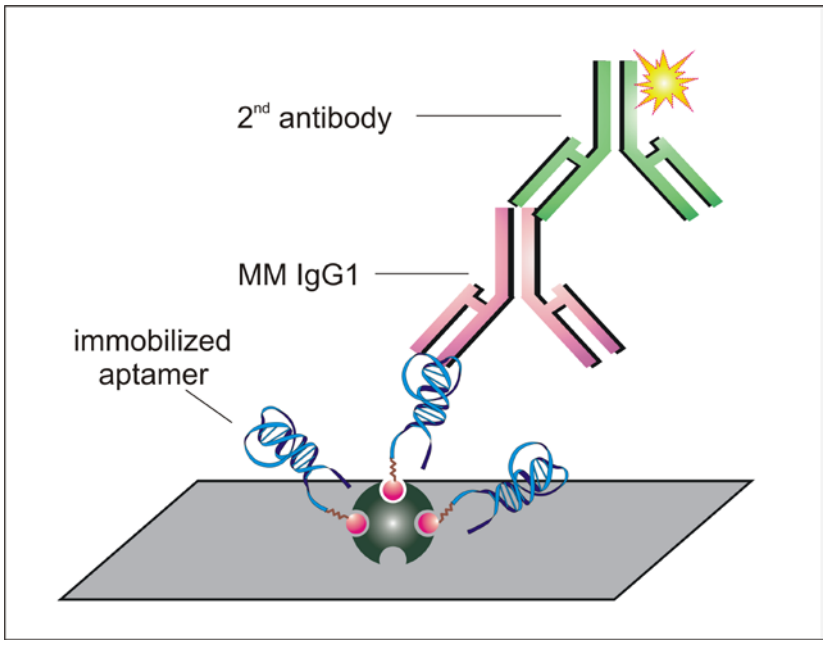

Figure 3.2 Mechanism of aptamer–based ELISA. The aptamer 3'–Bio–TEG–01a was immobilized on the streptavidin coated plate. MM IgG1 at different concentrations in 1% antibody–free human serum was added to the plate. HRP conjugated 2nd antiboby and TMB were added for MM IgG1 detection.

The coated wells were challenged with six different concentrations (500, 200, 100, 30, 10, 1 nM) of target MM IgG1 in 1% antibody–free human serum. The plate was then incubated at RT for 30 min for the binding to occur. The plate was washed three times with 200 µl PBS buffer, and the secondary antibody (1:5000 dilution), horseradish peroxidise (HRP)–conjugated goat anti–human IgG was added at 50 µl/well. The plate was incubated at RT for 30 min. The plate was then washed three times with 200 µl PBS buffer, and

3.3', 5.5'–tetramethylbenzidine (TMB) substrate solution was added at 50 µl/well. After approximately 5 min of incubation at RT, stop buffer (2N H_2SO_4) was added at 50 µl/well and the color development was measured spectrophotometrically at 450 nm.

3.5.2 Aptamer–based Affinity Capture Assay

An aptamer–based affinity capture method was established to evaluate the aptamer's application in capturing M protein from the serum of myeloma patient's. Immobilized NeutrAvidin^{TM} Protein (Pierce, USA) was used to bind the aptamer to the stationary phase. NeutrAvidin^{TM} Protein is a chemically modified version of avidin with a molecular weight of approximately 60 kDa. Unlike avidin, NeutrAvidin^{TM} Protein has no carbohydrate portion and a neutral isoelectric point (pI=6.3), resulting in minimal nonspecific binding (Hiller *et al.* 1987).

To immobilize the aptamers on the beads, 14 µg renatured aptamer 3'–Bio–TEG–01a was diluted into 50 µl of PBS and then added to 20 µl settled avidin gel. The sample was mixed for 30 min under rotation at RT. The binding efficiency was detected by measuring the UV absorbance of unbound aptamer at 260 nm. In order to determine the level of non–specific binding, a non–related 3'–biotinylated DNA sequence of 20 nt in length served as a control. The beads with immobilized DNAs were washed twice with 1 ml PBS before the assay. MM IgG1 (1µg) in 19 µl antibody–free human serum (1%) was added to the beads and incubated at RT for 30 min for the binding. The beads were then washed carefully and the bound antibody was eluted by boiling for 5 min in 20 µl of 2×SDS–PAGE loading buffer. The loading, the flow–through as well as the elution fractions were checked on 10% non–reducing SDS–PAGE gels.

4 Results

4.1 In Vitro Selection

A ssDNA library with a random sequence of 50 nt was used as precursor pool for the selection of aptamers for MM IgG1. The random region was flanked by primer binding sites of 18 nt each to facilitate PCR amplification. The reverse primer was synthesized with a 5' terminal phosphate for ssDNA generation from dsDNA PCR product by lambda (λ) exonuclease digestion (Fig. 4.1).

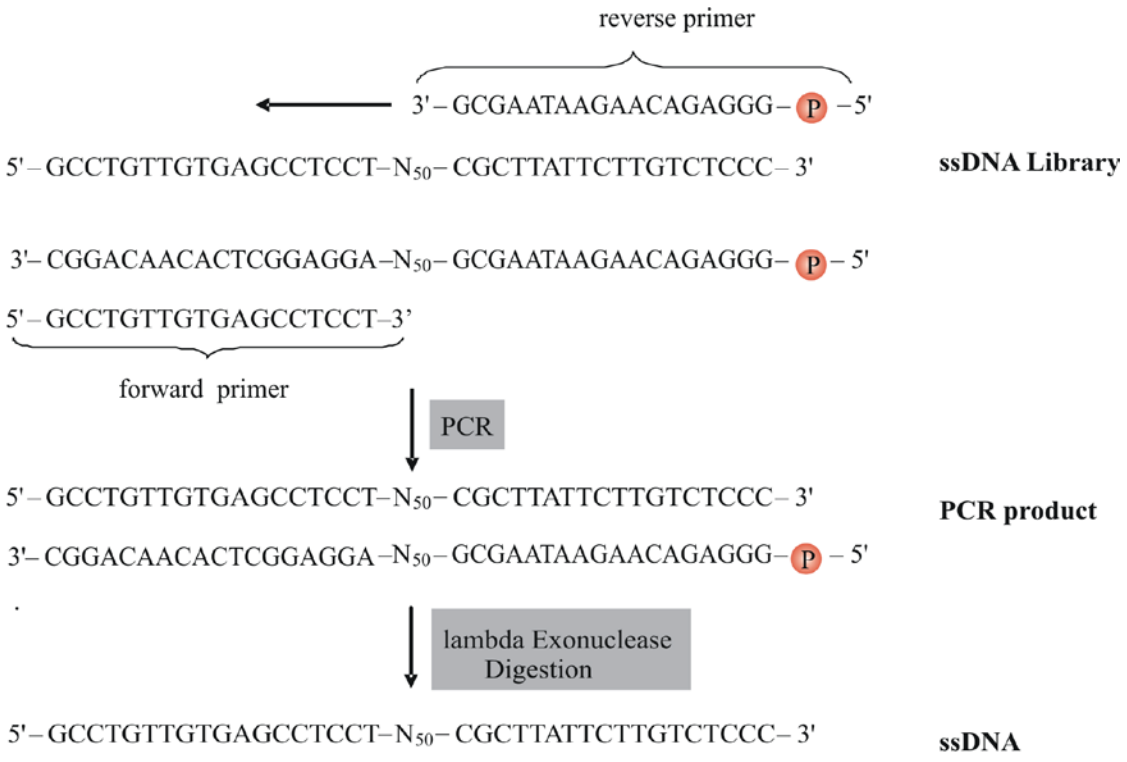

Figure 4.1 Design of the ssDNA library for MM IgG1 specific aptamers selection.

For the first round of selection, 5 nmol ssDNA (about 3×10^{15} different molecules) was used directly without PCR amplification. To monitor the formation of antibody–DNA complexes, a small fraction of the library (1%) was labelled with γ–^{32}P–ATP at the 5'–end and added back. For the following rounds of selection, 70 pmol ssDNA was employed in each round, and the ssDNA was

labelled for quantification with α–^{32}P–dCTP through PCR amplification. Before each round of selection, the nucleic acids were denatured and renatured to allow proper folding of the DNA into stable tertiary structures. The binding buffer used for the selection was phosphate buffered saline (PBS). PBS is a buffer solution commonly used in biochemistry and other branches of biological research. It contains NaCl, $Na_2HPO_4 \bullet 7H_2O$, KCl and KH_2PO_4. It was chosen for this *in vitro* selection experiment, because osmolarity and ion concentrations of the PBS solution usually match those of the human body.

After PCR amplification of selected sequences, the double–stranded product was treated with λ exonuclease, a 5' to 3' nuclease that specifically attacks dsDNA only if there was a 5' terminal phosphate (Higuchi *et al.* 1989). Therefore, the strand of DNA synthesized from the phosphorylated primer was digested by the exonuclease leaving the complementary strand for the next round of selection. The efficacy of the λ exonuclease was illustrated through gel electrophoresis by employing a model system of PCR product with strands of unequal length (Williams & Bartel 1995). The reverse primer was 5'–phosphorylated, and the forward primer was synthesized with a 5'–lengthener–terminator. The intervening terminator was non–nucleotide material that blocks negative strand elongation. The lengthener (20 dA) segment was responsible for the site difference of the two strands. Therefore, the two strands of PCR product differed significantly in length, and the digestion efficacy of λ exo-nuclease could be monitored by gel electrophoresis

For a 100 µl reaction mixture, 4 µg purified dsDNA and 20 U λ exonuclease was used following the instruction from the company (Fermentas, USA). After treatment of λ exonuclease, aliquots were taken at the indicated times. Samples were analyzed by denaturing PAGE. The positive strand of the PCR product migrated more slowly than the negative one (Fig. 4.2 lane 1). Treatment of PCR product with λ exonuclease resulted in complete removal of the phosphorylated strands. Digestion of the unphosphorylated strand could be detected after 30 min of incubation (Fig. 4.2 A). To avoid the digestion of the unphosphorylated strand, 10 U λ exonuclease was tested for 4 µg dsDNA in a 100 µl reaction mixture. Complete removal of the phosphorylated strands and

no evidence of digestion of the unphosphorylated strands were observed even after 50 min of incubation (Fig. 4.2 B). To accelerate the ssDNA preparation, the efficacy of λ exonuclease for the digestion of unpurified PCR product was also tested. Similar results were obtained (data not shown). According to these results, 10 U of λ exonuclease for about 4.0 µg unpurified PCR product was used with an incubation time of 30 min for ssDNA formation.

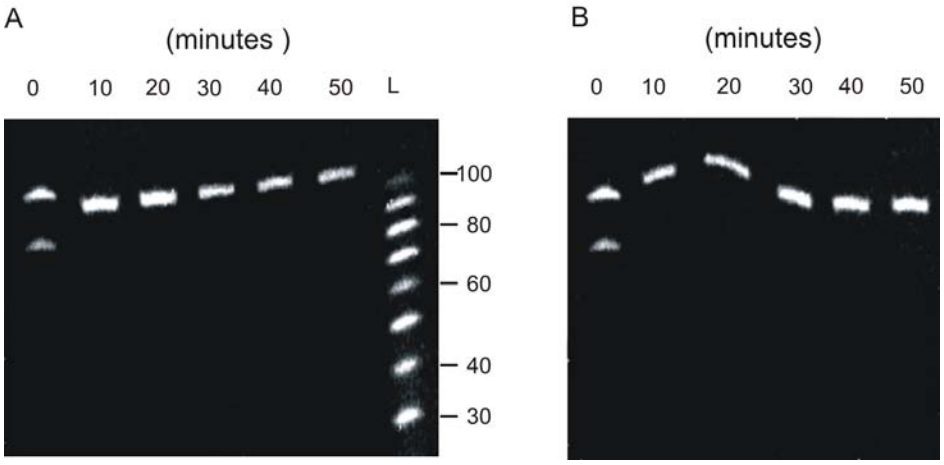

Figure 4.2 Optimization of lambda exonuclease digestion for ssDNA formation. For a 100 µl reaction mixture, 4 µg purified dsDNA was treated with 20 U (A) or 10 U (B) λ exonuclease, respectively. Aliquots were taken at the indicated times. L marks the size standard (10 bp DNA ladder). The results were reproduced in an independent experiment.

The formation of antibody–DNA complexes was monitored by using nitrocellulose filter binding assays. The filters were treated with alkaline before use to decrease unspecific binding of DNA to the filters. It turned out that neither ssDNA nor dsDNA was retained by alkaline–treated filters. The binding ability of human IgG to the filter was determined by Bradford protein assay. Almost no protein could be detected in the flow through and washing fractions, which indicated that the antibody could be retained on the filter efficiently. To prevent amplification of molecules that bind to the matrix, a pre–selection was performed before each round of selection. The pre–selection was carried out by filtration of the ssDNA pool in the absence of target. The flow–through containing the unbound ssDNA fraction was then collected for the following selection procedure. The amount of ssDNA obtained in both the pre–selection

and selection procedures was evaluated by Cerenkov counting of the fractions eluted from the filters. The percentage of DNA bound to the target increased from 0.02% in the first cycle to 2.1% in cycle 7. In cycle 8, it increased to 5.6% and reached 6% in cycle 9. Since there was no significant increase in cycle 10, the SELEX was assumed to have reached completion. This represented an improvement in affinity about 300–fold compared to the initial randomized DNA library. There was no obvious increase of DNA bound in the pre–selection procedure (Fig. 4.3).

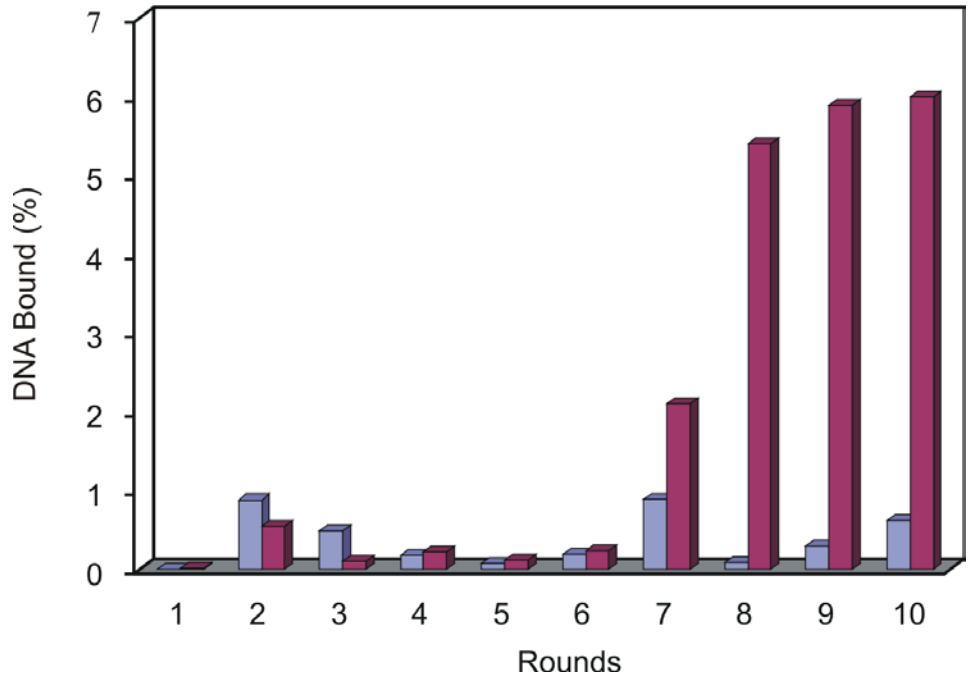

Figure 4.3 Fraction of ssDNA obtained in each selection round. The columns indicate the percentage of ssDNA eluted from the filters in the pre–selection (blue) and selection procedures (red). The fraction of ssDNA bound to the target reached a maximum of 6% after 9 cycles of selection.

4.2 Primary and Secondary Structures of the Aptamers

4.2.1 Sequence Analysis

The ssDNA obtained from round 9 was cloned and sequenced. Altogether, 48 individual clones were characterized and revealed 19 different variants. The

lengths of the sequences were from 83 to 88 nucleotides. Some of the selected DNAs were shorter than the original 86 nt pool DNAs because of deletions within the randomized region that presumably arose during PCR amplification. Based on the sequencing analysis, nine sequences were represented more than once in the 48 clones. Aptamer MA–01 was represented most frequently. The other nine variants (MA–10 to MA–19) were orphan sequences (Table 4.1).

Table 4.1 Sequence frequency of selected aptamers

aptamer	number of clones	length (nt)	frequency of sequence (%)
MA-01	9	84	18.8
MA-02	7	86	14.6
MA-03	5	86	10.4
MA-04	4	86	8.3
MA-05	4	85	8.3
MA-06	3	85	6.3
MA-07	2	86	4.2
MA-08	2	86	4.2
MA-09	2	86	4.2
MA-10	1	87	2.1
MA-11	1	84	2.1
MA-12	1	87	2.1
MA-13	1	83	2.1
MA-14	1	86	2.1
MA-15	1	86	2.1
MA-16	1	88	2.1
MA-17	1	83	2.1
MA-18	1	86	2.1
MA-19	1	85	2.1

The table shows the sequences frequency of the selected clones.

Alignment of these sequences revealed three distinct regions of conservation in 18 unique ligands (Fig. 4.4). These regions were highly guanosions (Gs) – rich. One conserved region contained six Gs (Box II), and the other regions had two Gs and one cytosine (Box I) or one thymine (Box III), respectively.

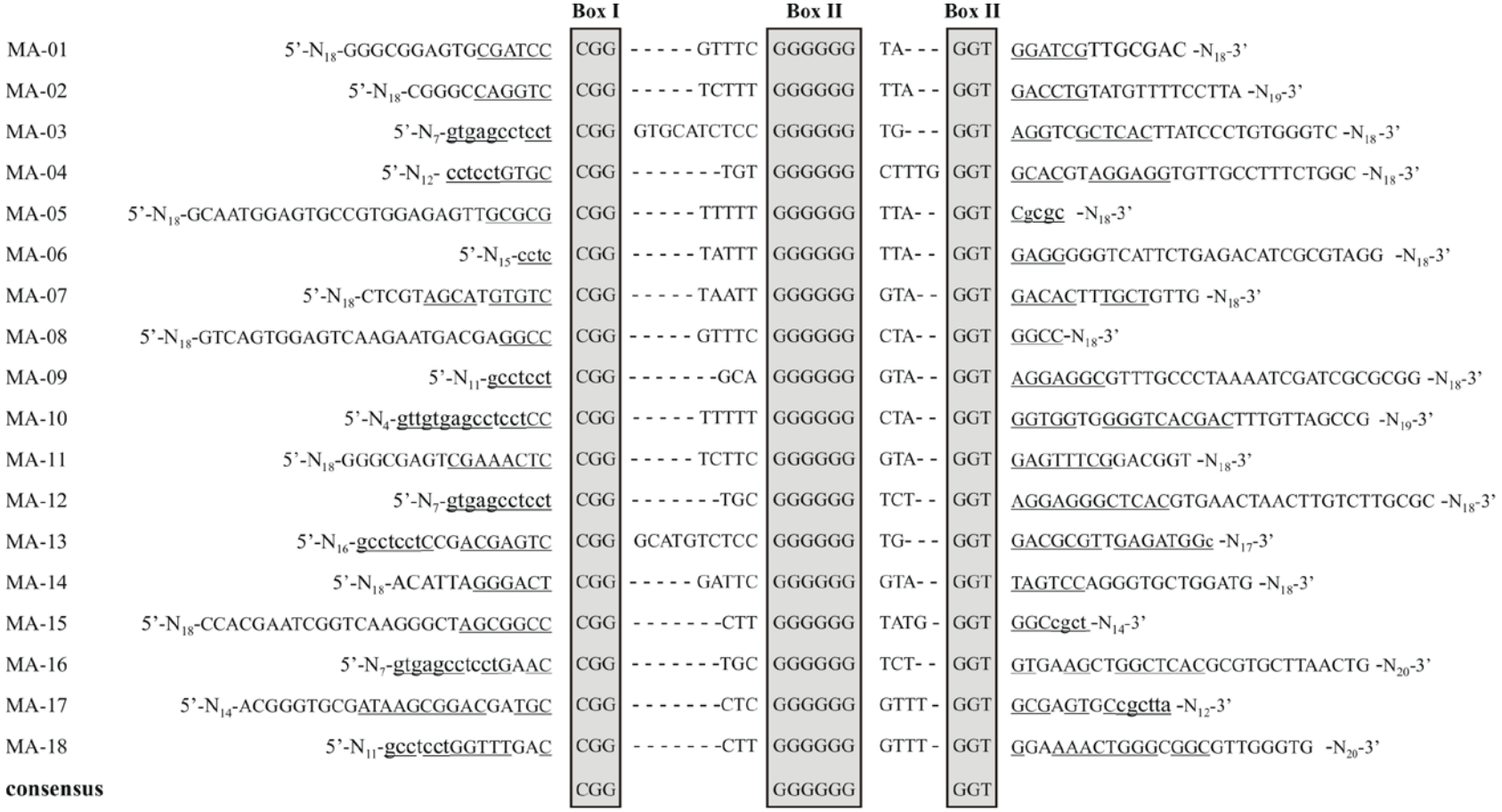

Figure 4.4 Alignment of sequences containing the consensus motif. Boxed nucleotides indicate areas of conserved sequence. Nucleotides of the initial random sequence are shown in upper case letters and nucleotides of primer regions in lower case letters. Underlined nucleotides are potentially involved in base pairing. The subscript numbers refer to the number of nucleotides in flanking regions.

These consensus motifs were located at different positions in the original random region of selected aptamers: close to the 5' terminal (9/18), close to the 3' terminal (5/18), or in the middle of the sequences (4/18). The order of the conserved motifs, however, followed a Box I – Box II– Box III orientation in all variants.

4.2.2 Secondary Structure Prediction

Secondary structures of the selected aptamers were predicted by the Zuker algorithm (Zuker 2003), using Mfold (version 3.2) with conditions set up at 0.15 M NaCl and 25°C. According to the proposed secondary structures, ten variants (MA–01, MA–02, MA–05, MA–06, MA–07, MA–08, MA–09, MA–11, MA–12, MA–15) could be folded into similar hairpin loop–stem structures. Surprisingly, the other eight variants (MA–03, MA–04, MA–10, MA–13, MA–14, MA–16, MA–17 and MA–18) were folded into different structures and no common secondary structure elements could be assigned to these variants. Considering the existence of the consensus motifs in these aptamers, constraint information was used to force the conserved sequences to be single stranded to search for common secondary structure elements. By doing this, these variants could be folded into similar loop–stem structures as MA–01 (Fig. 4.5).

In all predicted structures, the consensus motifs were located in the loops with the length of 19 to 24 nucleic acids. Nucleotides flanking these consensus motifs, which could base pair with each other (Fig. 4.4), formed stems with length of 4 to 12 base pairs. In nine aptamers (MA–03, MA–04, MA–06, MA–09, MA–10, MA–12, MA–13, MA–16, MA–18), the 5' fixed regions were involved in the stem structures; in three ligands (MA–05, MA–13, MA–15) the 3' fixed regions were involved in the stems.

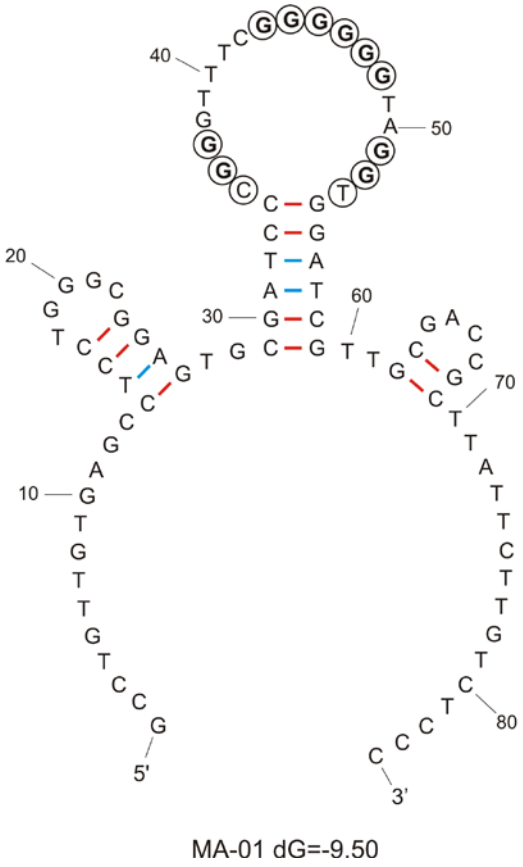

Figure 4.5 Potential secondary structure of aptamer MA–01. Positions 1–18 and 67–86 are the primers sequences. The conserved nucleotides are encircled. All sequences containing the conserved motif could be folded into similar secondary structures based on the folding algorithm of Zuker.

4.3 Binding Characteristics

4.3.1 Binding Affinity

The affinity of all unique ligands for the MM IgG1 was examined in a screening manner by determining the amount of DNA bound to the MM IgG1 at concentrations of 100 nM each. The 18 variants containing the conserved sequences displayed significant binding affinities to the target MM IgG1 compared with the random ssDNA library and the background control (Fig. 4.6). Clone MA–19, which did not contain the consensus motif, showed no affinity to the target molecule.

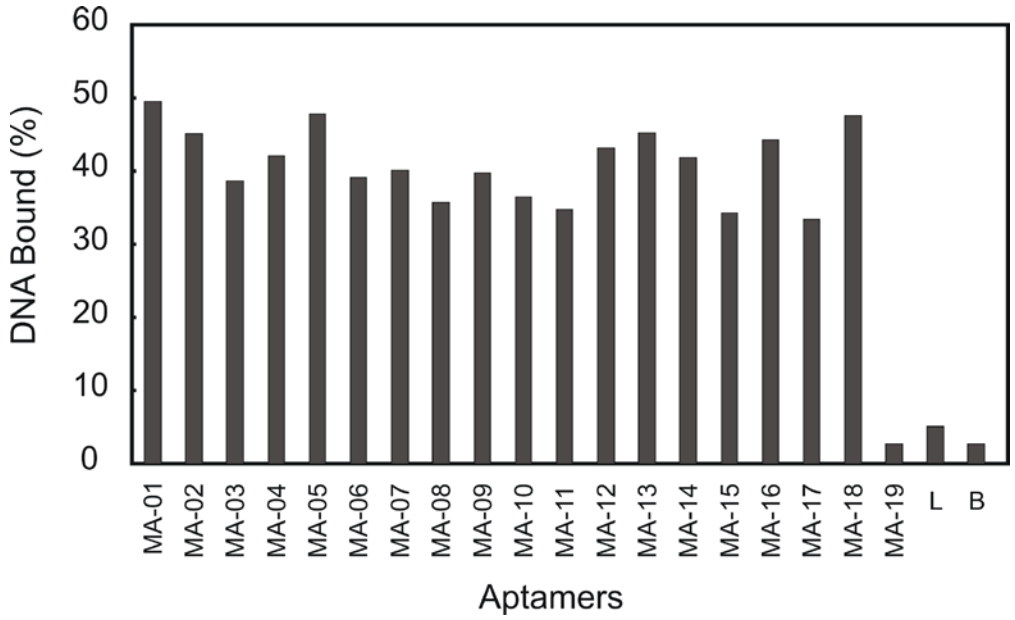

Figure 4.6 Binding test of all variants. The X axis shows the names of the aptamers. L and B indicate the library DNA and background control, respectively. The Y axis shows the fraction of DNA bound to the target.

Aptamer truncation and modification were carried out to define the sequences that are essential for binding as well as to obtain shorter and better binders for future applications. Since MA–01 appeared most frequently (18.8%) in the selected pool, and showed the highest binding affinity among the selected variants, this variant was truncated and modified based on the predicted secondary structure (Table 4.2).

Table 4.2 Sequence of MA–01 and the truncated aptamers.

	Sequence(5'-3')	Length (nt)	dG
MA-01	FP-GGGCGGAGTGCGATCCCGGGTTTCGGGGGGGTAGGTGGATCGTTGCGAC-RP	84	-9.50
MA-01a	CGATCCCGGGTTTCGGGGGGGTAGGTGGATCG	31	-4.85
MA-01c	**C**G**C**G**C**GCCCGGGTTTCGGGGGGGTAGGTGG**C**G**C**G**C**G**C**G	35	-11.66
MA-01g	CGGGTTTCGGGGGGGTAGGT	19	-2.37

The table shows the sequences of MA–01, MA–01a, MA–01c and MA–01g. FP indicates the forward primer and RP indicates the reverse primer binding region. The mutated bases in MA–01c are displayed in underlined letters and the two additional CGs are displayed in bold letters. dG indicates the predicted free energy of secondary structure formation.

To see if the conserved loops and the extended stems were sufficient for MM IgG1 binding, three ssDNA species were synthesized. MA–01a (31 nt) contained the conserved loop flanked by the covarying sequences of 12 nt forming a 6–bp stem calculated by the Mfold program. MA–01c (35 nt) was modified from MA–01a. The two AT sequences were replaced with two CG sequences in the flanking region, and the stem was extended with additional 5' CG and 3' GC residues. This resulted in a longer and more stable stem. The predicted free energy of secondary structure formation of MA–01c indicated a higher stability of this sequence as compared to MA–01a (Fig. 4.7). MA–01g (19 nt) contained only the conserved loop region. These three oligonucleotides were chemically synthesized. Binding assays were performed to define their binding affinities.

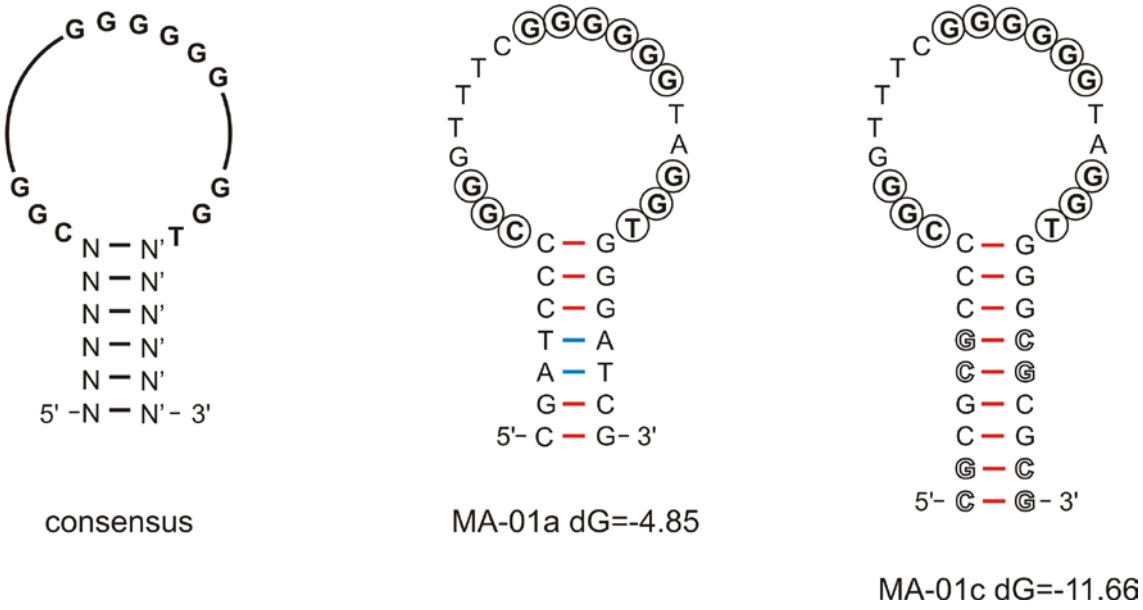

Figure 4.7 Potential structures of conserved motif, ligand MA–01a and ligand MA–01c. The consensus sequences for the ssDNA ligands can be folded into a stem–loop motif. The circled letters in the loops indicate the conserved nucleotides. The covariations in the stems are indicated by N–N' base pairs. Ligand MA–01a contains the conserved loop and the extended stem regions. Ligand MA–01c is a modification of MA–01a in the stem region to stabilize the secondary structure. The outline letters indicate the mutated bases and the additional bases.

The K_d values of the best binder MA–01 and the truncated form MA–01a were determined using the filter binding assay. MA–01 bound to the target with a K_d of 172 nM, and MA–01a bound to the target with a K_d of 372 nM (Fig. 4.8). MA–01c displayed a similar binding affinity as MA–01a (data not shown), indicating that the length and the sequences of the stems were not essential for binding. The truncated variant MA–01g did not bind to the MM IgG1 under this condition. These results suggested that the conserved loop structure might be the direct target binding motif, but that the stem formed by the 5' and 3' extensions were also critical for binding.

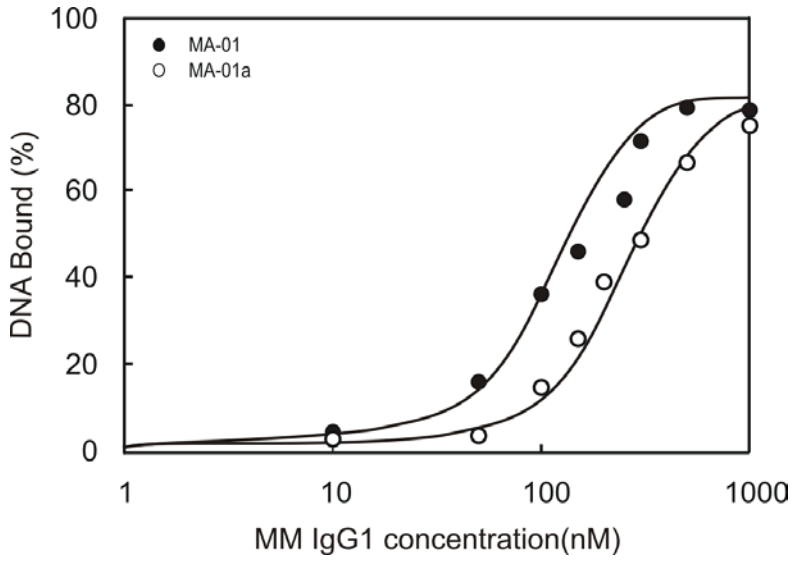

Figure 4.8 Binding curves of aptamers. The plots display the binding curve of selected full length aptamer MA–01 (solid circle) and truncated aptamer MA–01a (hollow circle).

The influence of pH on aptamer's binding performance was also evaluated by K_d determination in buffers with different pH. The aptamer MA–01 showed the best binding affinity to the target at pH 6.0, at which the aptamers was selected, with a K_d of 172 nM. The K_d of the aptamer changed to 290 nM at pH 6.6 and to 602 nM at pH 7.2, respectively (Fig. 4.9). This is likely due to the different neutralization of the phosphate backbone under different pH values, which had an impact on the aptamer's conformation and, therefore, on its binding capability.

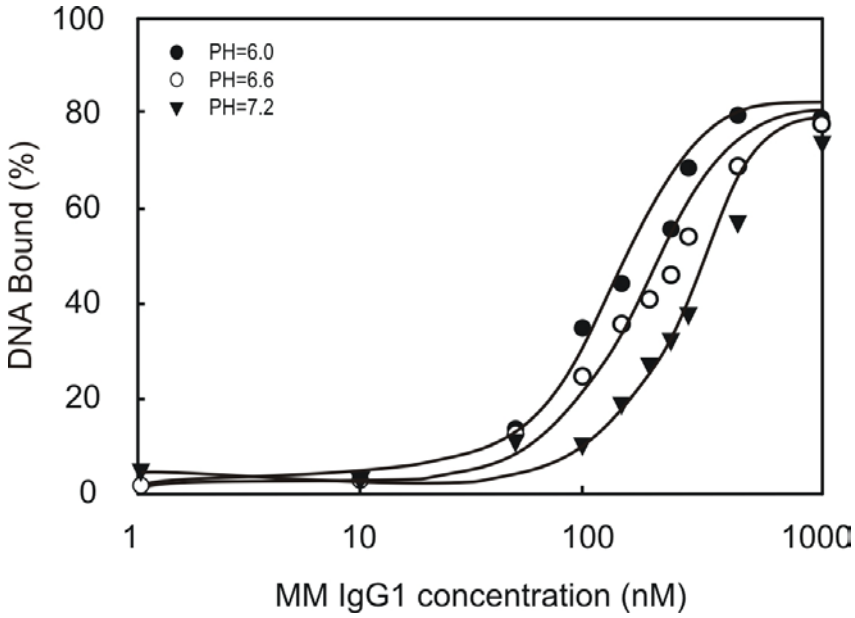

Figure 4.9 Binding curves of aptamer MA–01 under different pH values. Experiments were carried out in duplicate. pH condition: pH 6.0 (●), pH 6.6 (○) and pH 7.2 (▼).

To test whether antibody–aptamer complexes can dissociate by changing the pH value of the binding buffer, filter binding assays were carried out under different pH conditions (Fig. 4.10).

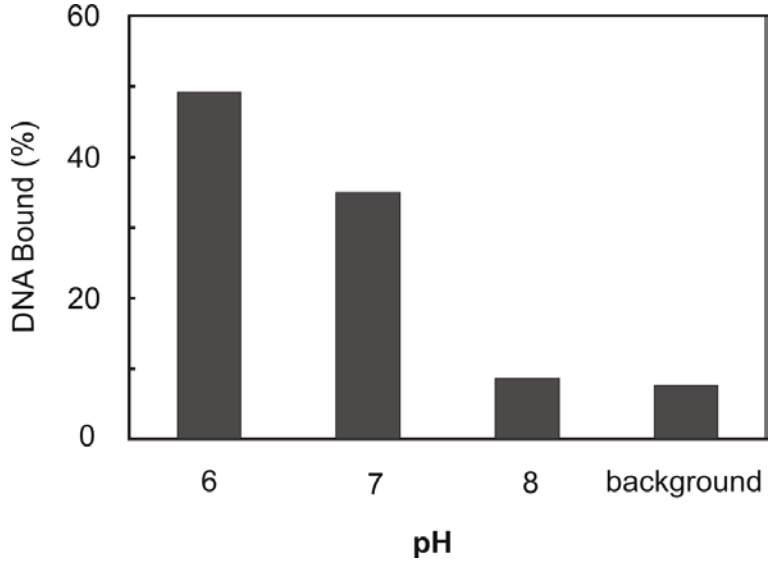

Figure 4.10 PH dependence antibody–aptamer dissociation assay. The experiments were carried out in duplicate.

About 50% of aptamer MA–01 bound to the target antibody to form aptamer–antibody complexes at pH 6.0. The fraction of the aptamer bound to target decreased to 35% as the pH increased from 6.0 to 7.0, indicating dissociation of 30% of the complexes. The fraction of bound DNA decreased to 17%, close to the background level, as the pH was raised from 6.0 to 8.0, indicating that almost all complexes dissociated under this condition. This pH dependence binding character of the aptamer could be utilized to elute the bound antibody from the immobilized aptamer. With this method, no special elution buffer is needed for the elution step. Moreover, the aptamer stationary phase can be regenerated easily by adjusting the pH of the binding buffer.

Because it has been discussed previously that the immobilization of aptamers may affect their binding properties (Nutiu & Li 2004; Baldrich *et al.* 2004), an aptamer–based immunoassay was performed to characterize the influence of immobilization on the MM IgG1 specific aptamers. Both 5'–biotinylated aptamer MA–01 and 5'–biotinylated ssDNA pool were immobilized on NeutrAvidin agarose beads. After incubation with MM IgG1 and horse radish peroxidase (HRP)–conjugated anti–human IgG 2nd antibody and HRP substrate, the absorbance was measured at 450 nm. A strong signal was obtained for the aptamer, indicating the binding of the MM IgG1 conjugate. The signal for the DNA pool was as low as the background, indicating no binding (Fig. 4.11).

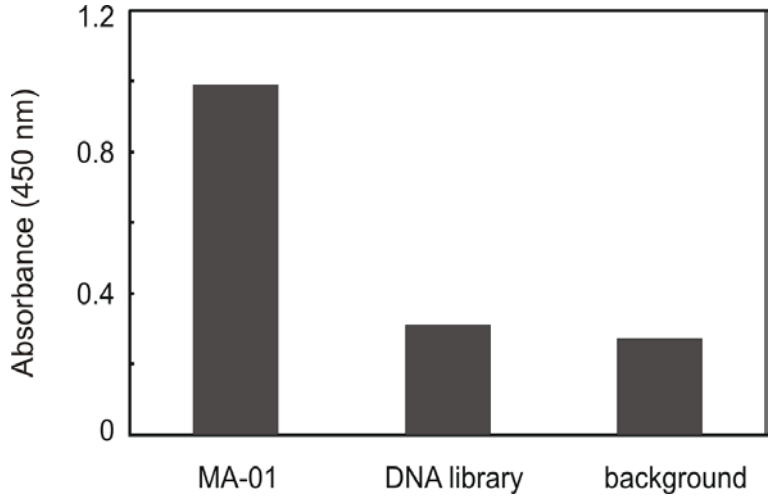

Figure 4.11 Binding test of aptamer MA–01 after immobilization. The experiments were carried out in duplicate.

4.3.2 Binding Specificity

To verify the binding specificity, MA–01 was subjected to filter binding experiments with the target antibody, a MM IgG1 from a different patient and one monoclonal human IgG1 (Fig. 4.12). The DNA to antibody ratio was 1:1 at a concentration of 100 nM each. About 40% of the aptamer bound to the target antibody under this condition. The aptamer did not cross–react with myeloma antibody from a different patient or the monoclonal IgG1, although they belonged to the same isotype. No binding of the aptamer could be detected to polyclonal human serum IgGs, Fab fragments or Fc fragments of human IgGs.

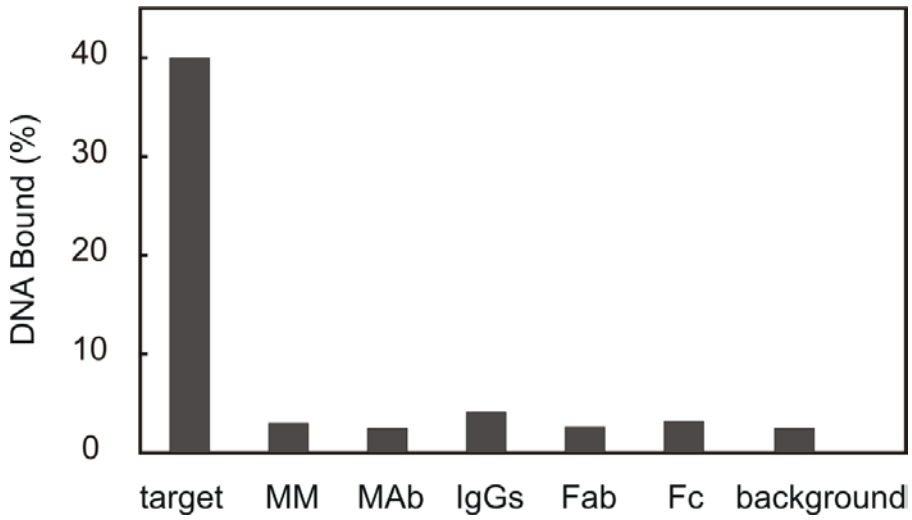

Figure 4.12 Binding specificity of aptamer MA–01. The experiments were carried out in duplicate.

This result implicated a high specificity of the MM IgG1 binding aptamer. Since the Fc fragments of antibodies of the same isotype are almost identical, the aptamer's specificity also suggested that the binding site of the aptamer was located in the variable region or even in the antigen binding pockets of the antibody.

4.4 Tertiary Structure Prediction

Nucleic acid sequences, which are rich in Gs are capable of forming four–stranded structures called G–quadruplexes. These consist of a square arrangement of Gs (a tetrad), stabilized by Hoogsteen hydrogen bonding. They are further stabilized by the existence of a monovalent cation in the center of the tetrads (Fig. 4.13 A). The relative strand orientation (5' to 3' polarity) of the four strands of the quadruplex may be parallel, antiparallel or mixed (Davis 2004). For a monomer quadruplex, the structure can be either monomer chair (antiparallel) or monomer basket (mixed) (Fig. 4.13 B).

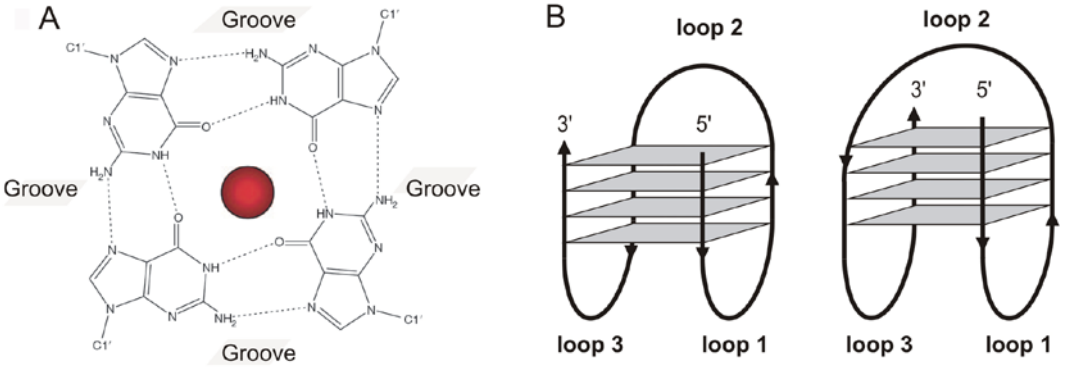

Figure 4.13 Schematic presentation of G–quartet structure. (A) G–quartet. The scheme displays the arrangement of guanine bases in a G–quartet, shown together with a centrally placed metal ion. Hydrogen bonds are shown as dotted lines, and the positions of the grooves are indicated. (B) Loop orientation of monomer G–quadruplexes. The left one shows the monomer chair G–quardruplex and the right one shows the monomer basket type (Dapić *et al.* 2003).

The consensus motif of selected aptamers is highly G–rich and fits the formula described for intramolecular quadruplexes (Burge *et al.* 2006) as follows:

GmXnGmXoGmXpGm

Where m is the number of G residues in each short G–tract, which are directly involved in G–tetrad interactions. Xn, Xo and Xp can be any combination of residues, including G, forming into loops. According to this formula, the G–rich

consensus motif of the MM IgG1 binding aptamers could potentially fold into a G–quadruplex structure. There are three different possible arrangements for the Gs that are directly involved in G–quartets (Fig. 4.14 A). According to the different strand polarities, there are two types of G–quadruplexes that are possibly folded by this motif, “chair” type or “basket” type (Fig. 4.14 B).

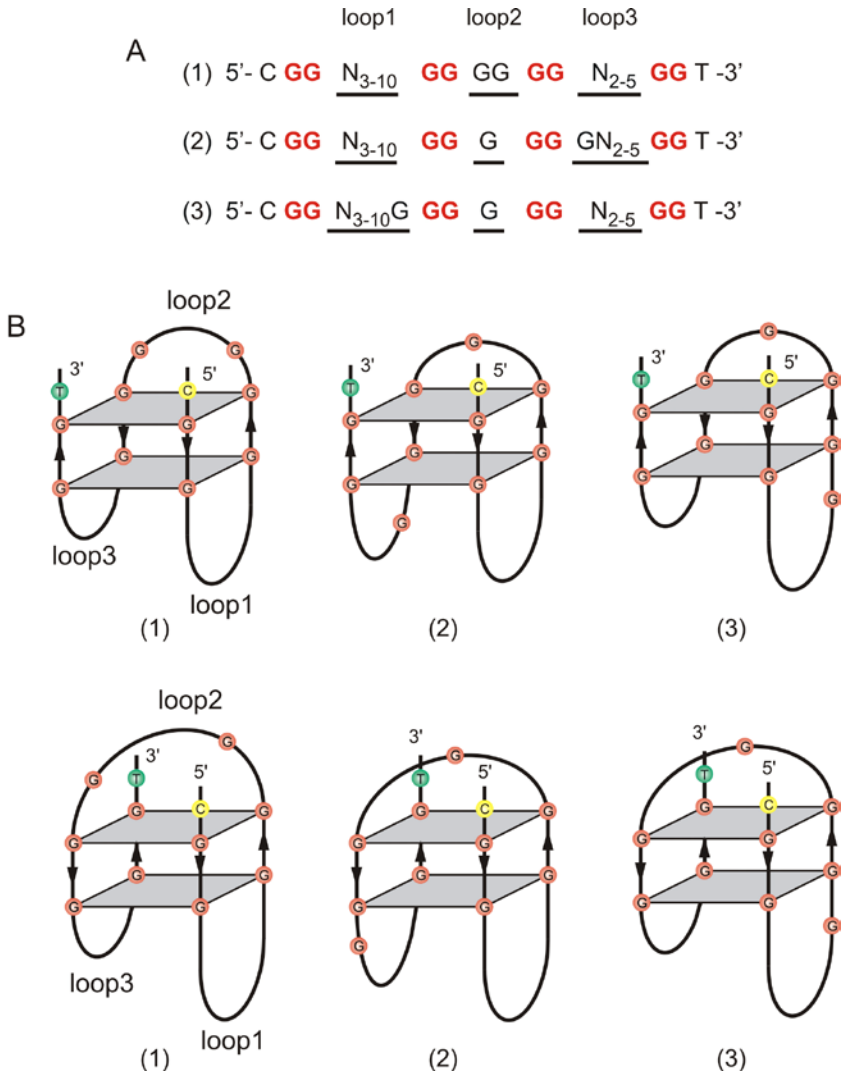

Figure 4.14 Prediction of G–quadruplexes folded by the consensus motif of the selected aptamers. (A) Three possible arrangements of the Gs forming the G–quartets. The Gs in red and bold form represent the Gs that are directly involved in the G–quartets. The Ns indicate the nonconserved nucleotides, and the subscript numbers indicate the number of nucleotides. The underlined letters indicate the sequences of the loops. (B) G–quadruplexe models folded by the consensus motif. The upper three figures indicate the chair type and the lower three show the basket type. The number under each structure indicates the corresponding G arrangements in this structure as shown in (A). Strand polarities are shown by arrows.

In all alternative options for G–quadruplexe formation, loop2 was highly conserved with either one or two guanine bases. For most of the aptamers (15/18), loop 1 and loop 3 differed in length. These aptamers could be classified into families, according to the common primary sequence elements of the loop1 and loop3 in the predicted G–quadruplex structures, as illustrated in Figure 4.15 (taking the first possible arrangement of Gs in the G–quartets).

		loop1	loop2	loop3
I	MA-01	G T T T C	G G	T A
	MA-02	T C T T T	G G	T T A
	MA-05	T T T T T	G G	T T A
	MA-06	T A T T T	G G	T T A
	MA-07	T A A T T	G G	G T A
	MA-08	G T T T C	G G	C T A
	MA-10	T T T T T	G G	C T A
	MA-11	T C T T T	G G	G T A
	MA-14	G A T T C	G G	G T A
	consensus	K H W T Y	G G	B T A
II	MA-03	G T G C A T C T C C	G G	T G
	MA-13	G C A T G T C T C C	G G	T G
	consensus	G Y R Y R T C T C C	G G	T G
III	MA-12	T G C	G G	T C T
	MA-16	T G C	G G	T C T
	consensus	T G C	G G	T C T
IV	MA-15	C T T	G G	T A T G
	MA-17	C T C	G G	G T T T
	MA-18	C T T	G G	G T T T
	consensus	C T Y	G G	K W T K

Figure 4.15 Classification of the aptamers into families sharing common primary sequence elements in loop1 and loop3 of the predicted G–quadruplex structures. K refers to G or T; H refers to A or C or T; W refers to A or T; Y refers to T or C; B refers to T or G; R refers to G or A.

Nine of the 18 sequences (family I) contained a consensus motif of five nucleotides, KHWTY, in loop1, and shared the motif BTA in loop3. The two aptamers of family II had the consensus motif, GYRYRTCTCC, in loop 1, while

six nucleotides were invariant and the other four were either a purine or a pyrimidine. The TG sequence of loop3 was invariant. The two aptamers of family III had identical loops. The three members of family IV had a CTY motif in loop1, and a TWTK motif in loop3. Two variants MA–04 and MA–09 did not belong to any of these families. It is notable that both loop1 and loop3 contained at least one T residues. It is conceivable that the G(s) in loop2 and the T(s) in loop1 and loop3 may be very importment for the target recognition for the aptamers.

CD spectroscopy is a powerful analytical tool for identifying quadruplex DNA structures. For parallel quadruplexes, in which all four strands are in the same orientation, CD minima and maxima are typically near 240 nm and 264 nm, respectively. For antiparallel quadruplexes, in which strands orientation alternates, the corresponding values are typically near 265 nm and 295 nm, respectively (Hardin *et al.* 1991). The CD spectra of aptamers MA–01a (Fig. 4.16 A) and MA–01g (Fig. 4.16 C), which annealed in buffer containing 100 mM Tris/HCl (black line) without any cation contained one positive peak around 260 nm and one negative peak around 240 nm. This suggested that no quadruplexes formation occurred under this condition. Interestingly, the spectra of MA–01a and MA–01g annealed in buffer containing 100 mM NaCl (blue line) or 100 mM KCL (red line) contained two positive peaks at both 295 nm and 264 nm. The appearance of these two peaks indicated that more than one molecular species (both chair and basket forms) were present in solution. The spectra of MA–01c (Fig. 4.16 B), which annealed in Tris/HCl buffer (black line), contained a broad positive peak around 280 nm and a negative one at 250 nm. The positive peak shifted a little to 290 nm in 100 mM NaCl (blue line) or 100 mM KCl buffers (red line). These spectra could not fit any one for. This suggested that aptamer MA–01c could not fold into quadruplex structures under these conditions. It is also possible these spectra resulted from the combination of spectra of G–quadruplex structures and the helical domain in this structure.

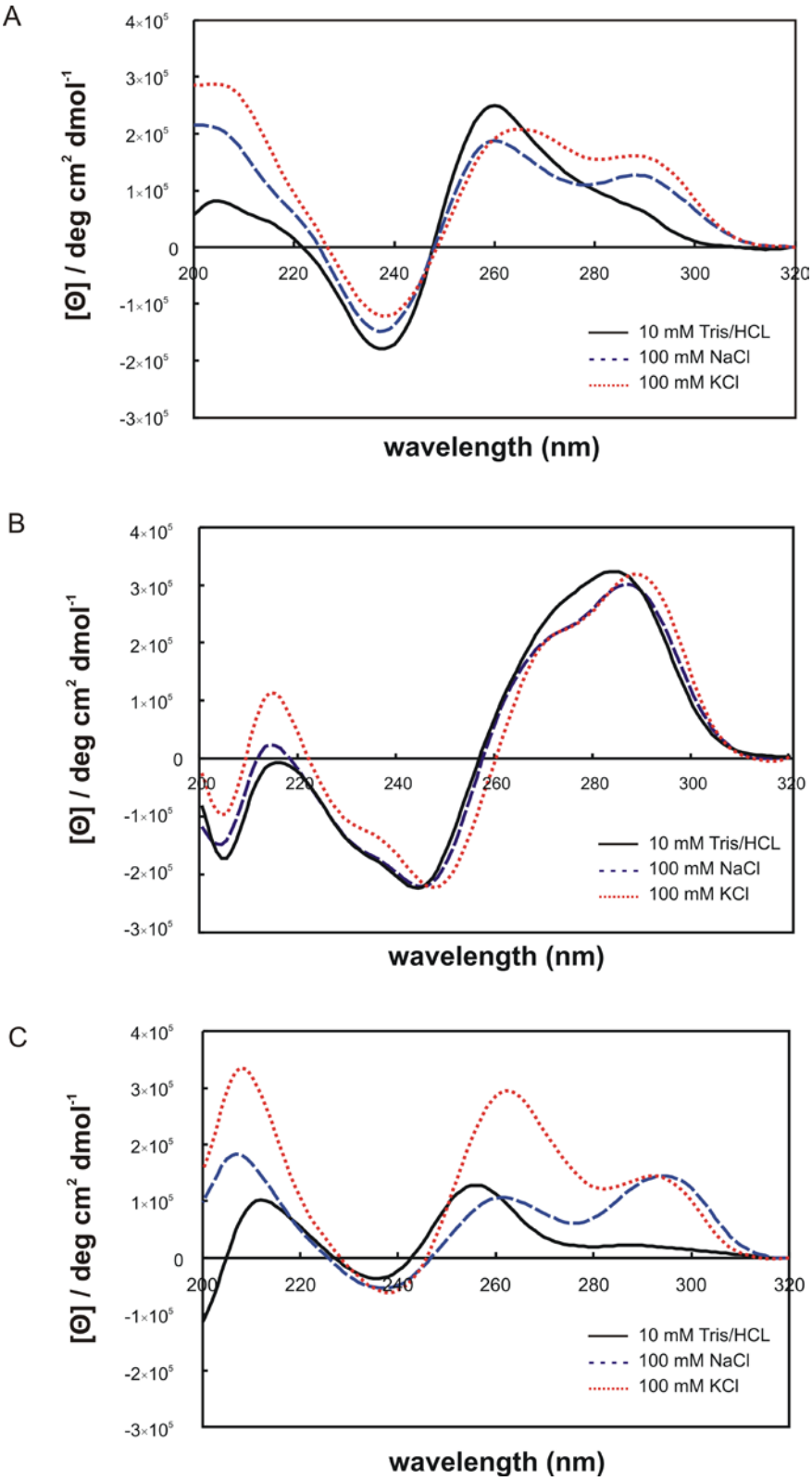

Figure 4.16 CD spectra of aptamers MA–01a (A), MA–01c (B) and MA–01g (C) in different buffer conditions. Buffer conditions: 10 mM Tris/Hl (solid line), 100 mM NaCl (dashed line) and 100 mM KCl (dotted line).

The formation and stability of a particular G–quadruplex can exhibit a strong dependence on the species of cation coordinated by its G–quartets. It was reported that the stabilization effect of different monovalent cations follows the trend K^+ > Rb $^+$> Na^+ > Li^+,Cs^+ and divalent cations have the trend $Sr^{2+} > Ba^{2+} > Ca^{2+} > Mg^{2+}$ (Phan *et al.* 2006). There were two cations, K^+ and Na^+, in the binding buffer used for aptamer selection. CD spectra of MA–01a (Fig. 4.17) and MA–01g (Fig. 4.18) annealed in various concentrations K^+ and Na^+ were measured to test the efficiency of cations on G–quadruplex formation.

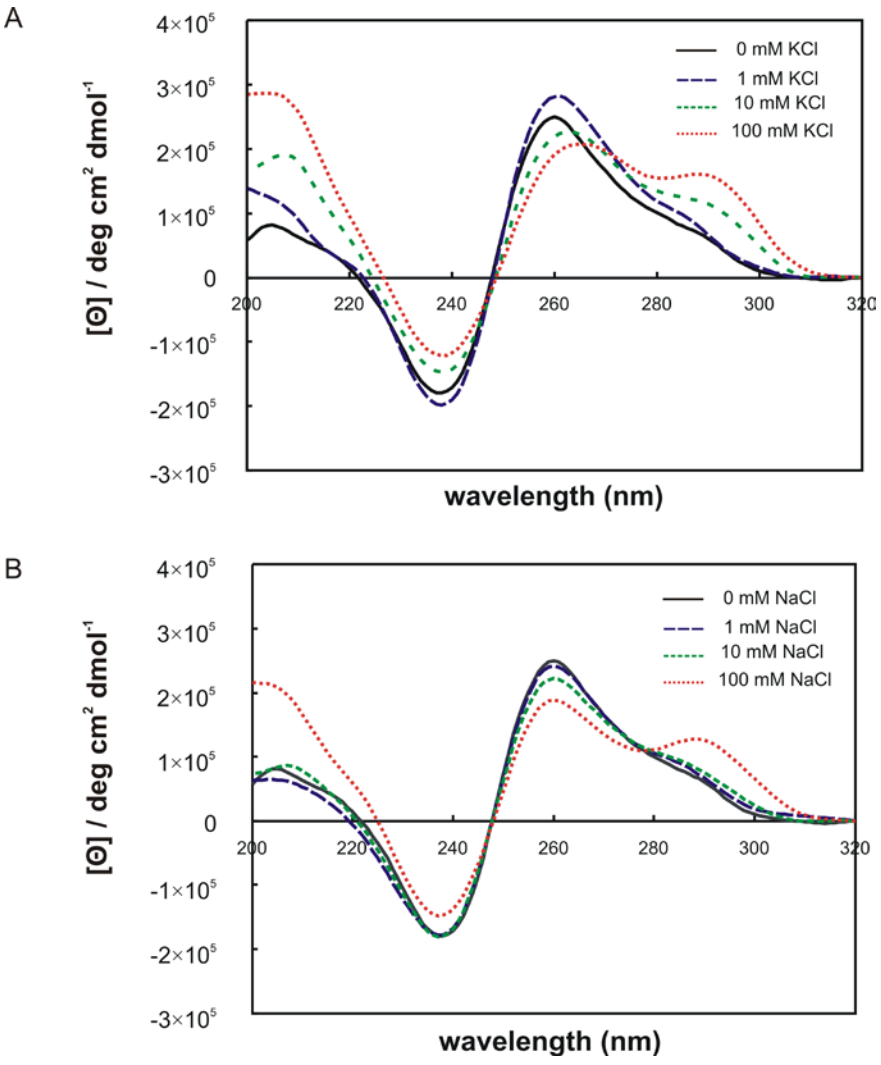

Figure 4.17 Efficiency of different cations on G–quarduplex of MA–01a. (A) CD spectra of MA–01a in various concentrations of K^+. (B) CD spectra of MA–01a in various concentrations of Na^+.

The positive peak of spectra of MA–01a around 260 nm in buffer containing no cations shifted towards 265 nm in buffers containing KCl (Fig. 4.17 A). A second positive peak appeared at 295 nm. The intensities of these two peaks increased as the ion concentrations were raised. Similar results were found in buffers containing NaCl (Fig. 4.17 B), but the CD intensities around both, 295 nm and 264 nm, were lower compared with those in KCl.

Similar results were obtained for aptamer MA–01g (Fig. 4.18). However, the changes of the CD spectra employing different ion concentrations for MA–01g

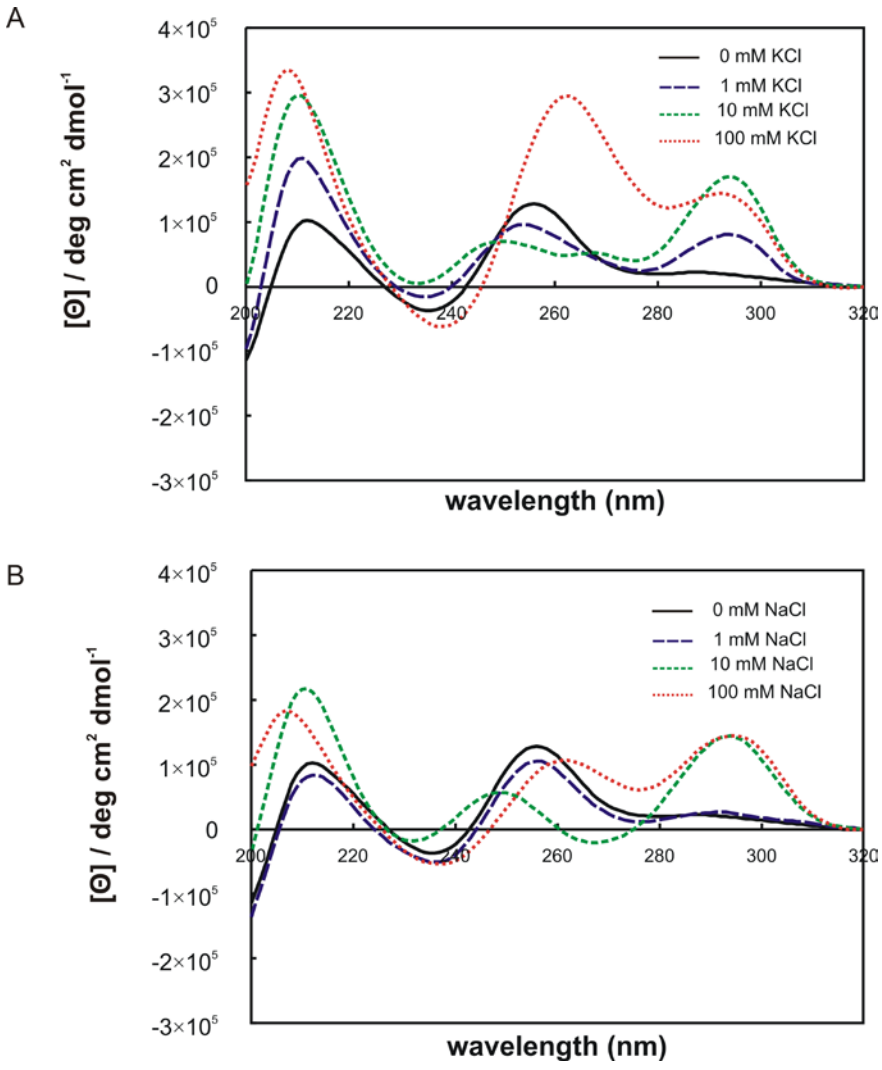

Figure 4.18 Efficiency of different cations on G–quarduplex of MA–01g. (A) CD spectra of MA–01g in various concentrations of K^+. (B) CD spectra of MA–01g in various concentrations of Na^+.

were much more obvious than those of MA–01a. This could be due to a higher flexibility of MA–01g, which lacked the stem structure as compared to MA–01a. Therefore, a conformational change might happen more easily. Interestingly, in 100 nM KCl, the intensity of the maximum at 264 nm was much higher than that at 295 nm; while in 100 mM NaCl, it was just the reverse. It is conceivable that KCl is more efficient in inducing a monomer “basket”, while NaCl is more efficient in inducing a “chair” type.

The cooling rate can influence the G–quadruplex structure formed by some DNA sequences (Bryan & Jarstfer 2007). This was determined by CD spectroscopy of MA–01a, which was annealed following fast or slow cooling procedures in different buffers (Fig. 4.19). In the buffers tested, the intensities of the positive peaks after slow cooling were a little higher than those after fast cooling. This result indicated a rapid formation of the G–quadruplex structure of the aptamer.

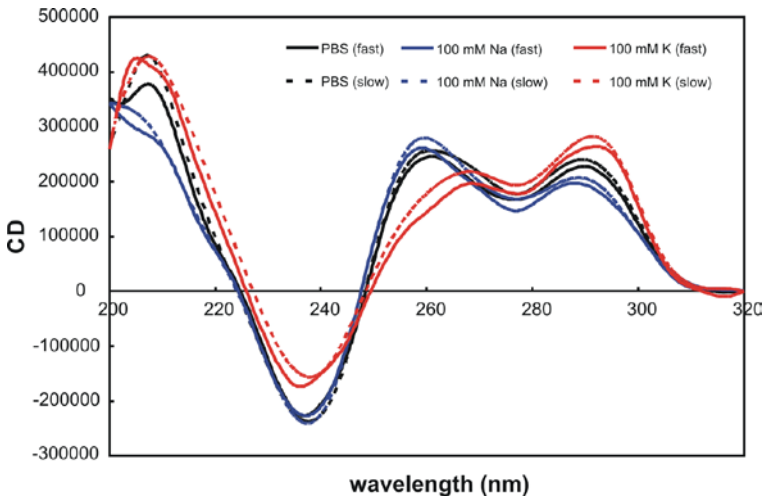

Figure 4.19 CD spectra of MA–04a after fast (full line) or slow (dotted line) annealing procedure. Buffer conditions: PBS pH 6.0 (black), 100 mM Na^+ (blue), and 100 mM K^+ (red). The results were reproduced in an independent experiment.

Thermal denaturation–renaturation studies can provide additional information about the thermodynamic stability and the kinetics of formation of secondary structures. The detection of G–quartet formation with UV–

spectroscopy was first described by Mergny *et al.* (1998). The thermal melting of quadruplex nucleic acids can be characterized by an inverse UV transition at 295 nm (Hardin *et al.* 1992). This technique relies on the observation that the absorbance of Gs at 295 nm is higher when they are in a G–quartet structure than when the structure is denatured. In the absence of stabilizing cations, the profile of aptamer MA–01a showed no clear transition at 295 nm, indicating the absence of stable G–quartets (or possibly the presence of a structure with a melting temperature>90°C). In 100 mM KCl or NaCl, the profiles of MA–01a showed a reversible transition at 295 nm, where melting and annealing curves were almost superimposable. The increase of absorbance from 70°C to 90°C could be explained by the dissociation of a helical domain within the structure. The T_m of MA–01a in 100 mM K^+ was determined to be 42.0°C, and 29.3°C in 100 mM Na^+(Fig. 4.20 A). The profiles showed an increase of absorbance at 260 nm (Fig. 4.20 B), indicating the dissociation of the G–tetrad structure.

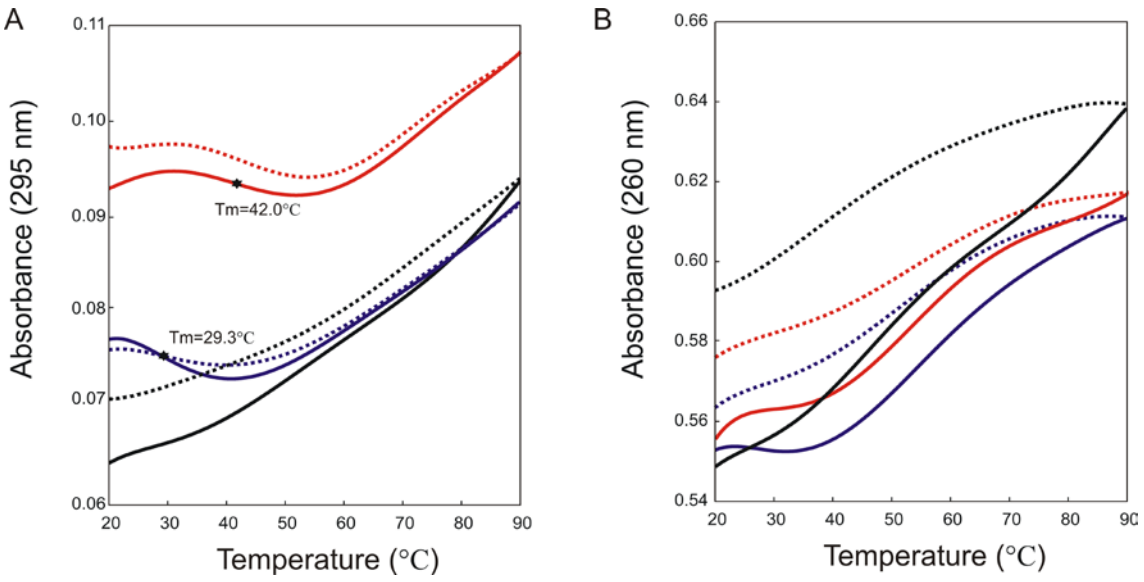

Figure 4.20 Thermal denaturation–renaturation curve of MA–01a. The melting curve is shown with a solid line, the annealing curve is shown with a dotted line (A) MA–01a at wavelength 295 nm. (B) MA–01a at wavelength 260 nm. Buffer conditions: 10 mM Tris/HCl (black), 100 mM Na^+ (blue), and 100 mM K^+ (red).

In Tris/HCl buffer, the UV–melting profile of MA–01g at 295 nm (Fig. 4.21 A) showed a similar profile compared with that of MA–01a. In 100 mM KCl or NaCl,

the profile showed reversible transitions with T_m values of 51.6°C and 46.9°C, respectively. The profiles showed an increase of absorbance at 260 nm (Fig. 4.21 B), indicating the dissociation of the G–tetrad structure. This indicated that both aptamers, MA–01a and MA–01g, were folded into very stable intramolecular G–quadruplexes. The monovalent ion dependence for stabilization of folded MA–01a and MA–01g, as judged by the T_m values, was in the order $K^+ > Na^+$, which was consistent with the data obtained by CD measurements.

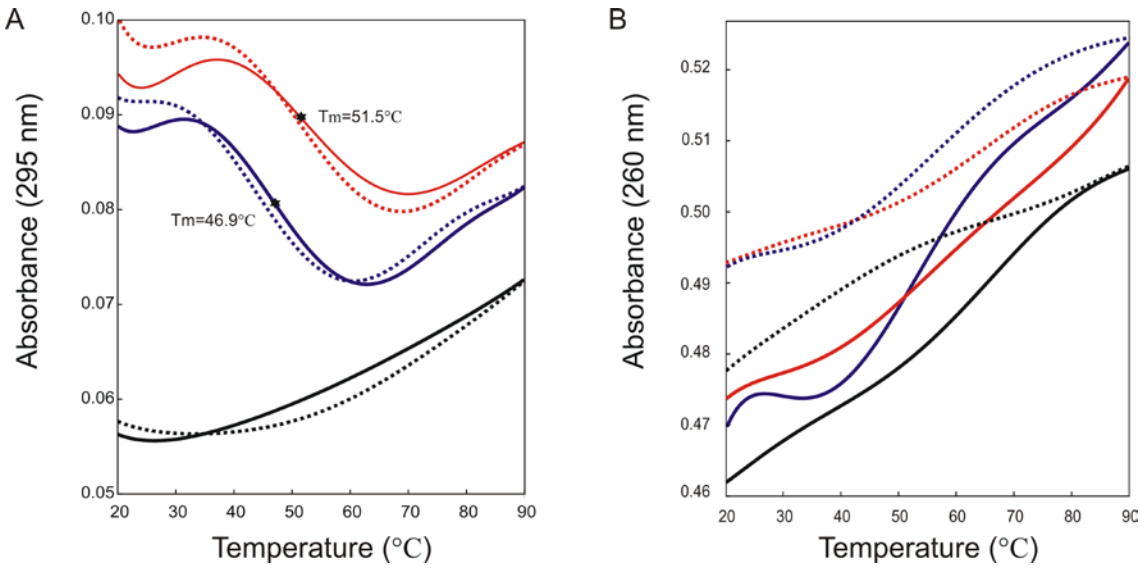

Figure 4.21 Thermal denaturation–renaturation curve of MA–01g. The melting curve is shown with a solid line, the annealing curve is shown with a dotted line. (A) MA–01g at wavelength 295 nM. (B) MA–01g at wavelength 260 nm. Buffer conditions: 10 mM Tris/HCl (black), 100 mM Na^+ (blue), and 100 mM K^+ (red).

4.5 Clinical Potential of MM IgG1 Aptamers

4.5.1 Serum Stability of MM IgG1 Aptamers

A prerequisite for a potential therapeutic use of the aptamers is a reasonable stability in mammalian serum. Different from RNA, which is very easily degraded in biological fluids, DNA is much more stable, which suggests an advantage of DNA aptamers for clinical applications. To test the stability of MM IgG1 specific aptamers in human serum, stability assays were carried out by

incubating the aptamer MA–01 in human serum for up to 48 h (Fig. 4.22 A). The ssDNA library used for the SELEX experiment was also tested side by side (Fig. 4.22 B).

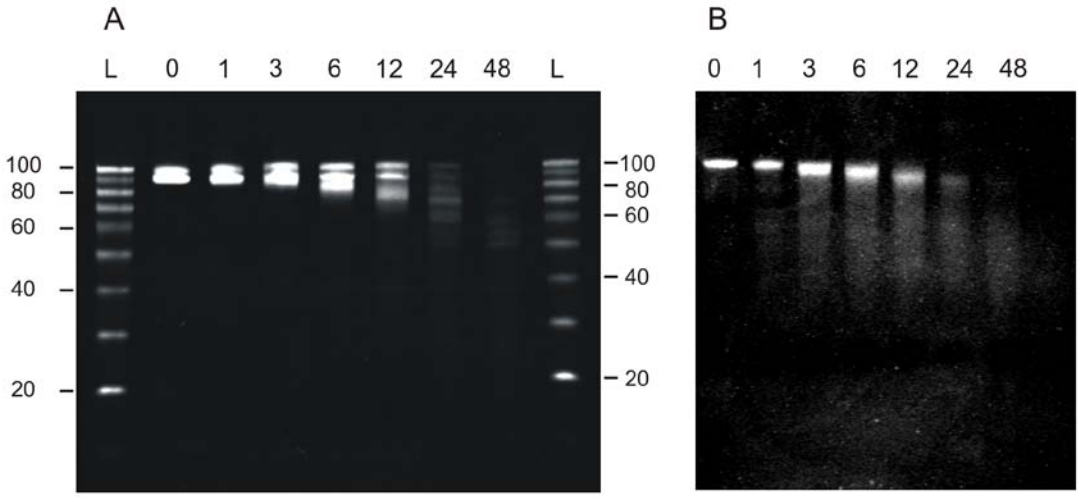

Figure 4.22 Stability of the aptamer MA–01 (A) and (B) the random ssDNA library in human serum. Aliquots were taken at the indicated times, L marks the size standard (10 bp DNA ladder). The results were reproduced in an independent experiment.

The incubation of aptamer MA–01 in human serum showed no evidence of degradation after one hour of incubation. Only partial degradation was observed after three hours. Even after 24 hours of incubation, the aptamer could still be detected on the gel. The stability of the library DNA was not as high as that of the aptamer, but was much higher than that of RNA, which degrades rapidly in human serum. This significant human serum stability of the MM IgG1 specific aptamer can be attributed to the G–quadruplexe structure, which made the aptamer less susceptible to nuclease degradation in human serum.

The serum of the patient containing the target antibody was required to evaluate the applicability of the MM IgG1 specific aptamers for MM diagnosis and therapy. However, the serum of this patient was unavailable according to the information from the company, which supplied the antibody. Therefore, a serum that could mimic the serum of the patient was prepared as a substitute (Fig. 4.23). Because the concentration of normal antibodies in the serum of a myeloma patient is very low, serum antibodies were removed from normal

human serum by ammonium sulphate precipitation to generate an antibody–free serum fraction. There was almost no antibody in this fraction, while all the other serum proteins remained (Fig. 4.23 lane 2). MM IgG1 of 2 µg was then added to 1 µl antibody–free serum to achieve a final concentration of 20 mg/ml, which is close to the level of MM antibody in the serum of the patient (Fig. 4.23 lane 4). The antibody–free serum and the mimic serum of the MM patient were used in aptamer–based assays designed for diagnostic and therapeutic purposes.

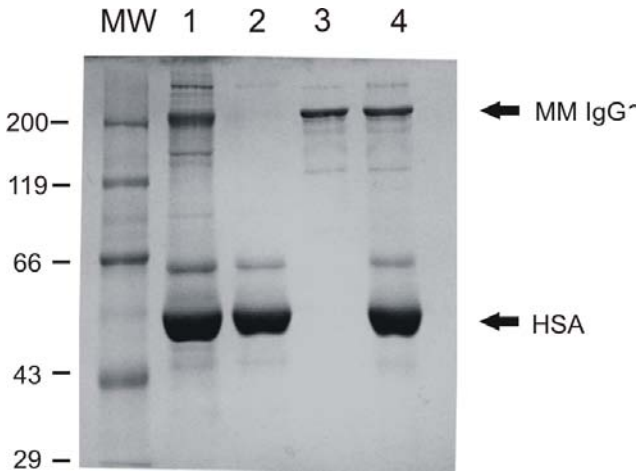

Figure 4.23 Preparation serum that mimics the serum of the MM patient. MW: protein ladder; lane 1: normal serum; lane 2: antibody–free serum fraction; lane 3: 2 µg MM IgG1; lane 4: serum that mimics the serum of the MM patient.

Detection of the M protein level can be very useful to evaluate the efficiency of the treatment as well as to monitor the recurrence of the disease. Thus, an aptamer–based ELISA was established to test the ability of the aptamers to detect low concentrations of M protein in the background of normal serum proteins. Both, the 3'–biotinylated aptamer MA–01a and a 3'–biotinylated ssDNA library, were immobilized on streptavidin coated plates. MM IgG1 was added to the antibody–free serum to achieve a series of final concentrations from 1 nM to 500 nM. The serum with MM IgG1 was added to the plates and incubated for 30 min. HRP–conjugated 2nd antibody and HRP substrate were added and absorbance was measured at 450 nm to detect the binding of MM IgG1 to the immobilized nucleic acids (Fig. 4.24).

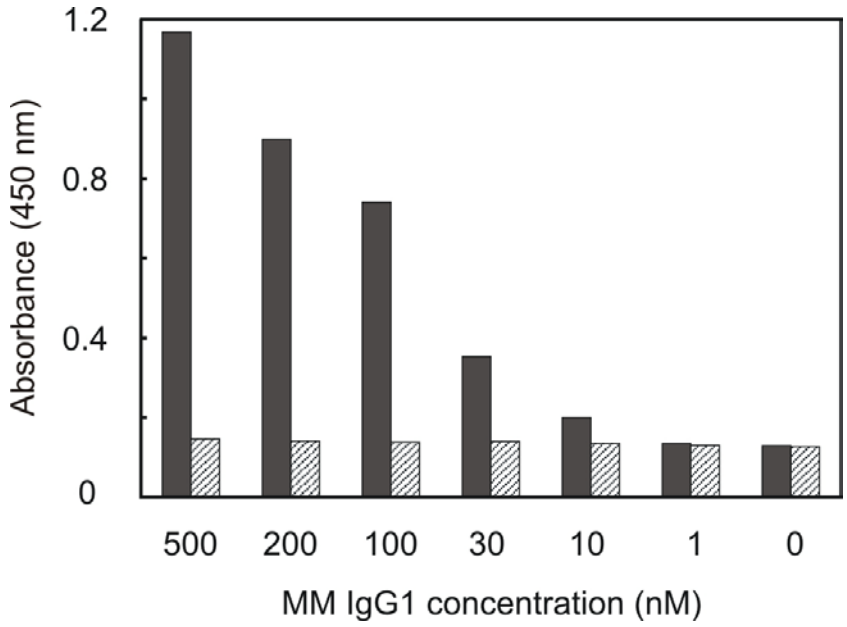

Figure 4.24 Aptamer–based ELISA for MM IgG1 detection. Biotinylated aptamer MA–01a (black) and the ssDNA library (white) were immobilized on a streptavidin–coated plate. The X axis indicates MM IgG1 concentration and the Y axis indicates the absorbance at 450 nm. Experiments were carried out in duplicate.

The results showed that the immobilized aptamer could detect the MM IgG1 from the human serum at concentrations as low as 10 nM. In contrast, almost no binding was detected for the immobilized library DNA. This was also an indication of the superior specificity of the aptamer since the other proteins and matrix in the serum did not interact with the aptamer. This aptamer–based ELISA will allow an easy, quantitative, and sensitive assay for serum M protein detection.

The large amount of M protein in the blood circulation of MM patients is the main cause of kidney damage and high blood viscosity. Removing M protein from the serum of the patients could release these symptoms. Therefore, an aptamer–based affinity capture assay was designed as a model to demonstrate the ability of aptamers for MM IgG1 to specifically eliminate the M protein from the human serum.

The 3'–biotinylated aptamer MA–01a was immobilized on NeutrAvidin agarose beads. Dilution of 1% antibody–free serum with 20 mg/ml MM IgG1

was added to the beads and incubated for 30 min. Bound proteins were then eluted. The loading sample, flow through fraction and elution fraction were checked on a SDS–PAGE gel (Fig. 4.25).

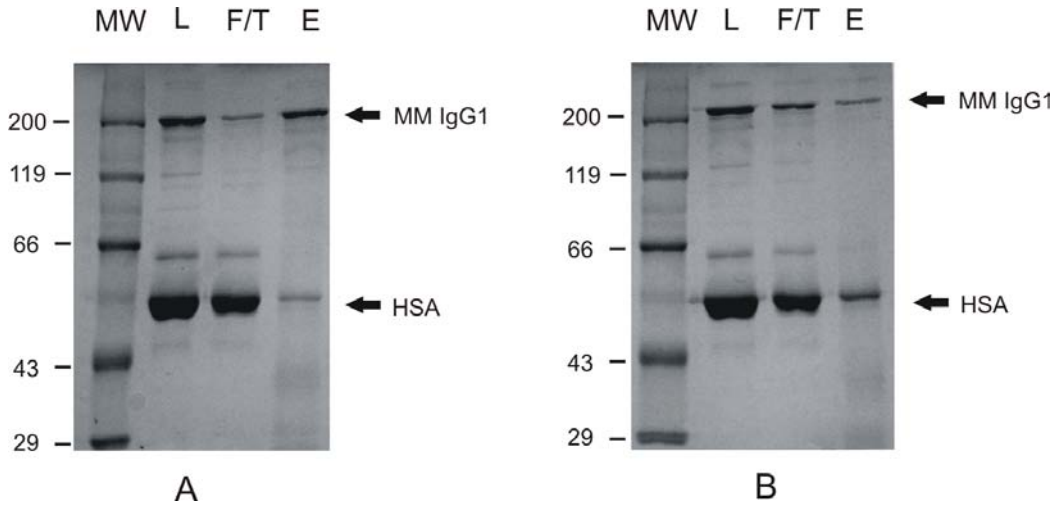

Figure 4.25 Capture of MM IgG1 from serum with immobilized aptamer. (A) 3'–biotinylated MA–04a and (B) A 3'–biotinylated library ssDNA were immobilized to NeutrAvidin agarose beads. Lanes contain the protein ladder (MW), column load (L), flow through (F/T), and elution (E) fractions, respectively.

For the immobilized aptamer, one clear band representing the MM IgG1 with about the same density as that of the loaded sample could be observed in the elution fraction (Fig. 4.25 E). This indicated that the MM IgG1 was effectively retained on the column, while other serum proteins were not retained and therefore collected in the flow through fraction (Fig. 4.25 A F/T). A column with immobilized library DNA was prepared to serve as control. In the elution fraction (Fig. 4.25 B E), a very weak band representing MM IgG1 could be observed, indicating that very few MM IgG1 was retained by the library DNA. In contrast, there was a strong band of human serum albumin (HSA) in this fraction, indicating non–specific binding of the library DNA to the HSA. This result suggested that the column modified with the aptamer for MM IgG1 could very specifically and efficiently retain myeloma protein from the human serum. Moreover, the binding of the aptamer to the target antibody was not interfered by the abundant proteins in the serum, which was an additional proof of the high specificity of the aptamer.

5 Discussion

In this thesis I have used *in vitro* selection and amplification to identify DNA aptamers that bound to a myeloma immunoglobulin. The best ligand bound to the target with a K_d of 172 nM in a very specific manner. Sequence alignment of selected ligands revealed a G–rich consensus motif among all high–affinity aptamers. This consensus motif could be folded into a common hairpin loop–stem motif by secondary structure prediction. CD spectra and UV melting profiles indicated the formation of G–quadruplex structures by this motif. The aptamers showed high stability in human serum. Furthermore, the results of aptamer–based ELISA and affinity capture assay approved that these myeloma protein specific aptamers could be very useful in myeloma diagnosis and therapy.

5.1 Optimization of In Vitro Selection Conditions

There is no standard SELEX protocol that is suitable for all targets. Therefore, the conditions of an individual *in vitro* selection need to be optimized according to the target properties and the requirements of selected aptamers.

One of the important aspects for oligonucleotide library design is the length of the central random region. The known simple single–stranded oligo-nucleotide motifs can be built from 30 nucleotides (Gold *et al.* 1995): hairpins, bulges within helices, pseudoknots, and G–quartets. Longer random region gives the library a greater structure complexity, which is particularly important for targets which are not known to be associated with or to bind to nucleic acids. Therefore, a longer random sequence pool may provide better opportunities for the identification of aptamers (Marshall & Ellington 2000). However, it was shown in several SELEX experiments that the efficiency of aptamer selection decreased, when the random region was longer than 70 nt (Legiewicz *et al.* 2005). Thus, in this project, a ssDNA library containing a 50–nt central block of random sequence was used for the *in vitro* selection of aptamers against a MM

IgG1. This length of the random region was considered to be ideal for the antibody target, because the complexity of the library is sufficient, the chemical synthesis of such library is cost–effective, and the amount of nucleic acids is easy to handle.

Analysis shows that there is no difference between RNA and DNA aptamers in terms of affinity and specificity (Gold 1995a). Moreover, DNA aptamers have certain advantages over RNA aptamers. The SELEX procedure for DNA aptamers is much faster and easier than that for RNA aptamers. DNA aptamers exhibit much higher stability in a broad range of conditions including biological fluids, which makes them more suitable for clinical applications. Therefore, a ssDNA library was chosen instead of a RNA library in this work.

For the first round of selection, a chemically synthesized ssDNA library was used directly without PCR amplification. Some researchers prefer a large scale amplification of the random library before initiating the selection process in order to eliminate damaged DNA synthesis products, which cannot be amplified by PCR (Marshall & Ellington 2000). However, it is assumed that chemically synthesized DNA molecules are amplified by the polymerase with different efficiency. Therefore, it is possible to lose some of the target–binding sequences in the original library. Moreover, the large scale PCR is a very time and material consuming process. The majority of the oligonucleotides in the original library showed intact length on the denaturing gel. Thus, a library with about 3×10^{15} sequences was used directly in the first round of selection.

Lambda exonulease digestion offered an easy and fast method for ssDNA preparation. Employing an optimized digestion condition, ssDNA for the next round of selection could be prepared in less than an hour. Since the ssDNA preparation is the most time consuming step in the standard SELEX procedure, the speed of SELEX was greatly improved and one round of selection could be achieved in one day.

Nitrocellulose filter partitioning was used to monitor the formation of antibody–DNA complexes. The pre–treatment of the filters with alkaline effectively decreased the nonspecific binding of ssDNA to the filters. The counter–selection step before each round of selection removed the matrix

binders from the library. Therefore, almost 98% of the sequenced variants obtained after nine cycles of selection turned out to be target binders.

5.2 Binding Affinity and Structural Features of the Aptamers

Eighteen out of nineteen selected variants were shown to bind to the target antibody with high affinity in the filter binding assays. The K_d of the best binder MA–01 was determined to be 172 nM. Furthermore, in the aptamer–based ELISA, the immobilized aptamer could detect MM IgG1 from human serum at concentrations as low as 10 nM. For certain applications, this binding affinity may not be sufficient. With a second selection experiment, employing a partially randomized pool based on the already selected aptamers, one could likely improve this affinity towards the low nanomolar or even picomolar range (Williams *et al.* 1997; Davis & Szostak 2002).

The variety of structural elements of DNA allows it to bind to its targets and accomplish its many functions. The alignment of the selected aptamers revealed three conserved sequences among all binders, which could be folded into a common motif of stem–loop structure by secondary structure prediction. Moreover, the consensus motif containes several Gs which are spaced in a regular pattern as G doublets, theoretically being able to fold into a tertiary structure called G–quadruplex (Davis 2004). However, the Zuker algorithm program for secondary structure prediction is unable to predict the G–quadruplex structures (Saito & Tomida 2005). Recently, CD spectrum and UV melting curve assay are used widely in G–quadruplex research to detect the existence of the structure and study the effects of different cations and solutions on G–quadruplex formation (Li *et al.* 2005). CD spectra and UV melting curves showed the existence of G–quadruplex structures of the aptamers MA–01a and MA–01g. The CD spectra suggested that there were both chair and basket types of G–quadruplex in solution. Potassium showed a stronger stabilization effect than sodium in both assays, which is consistent with literature (Phan *et al.*

2006). The CD spectra also demonstrated a rapid formation of the G–quadruplex structure of MA–01a.

Is the conserved G–quadruplex motif directly involved in the binding of the aptamer? This conserved motif was represented in almost 98% of clones sequenced. The DNAs containing this motif were able to bind to MM IgG1. In contrast, DNAs lacking this motif did not bind to the target. Therefore, it is conceivable that this motif is responsible for the binding of the aptamers to the targets. A 31–nt aptamer MA–01a was synthesized, containing the consensus motif and the extended stem, to answer this question. The affinity of MA–01a was more than 2–fold lower as compared to the full–length ligand. This result indicated that this conserved motif might be the binding motif of the aptamer, however, the flanking areas also contributed to the binding. The stem of selected aptamers showed little sequence conservation, indicating that its content is largely irrelevant for the target binding. This idea was supported by the fact that the replacement of the stem of MA–01a with a longer and more stable one (MA–01c) did not change the binding affinity of MA–01a. The truncated variant MA–01g, containing only the 19–nt consensus sequence, however, showed no binding activity at the tested concentrations despite the experimental confirmation of the G–quadruplex structure. These results highly suggested that the conserved G–quadruplex structure itself is not enough for binding, an extended stem is also required. The exact interaction of the aptamer and antibody will rely on the solution of the three–dimensional structure of the aptamer–antibody complex by X–ray or NMR methods.

There is a growing interest in DNA quadruplexes as they are important as lead molecules in drug design (Neidle & Parkinson 2008) and as a structural motif potentially adopted by telomere (Williamson 2004) and fragile X immunoglobulin switch regions (Kettani *et al.* 1995). Recently, this structure is also found in the core of a number of aptamers including the thrombin binding aptamer (Bock *et al.* 1992; Macaya *et al.* 1993; Schultze *et al.* 1994) and an inhibitor of HIV integrase (Jing & Hogan 1998). The structure of DNA aptamers for MM IgG1 appears to be similar to that for thrombin. The solution structure of the thrombin aptamer has been solved by NMR (Macaya *et al.* 1993;

Schultze *et al.* 1994). These studies indicate that this 15–mer aptamer 5'–GGTTGGTGTGGTTGG–3' forms two stacked G–quartets, with all adjacent strands antiparellel and a *syn–anti* alternation of G's around each quartet and along each strand. This structure has two minor and two major grooves, arranged such that the minor grooves are spanned by TT loops below the lower quartet (loop 1 and loop 3), while the TGT loop spans the major groove above the top quartet (loop 2). Thrombin is thought to recognize its aptamer mainly *via* the arrangement of phosphates on the outside of the aptamer (Paborsky *et al.* 1993)

The model for MM IgG1 aptamers invoke also two stacked G–quartets. Loop 2 of all aptamers were highly conserved with either one G or two Gs. According to the primary sequence of the loops, the aptamers could be divided into four families. Loop1 and loop3 were highly conserved for the aptamers from the same family and differed greatly in length and sequence for the aptamers from different families. The only common element found for all families was a highly conservation of a pyrimidine in loop3. However, despite the highly variable loop1 and loop3, aptamers from different families showed no obvious difference in terms of binding affinities. Therefore, the MM IgG1 specific aptamers most likely recognize the ligands with the highly conserved bases (5'–end C and 3'–end T) located above the top quartet, the highly conserved loop2 and the pyramidine in loop3. This is consistent with a model, where the stacked G–quartets act as a stable structural framework upon which important functional groups can be precisely arrayed.

5.3 Binding Specificity of the Aptamers

High specificity of aptamers for M protein is very important for future clinical applications. The results of binding specificity showed that the aptamer MA–01 had no binding affinity towards normal human serum IgGs and the Fab or Fc fragments of human IgGs. Moreover, the aptamer–based affinity capture assay showed that the immobilized aptamer could capture the MM IgG1 specifically from the human serum. These results indicated that the aptamer did not interact

with normal serum antibodies or other serum proteins of the patients. Therefore, the aptamers would have few side effects in applications.

The specificity of the aptamer is also an important hint towards the binding site of the aptamers on the MM antibody. Aptamers to proteins, like antibodies, recognize specific sites on the target surface, which are called aptatopes. It is assumed that most aptamers recognize structured aptatopes on protein targets (Eaton *et al.* 1995; Petach & Gold 2002). The specificity of the aptamers highly suggested that the variable (antigen recognition) domain rather than the constant domain was the aptatope for the MM IgG1 aptamer. A competition binding assay with the specific aptamer and the natural antigen of the antibody could be used to demonstrate this hypothesis. Unfortunately, the antigen of this myeloma antibody is unknown. However, the concept of aptamer binding to the variable domain can be deduced from the lack of interaction of the aptamer with a MM IgG1 from a different patient and a monoclonal human IgG1, since these target structures differed in the antigen binding pockets of the antibodies only.

Antibodies are large molecules possessing extensive surfaces with ridges, grooves, projections and depressions, all decorated with numerous H–bond donors and acceptors. However, the highly conserved motif in all aptamers suggested that all aptamers bound to one single aptatope on the antibody. Analysis of numerous protein SELEX experiments shows that in the course of selection, one aptatope of a protein target may become dominant in the presence of many other potential sites for oligonucleotide binding, and usually they are the receptor domains. The effect of domination of a limited number of different aptatopes is evidently explained by the nature of *in vitro* selection. During the SELEX process, only a small number of the most efficient binders are selected and amplified, whereas other sequences are gradually excluded from the library. This effect is revealed more clearly in complex SELEX in which just several classes of aptamers were obtained despite the presence of many thousand different protein targets. Fritter and James (2005) found during their selection of aptamers to human blood plasma that at initial rounds the enriched library contains different families of aptamers to many plasma proteins, whereas after further rounds of selection the number of different classes of aptamers

declined obviously. Therefore, the most efficient aptamers binding to certain aptatope can be achieved by increasing the number of selection rounds.

The specificity of the selected apatmers to the MM IgG1 suggested that mAb also has a dominant aptatope for aptamer binding, and this aptatope appears to coincide with the antigen binding site. This idea was supported by other published aptamers against mAbs (Doudna *et al.* 1995; Missailidis *et al.* 2005). Aptamers binding to the antigen–binding sites resemble anti–Id antibodies which react with the Id on a particular antibody molecule. Therefore, these aptamers can be called “anti–Id aptamers”. It should also be noted that the existence of a dominant aptatope on antibody does not preclude selection for ligands that bind to other sites. By reducing the number of selection rounds, or employing polyclonal antibodies or the constant fragments as the target in the *in vitro* selection, it is possible to obtain more aptamer classes binding to different aptatopes, such as the constant region of an antibody (Yoshida *et al.* 2008; Miyakawa *et al.* 2008).

5.4 Application of the Aptamers

As a real individual or patient–specific agent with high affinity and specificity to the myeloma monoclonal protein, the MM IgG1 specific aptamers could serve for several unique applications in both basic research and clinical areas.

The aptamers could be used in DNA–antibody recognition and interaction studies. Until now, much is known about how antibodies recognize protein antigens, where the general rules are similar to those that govern protein–protein recognition (Braden & Poljak 1995; Davies & Cohen 1996). There is little information about how antibodies recognize DNAs, because of the low antigenicity of DNAs and the difficulties in raising antibodies against them (Stollar 1986). The most frequently found anti–DNA autoantibodies are those related to the autoimmune disease – SLE (Stollar 1994). These antibodies are not specific to particular sequences of ssDNA or dsDNA. The aptamers specific for a mAb can provide an excellent model to study the DNA–antibody recognition and interaction. Therefore, analysis of the three–dimensional

structure of aptamer–antibody complexes could be very useful for our basic understanding of antibody–nucleic acid interaction.

One major hindrance to the clinical use of aptamers is their instability in body fluids due to high levels of nuclease activity. Without any modification to increase the stability, the aptamer MA–01 remained stable in human serum for several hours. This stability indicated its resistance to nucleases, which might be due to the G–quadruplex structure of the aptamer. The aptamer should be stable enough for most clinical assays. The results of aptamer–based MM IgG1 detection and the affinity capture assays in the presence of human serum supported this idea.

As a specific tumor cell marker, M protein is used to evaluate the effect of treatment as well as to monitor the expansion of the tumor. The MM IgG1 specific aptamers could overcome current limitations in myeloma diagnosis. For example, it has been proposed recently that the M protein must no longer be detectable by immunofixation, which is about 50–200 µg/ml of serum M protein, in order to qualify for the patient as having complete remission (Bladé *et al.* 1998). The sensitivity of the aptamer–based ELISA assay was as low as 1.5 µg/ml. This technology could thus provide a fast, sensitive and easy–to–use detection system for a M protein of a myeloma patient.

Another promising application of the aptamer in diagnosis could be *in vivo* imaging of a myeloma tumor. The use of aptamers for *in vivo* imaging is especially suitable because of the very wide range of possibilities available through defined chemical modifications that will modify their pharmacokinetic properties (Tavitian *et al.* 1998). For instance, the clearance rates of aptamers can be changed to keep them in circulation by anchoring them to liposome bilayers, by coupling them to inert large molecules such as polyethylene glycol or to other hydrophobic groups (Willis *et al.* 1998). The discrimination and targeting capacities of aptamers suit them exquisitely as imaging agents for non–invasive diagnostic procedures.

The anti–Id aptamers could be used in myeloma therapy as well. Over the last decade, a considerable amount of clinical data of Id vaccines in the treatment of MM has been published. However, MM likely represents the clinical

setting in which Id vaccines have collected the most disappointing results. This may be due to the large amount of M proteins secreted by myeloma cells, which block Id–specific antibodies before they can reach the surface of myeloma cells. The aptamer–based capture assay in this work showed a high potential to eliminate M proteins from the serum, which could possibly enhance the effect of anti–Id antibody therapy. Moreover, M protein is also the main reason for hyperviscosity syndrome and renal insuffiency in MM patients. So aptamer–based apheresis to eliminate the antibodies could release these syndromes without interfering with normal antibodies in the serum.

Anti–Id aptamers could also be utilized to eliminate MM cells from the bone marrow. By using the combinations of mAb and immunobeads, Shimazaki and colleagues (1988) successfully purged myeloma cells from bone marrow *ex vivo*. This is a reliable and nontoxic method to eliminate contaminating myeloma cells in preparing an autologous bone marrow transplantation in patients. Although not tested yet, according to their high binding affinities to the antibody and the stability in human serum, the aptamers should be highly eligible for this purpose.

In addition, anti–Id aptamers could be used in targeted therapy. Aptamers are suitable to serve as escort ligands in which the aptamer oligonucleotide may be used to deliver an active drug, radionuclide, toxin, or cytotoxic agent to the desired sites for targeted therapies (Hicke & Stephens 2000). Compared with antibodies, aptamers are smaller and travel better, penetrate tumor tissue better and have a faster circulation clearance rate. In case the stability of the aptamers can not meet the requirement for targeted therapies, many strategies can be utilized to improve the nuclease resistance of the aptamers, including the use of chemical modifications such as phosphoRothe, Germanyioate, locked nucleic acid, 2'–*O*methyl–and 2'–fluoro–nucleotides (Kurreck 2003), as well as mirror–image Spiegelmers (Vater & Klussmann 2003).

In conclusion, aptamers have been successfully obtained for a M protein from a myeloma patient. This methodology provides the possibility of rapidly selecting individual aptamers for any MM patients. Aptamer offers significant advantages over existing anti–Id antibodies in that they offer higher binding affinity and specificity to the target, lower immunogenicity and increased tumour

penetration. Therefore, they could be used in a number of applications in myeloma diagnosis and therapy, ranging from immunoassays to apheresis, enhancing immunotherapy efficiency, *in vivo* imaging and targeted therapies.

6 Summary

Multiple myeloma (MM) is a clonal B cell malignancy. The idiotype (Id) of the monoclonal (M) protein secreted by the tumor cells is a well–defined, tumor–specific marker. Thus, the Id has becomes an intriguing target for the treatment of MM. Aptamers binding to the Id with high affinity and specificity could be very useful in MM diagnosis and therapy.

This work focused on the selection and characterization of specific DNA aptamers for a MM IgG1 using the in vitro selection (SELEX) from an initial pool of 3×10^{15} different ssDNAs with a 50–nt central block of randomized sequence. After nine rounds of selection and amplification, 19 different variants were isolated and 18 of them proved to be target binders. Highly G–rich consensus sequence elements were identified and could be folded into a common stem–loop structure by the Mfold program. CD and UV spectra indicated that the loop forms a G–quadruplex in solution. The best binder MA–01 exhibited a dissociation constant (K_d) of 172 nM. Binding affinities of three truncated versions of MA–01 indicated that the G-quadruplex might be directly involved in target recognition, while the stem was also required for binding. The aptamer was proven to be very specific for the target antibody. The aptamer binds to the variable region of the antibody, or even to the antigen binding pocket of the antibody.

The potential of the aptamer was evaluated for future diagnosis and therapy. The aptamer exhibited high stability in human serum. An aptamer–based ELISA allowed the detection of MM IgG1 in human serum at concentrations as low as 10 nM. In addition, the chromatographic properties of the aptamer were tested. The immobilization of the aptamer did not change the binding ability. Moreover, the aptamer exhibited a pH dependent binding property, which could be used to regenerate the column matrix. The immobilized aptamer could specifically capture MM IgG1 from human serum.

Therefore, this work offers the possibility to generate anti–Id aptamers. Such patient and tumor specific aptamers could have a number of potential implications ranging from diagnosis, apheresis and targeted therapies of B cell malignancies.

7 Zusammenfassung

Das multiple Myelom (MM) ist eine maligne Erkrankung klonaler B-Zellen. Der Idiotyp (Id) des monoklonalen Antikörpers, der von den Tumorzellen sekretiert wird, ist ein gut definierter, Tumor-spezifischer Marker. Daher wird der Id zu einem interessanten Zielmolekül für die Behandlung von MM. Aptamere, die an den Id mit hoher Affinität und Spezifität binden, könnten sehr nützlich für die Diagnose und Therapie von MM werden.

Diese Arbeit konzentriert sich auf die Selektion und Charakterisierung von spezifischen DNA-Aptameren für ein MM IgG1 mit Hilfe der *in-vitro*-Selektion (SELEX) aus einem Pool von 3×10^{15} verschiedenen ssDNAs mit einem zentralen Block von 50 Nukleotiden mit Zufallssequenz. Nach neun Runden von Selektion und Amplifikation wurden 19 verschiedene Varianten isoliert, von denen 18 an das Zielmolekül binden konnten. Eine G-reiche Konsensus-Sequenz wurde identifiziert, die mit dem Mfold-Programm in eine gemeinsame Stem-Loop-Struktur gefaltet werden konnte. CD- und UV-Spektren weisen für den Loop auf die Ausbildung einer G-Quadruplex-Struktur. Der beste Binder MA-01 zeigte ein Dissoziationskonstante (K_d) von 172 nM. Bindungsaffinitäten von drei verkürzten Versionen von MA-01 weisen darauf hin, dass die G-Quadruplex-Struktur direkt mit dem Zielmolekül wechselwirkt, wobei auch der Stem für die Bindung benötigt wird. Es konnte gezeigt werden, dass das Aptamer den Ziel-Antikörper spezifisch erkennt. Das Aptamer bindet in der variablen Region des Antikörpers oder sogar in der Antigen-bindenden Tasche des Antikörpers.

Das Potenzial des Aptamers für die zukünftige Diagnose und Therapie wurde evaluiert. Das Aptamer zeigte hohe Stabilität in humanem Serum. Ein Aptamer-abhängige ELISA erlaubt den Nachweis von MM IgG1 in humanem Serum bis zu Konzentrationen von 10 nM. Zudem wurden die chromatographischen Eigenschaften des Aptamers getestet. Die Immobilisierung des Aptamers verhindert nicht die Bindung. Darüber hinaus ist die Bindung abhängig vom pH-Wert, was zur Regenerierung der Säulenmatrix genutzt werden kann. Das immobilisierte Aptamer konnte spezifisch MM IgG1 aus menschlichem Serum entfernen.

Diese Arbeit bietet die Möglichkeit, anti-Id Aptamere zu generieren. Diese Patienten- und Tumor-spezifischen Aptamere besitzen eine Mehrzahl potenzieller Anwendungen, wie Diagnose, Apherese und zielgerichtete Therapie von B-Zell-malignen Erkrankungen.

8 References

Adams GP & Weiner LM. Monoclonal antibody therapy of cancer. *Nat. Biotechnol.* **2005**, 23, 1147–1157.

Allen P, Worland S & Gold L. Isolation of high–affinity RNA ligands to HIV–1 integrase from a random pool. *Virology* **1995**, 209, 327–336.

Andreola ML, Calmels C, Michel J, Toulme JJ & Litvak S. Towards the selection of phosphoRothe, Germanyioate aptamers–optimizing *in vitro* selection steps with phosphoRothe, Germanyioate nucleotides. *Eur. J. Biochem.* **2000,** 267, 5032–5040.

Baldrich E, Restrepo A & O´Sullivan, CK. Aptasensor development: Elucidation of critical parameters for optimal aptamer performance. *Anal. Chem.* **2004**, 76, 7053–7063.

Bardeesy N & Pelletier J. Overlapping RNA and DNA binding domains of the wt1 tumor suppressor gene product. *Nucleic Acids Res.* **1998**, 26, 1784–1792.

Barlogie B, Shaughnessy J, Munshi N & Epstein J. Plasma cell myeloma. In: Beutler E, Lichtman M, Coller B, Kipps T, Seligsohn U, eds. Williams Hematology (ed 6). New York: McGraw–Hill, **2001**, 1279–1304.

Bartlett JM & Stirling D. A Short History of the Polymerase Chain Reaction. *Methods Mol. Biol.* **2003**, 226, 3–6.

Beigelman L, McSwiggen JA, Draper KG, Gonzalez C, Jensen K, Karpeisky AM, Modak AS, Matulic–Adamic J, DiRenzo AB & Haeberli P. et al. Chemical modification of hammerhead ribozymes Catalytic activity and nuclease resistance. *J. Biol. Chem.* **1995**, 270, 25702–25708.

Bell SD, Denu JM, Dixon JE & Ellington AD. RNA molecules that bind to and inhibit the active site of a tyrosine phosphatise. *J. Biol. Chem*. **1998**, 273, 14309–14314.

Berezovski M, Drabovich A, Krylova SM, Musheev M, Okhonin V, Petrov A & Krylov SN. Nonequilibrium capillary electrophoresis of equilibrium mixtures: a universal tool for development of aptamers. *J. Am. Chem. Soc.* **2005**, 127, 3165–3171.

Bergenbrant S, Yi Q, Osterborg A, Bjorkholm M, Osby E, Mellstedt H. Lefvert AK & Holm G. Modulation of anti–idiotypic immune response by immunization with the autologous M–component protein in multiple myeloma patients. *Br. J. Haematol.* **1996**, 92, 840–846.

Berglund JA, Charpentier B & Rosbash M. A high affinity binding site for the HIV–1 nucleocapsid protein. *Nucleic Acids Res*. **1997**, 25, 1042–1049.

Bianchini M, Radrizzani M, Brocardo MG, Reyes GB, Gonzalez SC & Santa–Coloma TA. Specific oligobodies against ERK–2 that recognize both the native and the denatured state of the protein. *J. Immunol. Methods* **2001**, 252, 191–197.

Bladé J, Samson D, Reece D, Apperley J, Björkstrand B, Gahrton G, Gertz M, Giralt S, Jagannath S & Vesole D. Criteria for evaluating disease response and progression in patients with multiple myeloma treated by high–dose therapy and haemopoietic stem cell transplantation. Myeloma Subcommittee of the EBMT. *Br. J. Haematol.* **1998**, 102, 1115–1123.

Blank M, Weinschenk T, Priemer M, Schluesener H. Systematic evolution of a DNA aptamer binding to rat brain tumor microvessels Selective targeting of endothelial regulatory protein pigpen. *J. Biol. Chem.* **2001**, 276, 16464–16468.

Bless NM, Smith D, Charlton J, Czermak BJ, Schmal H, Friedl HP & Ward PA. Protective effects of an aptamer inhibitor of neutrophil elastase in lung inflammatory injury. *Curr. Biol.* **1997**, 7, 877–880.

Bock C, Coleman M, Collins B. Davis J, Foulds G, Gold L, Greef C, Heil J, Heilig JS, Hicke B, Hurst MN, Husar GM, Miller D, Ostroff R, Petach H, Schneider D,Vant–Hull B, Waugh S, Weiss A, Wilcox SK & Zichi D. Photoaptamer arrays applied to multiplexed proteomic analysis. *Proteomics* **2004**, 4, 609–618.

Bock LC, Griffin LC, Latham JA, Vermaas EH & Toole JJ. Selection of single–stranded DNA molecules that bind and inhibit human thrombin. *Nature* **1992**, 35, 564–566.

Bogen B, Ruffini PA, Corthay A, Fredriksen AB, Frøyland M, Lundin K, Røsjø E, Thompson K & Massaia M. Idiotype–specific immunotherapy in multiple myeloma: suggestions for future directions of research. *Haematologica* **2006**, 91, 941–948.

Boiziau C, Dausse E, Yurchenko L & Toulmé JJ. DNA aptamers selected against the HIV–1 trans–activation–responsive RNA element form RNA–DNA kissing complexes. *J. Biol. Chem.* **1999**, 274, 12730–12737.

Braden BC & Poljak RJ Structural features of the reactions between antibodies and protein antigens. *FASEB J.* **1995**, 9, 9–16.

Bradford M. A rapid and sensitive method for the quantitation of microgram quantities of protein utilizing the principle of protein–dye binding. *Anal Biochem.* **1976**, 72, 248–254.

Breaker RR. DNA aptamers and DNA enzymes. *Curr. Opin. Chem. Biol.* **1997**, 1, 26–31.

Brown D & Gold L. Template recognition by an RNA–dependent RNA polymerase: identification and characterization of two RNA binding sites on Q beta replicase. *Biochemistry* **1995**, 34, 14765–14774.

Bryan TM & Jarstfer MB. Interrogation of G–quadruplex–protein interactions. *Methods* **2007**, 43, 332–339.

Burge S, Parkinson GN, Hazel P, Todd AK & Neidle S. Survey and summary quadruplex DNA: sequence, topology and structure. *Nucleic Acids Res.* **2006**, 34, 5402–5415.

Cerchia L, Hamm J, Libri D, Tavitian B & de Franciscis V. Nucleic acid aptamers in cancer medicine. *FEBS Lett.* **2002**, 528, 12–16.

Charlton J, Kirschenheuter GP & Smith D. Highly potent irreversible inhibitors of neutrophil elastase generated by selection from a randomized DNA–valine phosphonate library. *Biochemistry* **1997a**, 36, 3018–3026.

Charlton J, Sennello J & Smith D. *In vivo* imaging of inflammation using an aptamer inhibitor of human neutrophil elastase. *Chem. Biol.* **1997b**, 4, 809–816.

Chatterjee M, Chakraborty T & Tassone P. Multiple myeloma: monoclonal antibodies–based immnothrapeutic strategies and targeted radiotherapy. *Eur. J. Cancer* **2006**, 42, 1640–1652.

Chen CH, Chernis GA, Hoang VQ & Landgraf R. Inhibition of heregulin signaling by an aptamer that preferentially binds to the oligomeric form of human epidermal growth factor receptor–3. *Proc. Natl. Acad. Sci. USA*. **2003**, 100, 9226–9231.

Cho JS, Lee YJ, Shin KS, Jeong S, Park J & Lee SW. *In vitro* selection of specific RNA aptamers for the NFAT DNA binding domain. *Mol. Cells* **2004**, 18, 17–23.

Ciesiolka J, Gorski J & Yarus M. Selection of an RNA domain that binds Zn^{2+}. *RNA* **1995**, 1, 538–550.

Coscia M, Mariani S, Battaglio S, Di BC, Fiore F, Foglietta M. Pileri A, Boccadoro M & Massaia M. Long term follow–up of idiotype vaccination in human myeloma as a maintenance therapy after high–dose chemotherapy. *Leukemia* **2004**, 18, 139–145.

Cox JC & Ellington AD. Automated selection of anti–protein aptamers. *Bioorg. Med. Chem.* **2001**, 9, 2525–2531.

Cox JC, Hayhurst A, Hesselberth J, Bayer TS, Georgiou G & Ellington AD. Automated selection of aptamers against protein targets translated *in vitro*: from gene to aptamer. *Nucleic Acids Res.* **2002a**, 30, e108.

Cox JC, Rajendran M, Riedel T, Davidson EA, Sooter LJ, Bayer TS, Schmitz–Brown M & Ellington AD. Automated acquisition of aptamer sequences. *Comb. Chem. High. T. Scr.* **2002b**, 5, 289–299.

Crawley C, Lalancette M, Szydlo R, Gilleece M, Peggs K, Mackinnon S, Juliusson G, Ahlberg L, Nagler A, Shimoni A, Sureda A, Boiron JM, Einsele H, Chopra R, Carella A, Cavenagh J, Gratwohl A, Garban F, Zander A, Björkstrand B, Niederwieser D, Gahrton G, Apperley JF; Chromic Leukaemia Working Party of the EBMT. Outcomes for reduced–intensity allogeneic transplantation for multiple myeloma: an analysis of prognostic factors from the Chronic Leukaemia Working Party of the EBMT. *Blood* **2005**, 105, 4532–4539.

Dapić V, Abdomerović V, Marrington R, Peberdy J, Rodger A, Trent JO & Bates PJ. Biophysical and biological properties of quadruplex oligodeoxy-ribonucleotides. *Nucleic Acids Res.* **2003**, 31, 2097–107.

Davies DR & Cohen GH. Interactions of protein antigens with antibodies. *Proc. Natl. Acad. Sci. USA.* **1996**, 93, 7–12.

Davis JH & Szostak JW. Isolation of high–affinity GTP aptamers from partially structured RNA libraries. *Proc. Natl. Acad. Sci. USA.* **2002**, 99, 11616–11621.

Davis JT. G–quartets 40 years later: From 5'–GMP to molecular biology and supramolecular chemistry. *Angew. Chem. Intl, Ed.* **2004**, 43, 668–698.

Davis KA, Abrams B & Lin Y, Jayasena SD. Use of a high affinity DNA ligand in flow cytometry. *J. Clin. Ligand Assay* **1997**, 20, 90–97.

Deitiker P, Ashizawa T & Atassi MZ. Antigen mimicry in autoimmune disease. Can immune responses to microbial antigens that mimic acetylcholine receptor act as initial triggers of Myasthenia gravis? *Hum. Immunol.* **2000**, 61, 255–265.

Dhodapkar KM, Krasovsky J, Williamson B & Dhodapkar MV. Antitumor monoclonal antibodies enhance cross–presentation of cellular antigens and the generation of myeloma–specific killer T cells by dendritic cells. *J. Exp. Med.* **2002**, 195, 125–133.

Doudna JA, Cech TR, Sullenger BA. Selection of an RNA molecule that mimics a major autoantigenic epitope of human insulin receptor. *Proc. Natl. Acad. Sci. USA.* **1995**, 1492, 2355–2359.

Drabovich A, Berezovski M, Krylov SN. Selection of smart aptamers by equilibrium capillary electrophoresis of equilibrium mixtures (ECEEM). *J. Am. Chem. Soc.* **2005**, 127, 11224–11225.

Drolet DW, Moon–McDermott L & Romig TS. An enzyme–linked oligonucleotide assay. *Nat. Biotechnol.* **1996**, 14, 1021–1025.

Drolet DW. Nelson J, Tucker CE, Zack PM, Nixon K, Bolin R, Judkins MB, Farmer JA, Wolf JL, Gill SC & Bendele RA. Pharmacokinetics and safety of an anti–vascular endothelial growth factor aptamer (NX1838) following injection into the vitreous humor of rhesus monkeys. *Pharmaceutical Research* **2000**, 17, 1503–1510.

Duconge F & Toulme JJ. *In vitro* selection identifies key determinants for loop–loop interactions: RNA aptamers selective for the TAR RNA element of HIV–1. *RNA* **1999**, 5, 1605–1614.

Durie BG. Multiple myeloma: what's new. *CA. Cancer J. Clin.* **2001**, 51, 271–272.

Eaton BE, Gold L & Zichi DA. Let's get specific: the relationship between specificity and affinity. *Chem. Biol.* **1995**, 2, 633–638.

Ellington AD & Szostak JW. *In vitro* selection of RNA molecules that bind specific ligands. *Nature* **1990**, 346, 818–822.

Ellington AD & Szostak JW. Selection *in vitro* of single–stranded DNA molecules that fold into specific ligand–binding structures. *Nature* **1992**, 355, 850–852.

Eulberg D, Buchner K, Maasch C & Klussmann S. Development of an automated *in vitro* selection protocol to obtain RNA–based aptamers: identification of a biostable substance P antagonist. *Nucleic Acids Res.* **2005**, 33, e45.

Eulberg D, Klussmann S. Spiegelmers, biostable aptamers. *Chem. BioChem*. **2003**, 4, 979–983.

Eyetech Study Group. Antivascular endothelial growth factor therapy for subfoveal choroidal neovascularization secondary to age–related macular degeneration, phase II study results. *Ophthalmology* **2003**, 110, 979–86.

Eyetech Study Group. Preclinical and phase 1A clinical evaluation of an anti–VEGF pegylated aptamer (EYE001) for the treatment of exudative age–related macular degeneration. *Retina* **2002**, 22, 143–152.

Famulok M. Oligonucleotide aptamers that recognize small molecules. *Curr. Opin. Struct. Biol.* **1999**, 9, 324–329.

Fitter S & James R. Deconvolution of a complex target using DNA aptamers. *J. Biol. Chem.* **2005**, 280, 34193–34201.

Fukuda K, Vishnuvardhan D, Sekiya S, Hwang J, Kakiuchi N, Taira K, Shimotohno K, Kumar PK & Nishikawa S. Isolation and characterization of RNA aptamers specific for the hepatitis C virus nonstructural protein 3 protease. *Eur. J. Biochem.* **2000**, 267, 3685–3694.

Gal SW, Amontov S, Urvil PT, Vishnuvardhan D, Nishikawa F, Kumar PK & Nishikawa S. Selection of a RNA aptamer that binds to human activated protein C and inhibits its protease function. *Eur. J. Biochem*. **1998**, 252, 553–562.

Garber K. ODAC panel gives nod to Bexxar. *J. Natl. Cancer Inst.* **2003**, 595, 189.

Gilbert W. Origin of life: The RNA world. *Nature* **1986**, 319, 618.

Ginsberg JA, Crowther MA, White RH & Ortel TL. Anticoagulation therapy. *Hematology Am. Soc. Hematol. Educ. Program.* **2001**, 339–357.

Giver L, Bartel DP, Zapp ML, Green MR & Ellington AD. Selection and design of high–affinity RNA ligands for HIV–1 Rev. *Gene* **1993**, 137, 19–24.

Gold L, Polisky B, Uhlenbeck O & Yarus M. Diversity of oligonucleotide functions. *Annu. Rev. Biochem.* **1995a**, 64, 763–797.

Gold L. Oligonucleotides as research, diagnostic, and therapeutic agents. *Biol. Chem.* **1995b**, 270, 13581–13584

Goldman B. Next generation of targeted radiotherapy drugs emerging from the clinical pipeline. *J. Natl. Cancer Inst.* **2004**, 96, 903–904.

Goore MY, Dickson JH & Lipkin S. Human leukocyte interferon produced by use of an antibody–free human serum fraction. *Appl. Microbiol.* **1973**, 25, 325–326.

Gopinath SC. Methods developed for SELEX. *Anal. Bioanal. Chem.* **2007**, 387, 171–182.

Gounni AS, Lamkhioued B, Ochiai K. Delaporte E, Capron A, Kinet JP, Capron M. High–affinity IgE receptor on eosinophils is involved in defence against parasites. *Nature* **1994**, 367, 183–186.

Green LS, Jellinek D, Bell C, Beebe LA, Feistner BD, Gill SC, Jucker FM & Janjić N. Nucleaseresistant nucleic acid ligands to vascular permeability factor/vascular endothelial growth factor. *Chem. Biol.* **1995**, 2, 683–695.

Green LS, Jellinek D, Jenison R, Ostman A, Heldin CH & Janjic N. Inhibitory DNA ligands to platelet–derived growth factor B–chain. *Biochemistry* **1996**, 35, 14413–14424.

Greipp RP & Kyle RA. Clinical morphological and cell kinetic differences among multiple myeloma, monoclonal gammopathy of undetermined significance, and smoldering myeloma. *Blood* **1982**, 62, 161–171.

Guerrier–Takada C & Altman S. Catalytic activity of an RNA molecule prepared by transcription *in vitro*. *Science* **1984**, 223, 285–286.

Guhlke S, Famulok M & Biersack HJ. Aptamares, a novel class of radiopharmaceutical with diagnostic and therapeutic potential. *Eur. J. Nucl. Med. Mol. Imaging* **2003**, 30, 1441–1443.

Hajighasemi F, Gharagozlou S, Ghods R, Khoshnoodi J, Shokri F. Private idiotypes located on light and heavy chains of human myeloma proteins characterized by monoclonal antibodies. *Hybridoma (Larchmt)* **2006**, 25, 329–335.

Hallek M, Bergsagel PL & Anderson KC. Multiple myeloma: increasing evidence for a multistep transformation process. *Blood* **1998**, 91, 3–21.

Hardin CC, Henderson E, Watson T & Prosser JK. Monovalent cation induced structural transitions in telomeric DNAs: G–DNA folding intermediates. *Biochemistry* **1991**, 30, 4460–4472.

Hardin CC, Watson T, Corregan M & Bailey C. Cation–dependent transition between the quadruplex and Watson–Crick hairpin forms of d(CGCG3GCG). *Biochemistry* **1992**, 31, 833–841

Harousseau JL. Stem cell transplantation in multiple myeloma (0, 1, or 2). *Curr. Opin. Oncol.* **2005**, 17, 93–98.

Hermann T & Patel DJ. Adaptive recognition by nucleic acid aptamers. *Science* **2000**, 287, 820–825.

Hicke BJ, Marion C, Chang YF, Gould T, Lynott CK, Parma D, Schmidt PG & Warren S. Tenascin–C aptamers are generated using tumor cells and purified protein. *J. Biol. Chem.* **2001**, 276, 48644–48654.

Hicke BJ, Stephens AW, Gould T, Chang YF, Lynott CK, Heil J, Borkowski S, Hilger CS, Cook G, Warren S & Schmidt PG. Tumor targeting by an aptamer. *J. Nucl. Med.* **2006**, 47, 668–678.

Hicke BJ & Stephens AW. Escort aptamers: a delivery service for diagnosis and therapy. *J. Clin. Invest*. **2000**, 106, 923–928.

Higuchi RG & Ochman H. Production of single-stranded DNA templates by exonuclease digestion following the polymerase chain reaction. *Nucleic Acids Res.* **1989**, 17, 5865.

Hofmann HP, Limmer S, Hornung V, Sprinzl M. Ni^{2+}–binding RNA motifs with an asymmetric purine–rich internal loop and a G–A base pair. *RNA* **1997**, 3, 1289–1300.

Holliger P & Hudson PJ. Engineered antibody fragments and the rise of single domains. *Nat. Biotechnol.* **2005**, 23, 1126–1136.

Homann M & HU Goringer. Combinatorial selection of high affinity RNA ligands to live African trypanosomes*. Nucleic Acids Res.* **1999**, 27, 2006–2014.

Hwang B, Han K & Lee SW. Prevention of passively transferred experimental autoimmune myasthenia gravis by an *in vitro* selected RNA aptamer. *FEBS Lett*. **2003**, 548, 85–89.

Hwang B & Lee SW. Improvement of RNA aptamer activity against myasthenic autoantibodies by extended sequence selection. *Biochem. Biophys. Res. Commun.* **2002**, 290, 656–662.

Hybarger G, Bynum J, Williams RF, Valdes JJ & Chambers JP. A microfluidic SELEX prototype. *Anal Bioanal. Chem.* **2006**, 384, 191–198.

Ikebukuro K, Kiyohara C & Sode K. Novel electrochemical sensor system for protein using the aptamers in sandwich manner. *Biosens. Bioelectron* **2005**, 20, 2168–2172.

Irvine D, Tuerk C & Gold L. SELEXION. Systematic evolution of ligands by exponential enrichment with integrated optimization by non–linear analysis. *J. Mol. Biol.* **1991**, 222, 739–761.

Ishida S. Usui T, Yamashiro K, Kaji Y, Amano S, Ogura Y, Hida T, Oguchi Y, Ambati J, Miller JW, Gragoudas ES, Ng YS, D'Amore PA, Shima DT & Adamis AP. VEGF164–mediated inflammation is required for pathological, but not physiological, ischemia–induced retinal neovascularization. *J. Exp. Med.* **2003**, 198, 483–489.

Jellinek D, Green LS, Bell C, Lynott CK, Gill N, Vargeese C, Kirschenheuter G, McGee DP, Abesinghe P & Pieken WA, et al. Potent 2'–amino–2'–deoxypyrimidine RNA inhibitors of basic fibroblast growth factor. *Biochemistry* **1995**, 34, 11363–11372.

Jellinek D, Lynott CK, Rifkin DB & Janjić N. High–affinity RNA ligands to basic fibroblast growth factor inhibit receptor binding. *Proc. Natl. Acad Sci. USA.* **1993**, 90, 11227–11231.

Jeon SH, Ben–Yedidia T & Arnon R. Intranasal immunization with synthetic recombinant vaccine containing multiple epitopes of influenza virus. *Vaccine* **2002**, 20, 2772–2780.

Jing N & Hogan ME. Structure activity of tetrad forming oligonucleotides as a potential anti–HIV integrase therapeutic drug. *J. Biol. Chem.* **1998**, 273, 34992–34999.

Kettani A, Kumar RA & Patel DJ. Solution structure of a DNA quadruplex containing the fragile X syndrome triplet repeat. *J. Mol. Biol.* **1995**, 254, 638–656.

Kim, YM, Choi KH, Jang YJ, Yu J & Jeong S. Specific modulation of the anti–DNA autoantibody–nucleic acids interaction by the high affinity RNA aptamer. *Biochem. Biophys. Res. Commun.* **2003**, 300, 516–523.

Kleinjung F, Klussman S, Erdmann VA, Scheller FW, Fürste JP & Bier FF. High affinity RNA as a recognition element in a biosensor. *Anal. Chem.* **1998**, 328–331.

Klussmann S, Nolte A, Bald R, Erdmann VA & Fürste JP. Mirror–image RNA that binds D–adenosine. *Nat. Biotechnol.* **1996**, 14, 1112–1115.

Kopylov AM & Spiridonova VA. Combinatorial chemistry of nucleic acids: SELEX. *Mol. Biol.* **2000**, 34, 940–954.

Kubik MF, Stephens AW, Schneider D, Marlar RA & Tasset D. High–affinity RNA ligands to human alphathrombin. *Nucleic Acids Res.* **1994**, 22, 2619–2626.

Kumar PK, Machida K, Urvil PT, Kakiuchi N, Vishnuvardhan D, Shimotohno K, Taira K & Nishikawa S. Isolation of RNA aptamers specific to the NS3 protein of hepatitis C virus from a pool of completely random RNA. *Virology*, **1997**, 237, 270–282.

Kuriakose P. Targeted therapy for hematologic malignancies. *Cancer Control* **2005**, 12, 82–90.

Kurreck J. Antisense technologies. Improvement through novel chemical modifications. *Eur. J. Biochem* **2003**, 270, 1628–1644.

Kusser W. Chemically modified nucleic acid aptamers for *in vitro* selections: evolving evolution. *J. Biotechnol.* **2000**, 74, 27–38.

Kuwahara M, Hanawa K, Ohsawa K, Kitagata R, Ozaki H & Sawai H. Direct PCR amplification of various modified DNAs having amino acids: convenient preparation of DNA libraries with high–potential activities for *in vitro* selection. *Bioorg. Med. Chem.* **2006**, 14, 2518–2526.

Kyle A. Myeloma and related disorders. In: Wiemik PH, ed. Neoplastic Disease of the Blood. New York: Chuichill Livingstone, **1985**, 385–676.

Lebruska LL & Maher LJ. 3rd. Selection and characterization of a RNA decoy for transcription factor NF–kappa B. *Biochemistry* **1999**, 38, 3168–3174.

Lee JF, Stovall GM & Ellington AD. Aptamer therapeutics advance. *Curr. Opin. Chem. Biol.* **2006**, 10, 282–289.

Lee SW & Sullenger BA. Isolation of a nuclease–resistant decoy RNA that selectively blocks autoantibody binding to insulin receptors on human lymphocytes. *J. Exp. Med.* **1996**, 184, 315–324.

Legiewicz M, Lozupone C, Knight R & Yarus M. Size, constant sequences, and optimal selection. *RNA* **2005**, 11, 1701–1709.

Li J, Correla JJ, Wang L, Trent JO & Chaires JB. Not so crystal clear: the structure of the human telomere G–quadruplex in solution differs from that present in a crystal. *Nucleic Acids Res.* **2005**, 33, 4649–4659.

Lim SH, Zhang Y, Wang Z, Varadarajan R, Periman P, Esler WV. Rituximab administration following autologous stem cell transplantation for multiple myeloma is associated with severe IgM deficiency. *Blood* **2004**, 103, 1971–1972.

Liss M, petersen B, Wolf H, Prohaska E. An aptamer–based quartz crystal protein biosensor. *Anal. Chem.* **2002**, 74, 4488–4495.

Longo DL. Plasma cell disorders. In: Braunwald E, Kasper D & Fauci A, eds. Harrison's principles of internal medicine (ed 15). **2001**, 727–733.

Lorger M, Engstler M, Homann M & Göringer HU. Targeting the variable surface of African trypanosomes with variant surface glycoproteins–specific serum stable RNA aptamers. *Eukaryot Cell* **2003**, 2, 84–94.

Lynch RG, Graff RJ, Sirisinha S, Simms ES & Eisen HN. Myeloma proteins as tumour–specific transplantation antigens. *Proc. Natl. Acad Sci. USA.* **1972**, 69, 1540–1544.

Macaya RF, Schultze P, Smith FW, Roe JA & Feigon J. Thrombin–binding DNA aptamer forms a unimolecular quadruplex structure in solution. *Proc. Natl. Acad. Sci. USA.* **1993**, 90, 3745–3749.

Maloney DG, Donovan K & Hamblin TJ. Antibody therapy for treatment of multiple myeloma. *Semin. Hematol.* **1999**, 36, 30–33.

Marshall KA & Ellington AD. *In vitro* selection of RNA aptamers. *Methods Enzymol.* **2000**, 318, 193–214.

McEntee K, Weinstock GM & Lehman IR. recA proteincatalyzed strand assimilation: stimulation by Escherichia coli single stranded DNA–binding protein. *Proc. Natl. Acad. Sci. USA.* **1980**, 77, 857–861.

Mendonsa SD & Bowser MT. *In vitro* evolution of functional DNA using capillary electrophoresis. *J. Am. Chem. Soc.* **2004a**, 126, 20–21.

Mendonsa SD & Bowser MT. *In vitro* selection of high–affinity DNA ligands for human IgE using capillary electrophoresis. *Anal. Chem.* **2004b**, 76, 5387–5392.

Mergny JL, Phan AT & Lacroix L. Following G–quartet formation by UV–spectroscopy. *FEBS Lett.* **1998**, 43, 574–578.

Misono TS & Kumar PKR. Selection of RNA aptamers against human influenza virus hemagglutinin using surface plasmon resonance. *Anal. Biochem.* **2005**, 342, 312–317.

Missailidis S, Thomaidou D, Borbas KE & Price MR. Selection of aptamers with high affinity and high specificity against C595, an anti–MUC1 IgG3 monoclonal antibody, for antibody targeting. *J. Immunol. Methods* **2005**, 296, 45–62.

Miyakawa S, Nomura Y, Sakamoto T, Yamaguchi Y, Kato K, Yamazaki S & Nakamura Y. Structural and molecular basis for hyperspecificity of RNA aptamer to human immunoglobulin G. *RNA* **2008**, 14, 1154–1163.

Morris KN, Jensen KB, Julin CM, Weil M & Gold L. High affinity ligands from *in vitro* selection: complex targets. *Proc. Natl. Acad. Sci. USA.* **1998**, 95, 2902–2907.

Moshitzky S. Kukulansky T, Haimovich J & Hollander N. Growth inhibition of myeloma cells by anti–idiotype antibodies in the absence of membrane–bound immunoglobulin. *Immunol. Cell Biol.* **2008**, 86, 261–267.

Mosing RK, Mendonsa SD & MT Bowser. Capillary electrophoresis–SELEX selection of aptamers with affinity for HIV–1 reverse transcriptase. *Anal. Chem.* **2005**, 77, 6107–6112.

Murphy MB, Fuller ST, Richardson PM & Doyle SA. An improved method for the *in vitro* evolution of aptamers and applications in protein detection and purification. *Nucleic Acids Res.* **2003**, 31, e110.

Phan, AT, Kuryavyi V, Luu KN, Patel DJ. In: Neidle S, Balasubramanian S, eds. Quadruplex Nucleic Acids. Royal Society of Chemistry: UK. **2006**, 38−41.

Neidle S & Parkinson GN. Quadruplex DNA crystal structures and drug design. *Biochemie.* **2008**, 90, 1184–1196.

Ng EW, Shima DT, Calias P, Cunningham ET, Jr Guyer DR & Adamis AP. Pegaptanib, a targeted anti–VEGF aptamer for ocular vascular disease. *Nat. Rev. Drug Discov.* **2006**, 5, 123–132.

Nimjee SM, Rusconi CP & Sullenger BA. Aptamers, an emerging class of therapeutics. *Annu. Rev. Med.* **2005**, 56, 555–583.

Nolte A, Klussmann S, Bald R, Erdmann VA & Fürste JP. Mirror–design of L–oligonucleotide ligands binding to L–arginine. *Nat. Biotechnol.* **1996**, 14, 1116–1119.

Nutiu R & Li Y. *In vitro* selection of structure–switching signaling aptamers. *Angew. Chem. Int. Ed. Engl.* **2005**, 44, 1061–1065.

Nutiu R & Li Y. Structure–switching signaling aptamers: Transducing molecular recognition into fluorescence signalling. *Chemistry* **2004**, 10, 1868–1876.

O'Connell D, Koenig A, Jennings S, Hicke B, Han HL, Fitzwater T, Chang YF, Varki N, Parma D & Varki A. Calcium–dependent oligonucleotide antagonists specific for L–selectin. *Proc. Natl. Acad. Sci. USA.* **1996**, 93, 5883–5887.

Osterborg A, Yi Q, Henriksson L, Fagerberg J, Bergenbrant S, Jeddi–Tehrani M. Rudén U, Lefvert AK, Holm G, Mellstedt H. Idiotype immunization combined with granulocytemacrophage colony–stimulating factor in myeloma patients induced type I, major histocompatibility complex restricted, CD8– and CD4–specific T ell responses. *Blood* **1998**, 91, 2459–2466.

Paborsky LR, McCurdy SN, Griffin LC, Toole JJ & Leung LLK. The single–stranded DNA aptamer–binding site of human thrombin. *J. Biol. Chem.* **1993**, 268, 20808–20811.

Pagratis NC, Bell C, Chang YF, Jennings S, Fitzwater T, Jellinek D, Dang C. Potent 2'–amino–, and 2'–fluoro–2'–deoxyribonucleotide RNA inhibitors of keratinocyte growth factor. *Nat. Biotechnol.* **1997**, 15, 68–73.

Pan W, Craven RC, Qiu Q, Wilson CB, Wills JW, Golovine S & Wang JF. Isolation of virus neutralizing RNAs from a large pool of random sequences. *Proc. Natl. Acad. Sci. USA.* **1995**, 92, 11509–11513.

Petach H & Gold L. Dimensionality is the issue, use of photoaptamers in protein microarrays. *Curr. Opin. Biotechnol.* **2002**, 13, 309–314.

Potyrailo RA, Conrad RC, Ellington AD & Hieftje GM. Adapting selected nucleic acid ligands (aptamers) to biosensors. *Anal. Chem.* **1998**, 70, 3419–3425.

Proske D, Blank M, Buhmann R & Resch A. Aptamers – basic research, drug development, and clinical applications. *Appl. Microbiol. Biotechnol.* **2005**, 69, 367–374

Pyle AM. Ribozymes: a distinct class of metalloenzymes. *Science* **1993**, 261, 709–714.

Rakic JM, Blaise P & Foidart JM. Pegaptanib and age–related macular degeneration. *N. Engl. J. Med.* **2005**, 352, 1720–1721.

Rasmussen T, Hansson L, Osterborg A, Johnsen HE, Mellstedt H. Idiotype vaccination in multiple myeloma induced a reduction of circulating clonal tumor B cells. *Blood* **2003**, 101, 4607–4710.

Rhie A, Kirby L, Sayer N, Wellesley R, Disterer P, Sylvester I, Gill A, Hope J, James W, Tahiri–Alaoui A. Characterization of 2'–fluoro–RNA aptamers that bind preferentially to disease–associated conformations of prion protein and inhibit conversion. *J. Biol. Chem.* **2003**, 278, 39697–39705.

Riccardi A, Gobbi PG, Ucci G. et al. Changing clinical presentation of multiple myeloma. *Eur. J. Cancer* **1991**, 27, 1401–1405.

Sambrook J, Fritsh EF & Maniates T. *Molecular Cloning– A Laboratory Manuel*; Cold Spring Harbor Laboratory Press: Cold Spring Harbor, NY, 1989.

Saito T & Tomida M. Generation of inhibitory DNA aptamers against human hepatocyte growth factor. *DNA Cell Biol.* **2005**, 24624–24633.

Schneider DJ, Feigon J, Hostomsky Z & Gold L. High–affinity ssDNA inhibitors of the reverse transcriptase of type 1 human immunodeficiency virus. *Biochemistry* **1995**, 34, 9599–9610.

Schultze P, Macaya RF & Feigon J. Three–dimensional solution structure of the thrombin–binding DNA aptamer d(GGTTGGTGTGGTTGG). *J. Mol. Biol.* **1994**, 235, 1532–1547.

Shamah SM, Healy JM & Cload ST. Complex target SELEX. *Acc. Chem. Res.* **2008**, 41, 130–138.

Shearman LP, Wang SP, Helmling S. Stribling DS, Mazur P, Ge L, Wang L, Klussmann S, Macintyre DE, Howard AD & Strack AM. Ghrelin neutralization by an RNA–spiegelmer ameliorates obesity in diet–induced obese mice. *Endocrinology* **2006**, 147, 1517–1526.

Shimazaki C, Wisniewski D, Scheinberg DA, Atzpodien J, Strife A, Gulati S, Fried J, Wisniewolski R, Wang CY & Clarkson BD. Elimination of myeloma cells from bone marrow by using monoclonal antibodies and magnetic immunobeads. *Blood* **1988**, 72, 1248–1254.

Sirohi B & Powles R, Multiple myeloma. *Lancet* **2004**, 363, 875–887.

Spector T. Refinement of the coomassie blue method of protein quantitation. A simple and linear spectrophotometric assay for less than or equal to 0.5 to 50 microgram of protein. *Anal. Biochem.* **1978**, 86, 142–146.

Stevenson FK, Bell AJ, Cusack R, Hamblin TJ, Slade CJ, Spellerberg MB & Stevenson GT. Preliminary studies for an immunotherapeutic approach to the treatment of human myeloma using chimeric anti–CD38 antibody. *Blood* **1991**, 77, 1071–1079.

Stollar BD. Antibodies to DNA. *CRC. Crit. Rev. Biochem.* **1986**, 20, 1–36.
Stollar BD. Molecular analysis of anti–DNA antibodies. *FASEB J.* **1994**, 8, 337–342.

Stoltenburg R, Reinemann C & Strehlitz B. FluMag–SELEX as an advantageous method for DNA aptamer selection. *Anal. Bioanal. Chem.* **2005**, 383, 83–91.

Stoltenburg R, Reinemann C & Strehlitz B. SELEX–A (r)evolutionary method to generate high–affinity nucleic acid ligands. *Biomolecular Engineering* **2007**, 24, 381–403.

Sutton BJ & Gould HJ. The human IgE network. *Nature* **1993**, 366, 421–428.

Tai YT, Li X, Tong X, Santos D, Otsuki T, Catley L, Tournilhac O, Podar K, Hideshima T, Schlossman R, Richardson P, Munshi NC, Luqman M & Anderson KC. Human anti–CD40 antagonist antibody triggers significant antitumor activity against human multiple myeloma. *Cancer Res.* **2005**, 65, 5898–5906.

Tavitian B, Terrazzino S, Kuhnast B. Marzabal S, Stettler O, Dollé F, Deverre JR, Jobert A, Hinnen F, Bendriem B, Crouzel C & Di Giamberardino L. *In vivo* imaging of oligonucleotides with positron emission tomography. *Nat. Med.* **1998**, 4, 467–471.

Terness P, Welschof M, Moldenhauer G, Jung M, Moroder L, Kirchhoff F, Kipriyanov S, Little M & Opelz G. Idiotypic vaccine for treatment of human B–cell lymphoma. Construction of IgG variable regions from single malignant B cells. *Hum. Immunol.* **1997**, 56, 17–27.

Titzer S, Christensen O, Manzke O, Tesch H, Wolf J, Emmerich B. Carsten C, Diehl V, Bohlen H. Vaccination of multiple myeloma patients with idiotype–pulsed dendritic cells: immunological and clinical aspects. *Br. J. Haematol.* **2000**, 108, 805–816.

Tombelli S, Minunni A, Luzi E & Mascini M. Aptamer–based biosensors for the detection of HIV–1 Tat protein. *Bioelectrochemistry* **2005**, 67, 135–141.

Toulme JJ, Darfeuille F, Kolb GL, Chabas S & Staedel C. Modulating viral gene expression by aptamers to RNA structures. *Biol. Cell* **2003**, 95, 229–238.

Treon SP, Agus TB, Link B, Rodrigues G, Molina A, Lacy MQ, Fisher DC, Emmanouilides C, Richards AI, Clark B, Lucas MS, Schlossman R, Schenkein D, Lin B,

Kimby E, Anderson KC & Byrd JC. CD20–directed antibody–mediated immunotherapy induces responses and facilitates hematologic recovery in patients with Waldenstrom's macroglobulinemia. *J. Immunother.* **2001**, 24, 272–279.

Tsai RYL, Reed RR. Identification of DNA recognition sequences and protein interaction domains of the multiple–Zn–finger protein Roaz. *Mol. Cell Biol.* **1998**, 18, 6447–6456.

Tucker CE, Chen LS, Judkins MB, Farmer JA, Gill SC, Drolet DW. Detection and plasma pharmacokinetics of an anti–vascular endothelial growth factor oligonucleotide–aptamer (NX1838) in rhesus monkeys. *J. Chromatogr. B. Biomed. Sci. Appl.* **1999**, 732, 203–212.

Tuerk C & Gold L. Systematic evolution of ligands by exponential enrichment: RNA ligands to bacteriophage T4 DNA polymerase. *Science* **1990**, 249, 505–510.

Tuerk C, MacDougal S & Gold L. RNA pseudoknots that inhibit human immunodeficiency virus type 1 reverse transcriptase. *Proc. Natl. Acad. Sci. USA.* **1992**, 89, 6988–6992.

Tuerk C & MacDougal–Waugh S. *In vitro* evolution of functional nucleic acids, high–affinity RNA ligands of HIV–1 proteins. *Gene* **1993**, 137, 33–39.

Vater A & Klussmann S. Toward third–generation aptamers: Spiegelmers and their therapeutic prospects. *Curr. Opin. Drug Discov. Devel.* **2003**, 6, 253–261.

Vinores SA. Technology evaluation, Pegaptanib, Eyetech/Pfizer. *Curr. Opin. Mol. Ther.* **2003**, 5, 673–679.

Wang J, Jiang H & Liu F. *In vitro* selection of novel RNA ligands that bind human cytomegalovirus and blockviral infection. *RNA* **2000**, 6, 571–583.

Wiegand T, Williams P, Dreskin S. Jouvin MH, Kinet JP & Tasset D. High–affinity oligonucleotide ligands to human IgE inhibit binding to Fc epsilon receptor I. *J. Immunol.* **1996**, 157, 221–230.

Williams KP & Bartel DP. PCR product with strands of unequal length. *Nucleic Acids Research* **1995**, 234, 220–4221

Williams KP, Liu XH, Schumacher TNM, Lin HY, Ausiello DA, Kim PS & Bartel DP. Bioactive and nuclease–resistant L–DNA ligand of vasopressin. *Proc. Natl. Acad. Sci. USA.* **1997**, 94, 11285–11290

Willems PM, Hoet RM, Huys EL, Raats JM, Mensink EJ & Raymakers RA. Specific detection of myeloma plasma cells using anti–idiotypic single chain antibody fragments selected from a phage display library. *Leukemia* **1998**, 12, 1295–1302.

Williamson JR. G–quartet structures in telomeric DNA. *Annu. ReV. Biophys. Biomol. Struct.* **1994**, 23, 703–730.

Willis MC, Collins BD, Zhang T, Green LS, Sebesta DP, Bell C, Kellogg E, Gill SC, Magallanez A, Knauer S, Bendele RA, Gill PS & Janjić N. Liposome–anchored vascular endothelial growth factor aptamers. *Bioconjug. Chem.* **1998**, 9, 573–582.

Wochner A, Menger M, Orgel D, Cech B, Rimmele M, Erdmann VA & Glökler JA. DNA aptamer with high affinity and specificity for therapeutic anthracyclines. *Anal. Biochem.* **2008**, 1373, 34–42.

Würflein D, Dechant M, Stockmeyer B, Tutt AL, Hu P, Repp R, Kalden JR, van de Winkel JG, Epstein AL, Valerius T, Glennie M & Gramatzki M. Evaluating antibodies for their capacity to induce cell–mediated lysis of malignant B cells. *Cancer Res.* **1998**, 58, 3051–3058.

Yamamoto R, Katahira M, Nishikawa S, Baba T, Taira K & Kumar PK. A novel RNA motif that binds efficiently and specifically to the Tat protein of HIV and inhibits the transactivation by Tat of transcription *in vitro* and *in vivo. Genes Cells* **2000**, 5, 371–388.

Yan X, Gao X & Zhang Z. Isolation and Characterization of 2'–amino–modified RNA aptamers for human TNF–alpha. *Genomics Proteomics Bioinformatics* **2004**, 2, 32–42.

Yang JC, Haworth L, Sherry RM, Hwu P, Schwartzentruber DJ, Topalian SL, Steinberg SM, Chen HX & Rosenberg SAA. Randomized trial of bevacizumab, an anti–vascular endothelial growth factor antibody, for metastatic renal cancer. *N. Engl. J. Med.* **2003**, 349, 427–434.

Yarus M & Berg P. On the properties and utility of a membrane filter assay in the study of isoleucyl–tRNA synthetase. *Anal. Biochem.* **1970**, 35, 450–465.

Yi Q, Desikan R, Barlogie B & Munshi N. Optimizing dendritic cell–based immunotherapy in multiple myeloma. *Br. J. Haematol.* **2002**, 117, 297–305.

Yoo S & Dynan WS. Characterization of the RNA binding properties of Ku protein. *Biochemistry* **1998**, 37, 1336–1343.

Yoshida Y, Sakai N, Masuda H, Furuichi M, Nishikawa F, Nishikawa S, Mizuno H & Waga I. Rabbit antibody detection with RNA aptamers. *Anal. Biochem.* **2008**, 15375, 217–222.

Zaug AJ & Cech TR. The intervening sequence RNA of Tetrahymena is an enzyme. *Science* **1986**, 231, 470–475.

Zhang B & Rothe, Germany R. A region of the insulin receptor important for ligand binding (residues 450–601) is recognized by patients´ autoimmune antibodies and inhibitory monoclonal antibodies. *Proc. Natl. Acad. Sci. USA.* **1991**, 88, 9858–9862.

Zhang YM, Liu N, Zhu ZH, Rusckowski M & Hnatowich DJ. Influence of different chelators (HYNIC, MAG3 and DTPA) on tumor cell accumulation and mouse biodistribution of technetium–99m labeled antisense DNA. *Eur. J. Nucl. Med.* **2000**, 27, 1700–1707.

Zuker M. Mfold web server for nucleic acid folding and hybridization prediction. *Nucleic Acids Res.* **2003**, 31, 3406–3415.

9 Appendix

9.1 Materials

9.1.1 Chemicals

Acetic Acid	Rothe, Germany
Acrylamide	Rothe, Germany
Agar	Gibco BRL
Agarose	Biozyme, Oldendorf, Germany
Ammonium sulfate	Fluka, St Quentin Fallavier, France
Ampicillin	Sigma, Germany
APS	Rothe, Germany
Bromophenol Blue	Serva, Heidelberg, Germany
BSA	Biolabs, Beverly, USA
DNA Ladder (10 bp)	Biolabs, Beverly, USA
dNTPs	Roche, Germany
DTT	BD Biosciences, USA
EDTA	Merck, Germany
Ethanol	Merck, Germany
Ethidium Bromide	Fluka, St Quentin Fallavier, France
Glucose	Merck, Germany
Glycerol	Merck, Germany
Glycogen	Fermentas, Burlington, Canada
Hydrochloric Acid	Merck, Germany
IPTG	Merck, Germany
Magnesium Chloride	Merck, Germany
Methanol	Rothe, Germany
Magnesium Sulfate	Merck, Germany
r–^{32}P–dCTP	Amersham/GE Healthcare, UK
α–^{32}P–ATP	Amersham/GE Healthcare, UK
Pepton Nr. 140	Gibco BRL, Eggenstein, Germany

Phenol/chloroform/Isoamylethanol	Rothe, Germany
Potassium Chloride	Merck, Germany
Potassium Phosphate	Merck, Germany
Protein Marker	Serva, Heidelberg, Germany
Sodium acetat	Riedel de Häen
Sodium chloride	Merck, Germany
Sodium Hydroxide	Merck, Germany
Sodiumdodecylsulfate (SDS)	Merck, Germany
Sulfuric acid	Rothe, Germany
TEMED	Rothe, Germany
TMB	Calbiochem, San. Diego, CA, USA
Tris–HCl	Rothe, Germany
Tween 20	Serva, Heidelberg, Germany
Urea	Rothe, Germanye, Germany
Yeast extract	Gibco BRL, Eggenstein, Germany

9.1.2 Special Materials

9.1.2.1 Antibodies

Human MM IgG1 (target)	Alexis, CA, USA
Human MM IgG1	AbD Serotec, Oxford, UK
Human anti–lysozyme IgG1	AbD Serotec, Oxford, UK
Human normal serum IgG	Bethyl, TX, USA
Human IgG Fab fragment	Bethyl, TX, USA
Human IgG Fc fragment	Calbiochem, CA, USA
Goat anti–human IgG (conjugated with HRP)	Abcam, Cambridge, UK

9.1.2.2 Enzymes

Lambda Exonuclease	Fermentas, Burlington, Canada
T4–DNA–Ligase	New England Biolabs, Beverly, USA
T4 Polynucleotide Kinase	Promega, Madison, WI, USA
Taq DNA Polymerase	New England Biolabs, Beverly, USA

9.1.3 Kits

Nucleospin® Extract II	Macherey–Nagel, Düren, Germany
NucleoSpin® Plasmid	Macherey–Nagel, Düren, Germany
GFX PCR DNA and Gel Band Purification Kit	Amersham/GE Healthcare, UK
pGEM®–T Easy Vector Systems	Promega, Madison, WI, USA
BioRad protein assay	Biorad, Sweden

9.1.4 Cells and Plasmids

E. Coli BL21/DE3	Stratagene, La Jolla, CA, USA
E. Coli JM 109	Promega, Madison, WI, USA
pGEM®–T Easy	Promega, Madison, WI, USA

9.1.5 Media

LB–Medium

10 g/l peptone Nr. 140
5 g/l yeast extract
10 g/l NaCl,
Adjust the pH to 7.5 with NaOH
Autoclave 20 mins, 120°C

LB–Agar Plates

12 g/l agar (w/v) in LB–medium
Autoclave 20 mins, 120°C
Cool down to ~50°C

SOC Medium

20 g/l peptone Nr.140
5 g/l yeast extract
10 mM NaCl
2.5 mM KCl
Autoclave 20 min, 120°C
Add ampicillin to 100 mg/ml
Pour into sterile petri plates
Add 20 mM $MgCl_2$
Add 20 mM Glucose, Adjust the pH to 7.0 with NaOH

9.1.6 Buffers

Dulbecco's Phosphate–Buffered Saline (D–PBS) (1×)

137.9 mM NaCl
8.06 mM Na_2HPO_4–$7H_2O$
2.67 mM KCl
1.47 mM KH_2PO_4

Lambda Exonuclease Buffer (10×)

670 mM glycine–KOH (pH 9.4)
25 mM $MgCl_2$
0.1% Triton X–100

Laemmli–Loading buffer (2×)

0.5M Tris–HCl (pH 6.8)
4.4% (w/v) SDS
20% (v/v) glycerol
2% (v/v) 2–mercaptoethanol
2% (v/v) bromophenol blue

SDS–PAGE Running Buffer (5×)

192 mM Tris–HCl
1.9 M Clycin
0.5% SDS

Urea PAGE Loading Buffer (2×) 2×TBE

16 M Harnstoff
0.04 % Bromphenolblue
0.04 % Xylencyanol

T4 Polynucleotide Kinase Reaction Buffer (10×)

500 mM imidayole–HCl (pH 6.6)
100 mM $MgCl_2$
50 mM DTT
1 mM spermidine
1 mM EDTA

ThermoPol PCR Buffer (10×)

100 mM KCl
100 mM $(NH_4)_2SO_4$
200 mM Tris–HCl
20 mM $MgSO_4$
1% Triton X–100

TAE Buffer (10×)

400 mM Tris– Acetat (pH 8.0)
10 mM EDTA

TBE Buffer (10×)

900 mM Tris–borate (pH 8.0)
20 mM EDTA

TE Buffer

10 mM Tris–HCl (pH 8.0)
1 mM EDTA

9.1.7 Laboratory Equipment

Agarose Gel Chamber	Bio-Rad, USA
Agilent 8452 Diode Array Spectrophotometer	Hewlett Packard, Palo Alto, CA, USA
Autoclave 500–D	Sterico, AG, Dietikon, Switzerland
CD–Spektropolarimeter J–600	JASCO, Japan
Centrifuge 5415D	Eppendorf, Germany
Cool Centrifuge J2–21	Beckman, Fullerton, CA, USA
ELISA Plate Reader	Anthos Labtec Instruments, Austria
Gel Document Gel Dol 2000	Bio–Rad, USA
Gel Dryer	Biometra, Göttingen, Germany
Gel Electrophoresis System	Renner GmBH, Darmstadt, Germany
Freezer –20ºC	Bosch, Germany
Freezer –80ºC	Heraeus, Hanau, Germany
Freezer 4ºC	Bosch, Germany
Lyophilizer SC110AR	Savant, Instruments, Farmingdale, NY, USA
Magnetic Stirrer	IKA–Combimag RCT, Staufen, Germany
Mini–gel apparatus	Bio–Rad, USA
Microcentrifuge ProFuge 10K	Stratagene, La Jolla, CA, USA
Microwave	Toshiba, Japan
Oil Pump	Alcatel, Germany
PCR Apparatus	Biometra, Göttingen, Germany
Pipettes P2, P20, P200, P1000	Abimed, Langenfeld, Germany

pH–Meter 766 Calimatic	Knick, Berlin, Germany
Photometer UV–1202	Shimadzu, USA
Plexis Container	Nalgene, Germany
Plexis Shield	Jencons
Power Supply	ECPS 3000/150, Pharmacia
Purest Water Installation (Milli–Q)	Millipore, Bedford, MA
Refrigerated Vapor Trap	RVT400, Savant
Shaker (Isotope Laboratory)	Yellow line, FHG–VERW
Scintillation Counter LS 6000	Beckman, Fullerton, CA, USA
Table–top Centrifuge	Eppendorf, Germany
Thermomixer comfort	Eppendorf, Germany
UV–Visible Spectrophotometer (UV–1202)	Shimadzu, Duisburg, Germany
Vortex	Scientific Industries, Bohemia, NY, USA
Water Bath	GFL, Germany

9.1.8 Other Materials

NeutrAvidin Agarose Resins	Thermo Scientific Pierce
Roti–Blue (Colloidal Coomassie Staining)	Rothe, Germany
StrataClean™ resin	Stratagene, CA, USA
96–Well PCR Tube Racks	Rothe, Germany
96–Well Plates	Nunc,Roskilde, Denmark
Gel Filtration Columns (NAP–5, 10 Column)	Pharmacia Biotech, Sweden
Gel Filtration Columns (Nick™ Column)	Pharmacia Biotech, Sweden
Gloves	Meditrade, Germany
PCR Tubes	Rothe, Germany
Pipette Tips	Greiner bio–one, Germany
Plate Sealing Film	American National Can TM, USA
Streptavidin Coated 96–Well Plates	Pierce, Bonn, Germany
Microcon YM–10, 30, 50 Spin Filters	Millipore, Bedford, MA

Nap 5, 10, 25–Column	GE Healthcare, Uppsala, Sweden
Reaction Tubes, 0.5 ml	Rothe, Germany
Syringe Filter 0.22µm	Rothe, Germany
Nitrocellulose Membrane 0.45 µm	Millipore, Bedford, MA
Reaction Tubes, 1.5 ml, 2.0ml	Rothe, Germany

9.2 Abbreviations

A	adenosine
A_{260}	absorption at λ=260 nm
A_{295}	absorption at λ=295 nm
A_{595}	absorption at λ=595 nm
AChRs	acetylcholine esterase receptors
ADCC	antibody dependent cellular cytotoxicity
AMD	age–related macular degeneration
AMP	Ampicillin
APS	Ammonium persulfate
ATP	adenosine 5'–triphosphate
Bio	biotin
Bis	N, N'–methylene bisacrylamide
BM	bone marrow
bp	base pair(s)
BSA	bovine serum albumin
C	cytosine
°C	temperature in degrees Celsius
CD	circular dichroism
CDC	complement dependent cytotoxicity
CDR	complementary–determining regions
CE	capillary electrophoresis
Ci	curie, 1 Ci=37 MBq
cpm	counts per minute
Da	Dalton

DEXA	dual energy X–ray absorptiometry
DNA	deoxyribonucleic acid
DNase	desoxyribonuclease
dNTP	deoxyribonucleotide triphosphate
ds	double–stranded
DTT	Dithiothreitol
E. coli	Escherichia coli
EDTA	Ethylenediaminetetraacetic Acid
EMSA	electrophoretic mobility shift assay
ESR	erythrocyte sedimentation rate
EtBr	3, 8–diamino–5–Ethyl–6–phenyl phenanthridinium Bromide
FC	flow cytometry
FDA	Food and Drug Administration
Fig.	figure
FISH	fluorescence in–situ hybridisation
FITC	fluorescein isothiocyanate
FLAA	fluorescent dye–linked aptamer assay
g	gram
G	guanosine
GM–CSF	granulocyte–marcrophage colony–stimulating factor
h	hour(s)
HIV	human immunodeficiency virus
HPLC	high performance liquid chromatography
HRP	horseradish peroxidise
HSCT	haematopoietic stem cell transplantation
IC_{50s}	50% inhibitory concentrations
Id	idiotype
Id–KLH	Id–keyhole–limpet hemocyanin
Ig	Immunoglobulin
IPTG	Isopropyl-β-D-thiogalactopyranosid
J	joining
K_d	dissociation constant
K_i	inhibition constant

l	liter
LB	Luria Bertani medium
LDH	lactate dehydrogenase.
m	meter
M	mol/l, molar
M protein	monoclonal protein
mAb	monoclonal antibody
MG	myasthenia gravis
MGUS	monoclonal gamopathy of undetermined significance
min	minute(s)
mM	micromolar
MM	multiple myeloma
mRNA	messenger ribonucleic acid
MVD	microvascular density
NCFBAs	nitrocellulose filter binding assays
nM	nanomolar
NMR	nuclear magnetic resonance
nt	Nucleotide(s)
NTP	nucleotide triphosphate
OD	optical density
PAGE	polyacrylamide gel electrophoresis
PBS	phosphate buffered saline
PCR	polymerase chain reaction
PEG	polyethylene glycol
rcf	relative centrifugal force
RNA	ribonucleic acid
rpm	rotations per minute
RT	room temperature
s	second(s)
SAP	serum amyloid protein
SDS	Sodium dodecyl sulfate
SLE	systemic lupus erythematosus
SPR	surface plasmon resonance

ss	single–stranded
T	thymine
t	time
TAA	tumor–associated antigens
TAE	Tris–Acetic Acid–EDTA
TBE	3.3', 5.5'–tetramethylbenzidine
TEMED	N,N,N',N'–Tetramethylethylenediamine
TMB	Tetramethylbenzidine
Tris	Tris–(Hydroxymethyl)–Aminomethane
U	units of enzymatic activity
UV	ultraviolet
V	variable
V	volt (s)
v/v	volume per volume
VEGF	vesicular endothelial growth factor
VSG	variant surface glycoprotein
W	watt (s)
w/v	weight per volume
X–gal	5'–Bromo–4'–Chloro–3'–Indolyl–β–D–galactoside
λ	lambda
µl	micro liter
µM	micro molar

9.3 Publications Related to this Work

Articals

Yan Wang. SELEX and the applications in medicine (review in Chinese). Basic and Clinic Medicine 2007; 27 (7). 834–840.

Yan Wang, Jens P. Fürste and Volker A. Erdmann. High affinity and specificity DNA aptamers to a mouse anti–streptavidin IgG1 monoclonal antibody. manuscript in preparation

Yan Wang, Jens P. Fürste and Volker A. Erdmann. *In vitro* selection and chracterizaiton of DNA aptamers against a human multiple myeloma antibody. manuscript in preparation

Poster Presentitions

Yan Wang Jens P. Fürste, Volker A. Erdmann. DNA aptamers to a human multiple myeloma IgG1 for diagnostic and therapeutic applications. RNA 2008 Thirteenth Annual Meeting of the RNA Society. 28 July–3 August 2008, Berlin.

Yan Wang, Jens P. Fürste, Volker A. Erdmann. High affinity DNA aptamers to a human myeloma IgG1. the 22nd international symposium on Microscale Bioseparations and methods for systems biology, MSB. 9–13 March 2008, Berlin.

Yan Wang, Siegfried Neumann, Jens P. Fürste, Volker A. Erdmann. Selection of DNA aptamers that bind a specific antibody. Annual fall meeting, German Society for Biochemistry and Molecular Biology, GBM 18–21 September 2005 ,Berlin.

Patent One patent in application.

9.4 Curriculum Vitae

For reason of data protection,
the curriculum vitae is not included in the online version

9.5 Acknowledgements

First and foremost, I would like to express my highest gratitude to Prof. Volker. A. Erdmann for giving me the opportunity to perform the research for my doctoral thesis in his laboratory, for the guidance during the last five years and for reviewing this thesis.

I am indebted to Prof. Roland Tauber for being my second supervisor and for reviewing this thesis.

Great thanks go to Dr. Jens Peter Fürste for all his supervision, discussion and supports on my Ph.D. program, and for his correction of this dissertation.

I am also very much indebted to the members of the Erdmann laboratory for their stimulating discussions and valuable suggestions as well as their friendships.

I would like to thank Prof. Heinz Zeichhardt for kindly providing normal human serum. I would also like to thank Prof. Wolfram Saenger for offering the use of CD spectroscopy in his group, and Prof. Multhaup and Dr. Münter for offering and helping me to use the ELISA plate reader.

I would not have been able to achieve all this without the support of my family. To my family I owe more than to anyone else. They have guided me, encouraged me, and sustained me. Most of all, they have always believed in me and loved me. All of this means more to me than I am able to express here in words.